

Phase I Report

Project: DTFH61-11-C-00025

The Impact of Wide-Base Tires on Pavement – A National Study

Submitted to the

**FEDERAL HIGHWAY ADMINISTRATION
(FHWA)**

August 2011

Submitted by

**University of Illinois at Urbana-Champaign
1207 Newmark Lab, 205 N. Mathews, M/C 250
Urbana, IL 61801**

Particiapants: UC Davis, FLDOT, Delft, CSIR

TABLE OF CONTENTS

List of Tables	Page
	v
List of Figures	vi
1. Introduction and Overview of the Report	1
2. Synthesis of the Literature Review	4
3. Numerical Modeling	7
3.1. The Finite Element Method	7
3.1.1. Viscoelastic Asphalt Material	7
3.1.2. Dynamic Analysis	7
3.1.3. Three-dimensional Contact Stresses	8
3.1.4. Continuous Moving Load	8
3.1.5. Layer Interaction	8
3.1.6. Nonlinear Granular Material	9
3.2. Material Characterization	9
Material characteristics are needed as inputs for pavement modeling. The following tests are suggested.	9
3.2.1. Complex (Dynamic) Modulus	9
3.2.2. Semi-Circular Beam (SCB)	10
3.2.3. Cross-Anisotropic Characterization of Granular Materials	11
3.2.4. Volumetric Properties of Asphalt Mixtures	11
3.3. Tire Contact Stress Measurements	11
3.4. Load-Deflection curves	13
4. Validation of Numerical Modeling	14
4.1. Proposed Pavement Structures	14
4.1.1. New Test Sections in UIUC-ATREL	14
4.1.2. New Test Sections in UC-Davis	14
4.1.3. New Test Sections in Florida	15
4.2. Overview of Available Data	17
4.2.1. Virginia Smart Road	17
4.2.2. UIUC-ATREL Thin Pavement Sections	19
4.2.3. UIUC-ATREL Full Depth Sections	19
4.2.4. Ohio SPS-8 Sections	20

4.2.5.	UC-Davis Permanent Deformation Profiles	20
4.2.6.	Florida DOT	20
4.3.	Testing Program	21
4.3.1.	Accelerated Pavement Testing	21
4.3.2.	Pavement Response	21
5.	Evaluation of Pavement Damage	22
5.1.	Fatigue Cracking (bottom-up and top-down)	22
5.2.	AC Rutting	23
5.3.	Subgrade Rutting	23
5.4.	Combined Damage Ratio	23
6.	Use of Modeling results in Analysis Tool	25
6.1.	Artificial Neural Network (ANN) Based Prediction Model for Pavement Damage Based on Finite Element Analyses	25
6.2.	Life Cycle Cost Analysis Results and Environmental Life Cycle Assessment Framework	25
6.2.1.	Life Cycle Cost Analysis	25
6.2.2.	Life Cycle Assessment (LCA)	26
6.3.	Suggested Options for utilization of modeling results	30
6.3.1.	Consider Analysis of Full Factorial Pavement System	30
6.3.2.	ANN on Specific Scenarios	31
6.3.3.	Postpone ANN for a Future Work	31
7.	Implementation	32
8.	References	33
9.	Appendix A: Detailed Literature Review	36
9.1.	Impact on Road Infrastructure	36
9.1.1.	Accelerated Pavement Testing	36
9.1.2.	Numerical Modeling and Analytical Methods	42
9.1.3.	Sections subjected to real traffic	47
9.2.	Impact on Dynamic Tire Loading	47
9.3.	Impact on Trucking Operations	48
9.3.1.	Fuel Economy	48
9.3.2.	Hauling Capacity	49
9.3.3.	Tire Cost and Repair	50

9.3.4.	Truck Operation and Safety	50
9.3.5.	Ride and Comfort	50
9.4.	Impact on Environment	50
9.4.1.	Gas Emission	50
9.4.2.	Tire Recycling	51
9.4.3.	Noise	51
10.	Appendix B: Available Pavement Structures and Instrumentation – Virginia Smart Road	52
11.	Appendix C: Available Pavement Structures and Instrumentation – ATREL-UIUC Thin Sections	64
12.	Appendix D: Available Pavement Structures and Instrumentation – ATREL-UIUC Full Depth Sections	70
13.	Appendix E: Available Pavement Structures and Instrumentation – Ohio SPS-872	
14.	Appendix F: Available Pavement Structures and Instrumentation – UC-Davis	74

LIST OF TABLES

Table 1. Test Matrix for SIM testing in South Africa	Page 12
Table 2. Damage Ratios between the NG-WBT and a Dual-Tire Assembly Based on the COST TCF Models.	39

DRAFT

LIST OF FIGURES

	Page
Figure 1. Flowchart of the Work-Plan	3
Figure 2. Dynamic modulus test set-up	10
Figure 3. SCB test configuration	10
Figure 4. Measurement of tire contact stress using SIM	12
Figure 5. 3D air-inflated tire model for tire-pavement interaction simulation as developed by the research team	13
Figure 6. Plan and profile view of possible pavement structure and instrumentation of proposed section at UIUC	14
Figure 7. Plan and profile view of typical pavement structure and instrumentation of proposed section at UC-Davis	16
Figure 8. Plan and profile view of typical pavement structure and instrumentation of proposed section at Florida DOT	17
Figure 9. Proposed framework for pavement LCA ¹	27
Figure 10. Procedure to address additional fuel consumption adopted by UCPRC.	29
As indicated earlier, the results of the FE models would be used to calculate a combined damage ratio for the various pavement-loading scenarios. The scenarios parameters include layer thicknesses, material properties of each layer, pavement structure, type of tire, applied load, and inflation pressure. The total number of cases can be divided by the number of possible pavement structures and loading cases.	30
Table 2. Total number of loading combinations	30
Table 3. Possible structures for Interstate pavement design	30
Table 4. Total cases for low-volume road pavements	31
Figure B- 1. Plan and profile view of pavement structure and instrumentation of Section A, Virginia Smart Road	52

Figure B- 2. Plan and profile view of pavement structure and instrumentation of Section B, Virginia Smart Road	53
Figure B- 3. Plan and profile view of pavement structure and instrumentation of Section C, Virginia Smart Road	54
Figure B- 4. Plan and profile view of pavement structure and instrumentation of Section D, Virginia Smart Road	55
Figure B- 5. Plan and profile view of pavement structure and instrumentation of Section E, Virginia Smart Road	56
Figure B- 6. Plan and profile view of pavement structure and instrumentation of Section F, Virginia Smart Road	57
Figure B- 7. Plan and profile view of pavement structure and instrumentation of Section G, Virginia Smart Road	58
Figure B- 8. Plan and profile view of pavement structure and instrumentation of Section H, Virginia Smart Road	59
Figure B- 9. Plan and profile view of pavement structure and instrumentation of Section I, Virginia Smart Road	60
Figure B- 10. Plan and profile view of pavement structure and instrumentation of Section J, Virginia Smart Road	61
Figure B- 11. Plan and profile view of pavement structure and instrumentation of Section K, Virginia Smart Road	62
Figure B- 12. Plan and profile view of pavement structure and instrumentation of Section L, Virginia Smart Road	63
Figure C- 1. Plan and profile view of pavement structure and instrumentation of thin Section A-1 and A-2 at ATREL-UIUC	64
Figure C- 2. Plan and profile view of pavement structure and instrumentation of thin Section A-3 and B-1 at ATREL-UIUC	65

Figure C- 3. Plan and profile view of pavement structure and instrumentation of thin Section B-2 and C-1 at ATREL-UIUC	66
Figure C- 4. Plan and profile view of pavement structure and instrumentation of thin Section D-1 at ATREL-UIUC	67
Figure C- 5. Plan and profile view of pavement structure and instrumentation of thin Section D-2 at ATREL-UIUC	68
Figure C- 6. Plan and profile view of pavement structure and instrumentation of thin Section D-3 at ATREL-UIUC	69
Figure D- 1. Plan and profile view of pavement structure and instrumentation Sections A and B, ATREL-UIUC full depth pavements.	70
Figure D- 2. Plan and profile view of pavement structure and instrumentation Sections A and B, ATREL-UIUC full depth pavements.	71
Figure E- 1. Plan and profile view of pavement structure and instrumentation of 4 in section, Ohio SPS-8.	72
Figure E- 2. Plan and profile view of pavement structure and instrumentation of 8-in section, Ohio SPS-8.	73
Figure F- 1. Profile view of pavement structure UC-Davis Sections.	74

1. INTRODUCTION AND OVERVIEW OF THE REPORT

After more than two decades of research by the tire industry in conjunction with pavement researchers, a new generation of wide-base tires (445/50R22.5 and 455/55R22.5) was recently introduced to reduce pavement damage and to offer other improved safety, environment, and cost-savings characteristics. This new generation of wide-base tires is wider than its predecessors and has improved structure and design. Experiments have shown that, compared to dual-tire assemblies, wide-base tires have better contact stress distribution and possess capabilities for improved dynamic damping. The new generation of wide-base tires offers a rolling tread width (RTW) increase of 15 to 36% compared to first generation wide-base tires, and these new tires are legal for the “inch-width” law in all 50 states of the United States for 5-axle, 79.8 kip gross-vehicle-weight (GVW) trucks.

In Europe, wide-base tires (having a different design than the ones introduced in the U.S.) have been used successfully on trucks since the early 1980s. In 1997, around 65% of trailers and semi-trailer tires in Germany used wide-base tires (COST 334, 2001). In April 2008, Canada increased the allowable weight limit on axles with wide-base tires. The law now requires that axle loads do not exceed 17 kip for single axles and 34 kip for tandem axle groups when an axle is fitted with two single tires (each 445 mm wide or greater), compared to 20.2 and 37.4 kip, respectively for dual tire assemblies.

For this study, after a thorough literature review, the logical next step is to quantify the impact of vehicle-tire interaction on pavement damage for various pavement structures utilizing advanced theoretical modeling and to validate that impact by performing full-scale pavement testing and or make use of available data. There is also a need to further assess the economic, safety, and environmental effects of using wide-base tires as related to pavement performance. Finally, to allow the use and implementation of wide-base tires by state Departments of Transportation, a simple user-friendly tool may need to be developed to assess the impact of wide-base tires on pavement networks and to facilitate decision-making.

This report summarizes the literature to date on testing and modeling as related to the impact of wide-base tires on pavements and presents the research plan that introduces an innovative and performance-based approach to address the objectives of the project, which include the following:

- Quantify the impact of vehicle-tire interaction on pavement damage utilizing advanced theoretical modeling that is validated via full-scale pavement testing. This includes the determination of the relative effects of wide-base tires and dual-tire assemblies on pavement performance. This should also include the determination of the relationship between the reported tire width and aspect ratio, load, tire inflation pressure and actual tire tread width;
- Develop a tool and methodology that allows state Departments of Transportation to assess the impact of wide-base tires on pavements; and
- Perform an analysis of the economic, safety, and environmental effects of using wide-base tires relative to the impact on pavement performance.

The research team will use advanced modeling to predict pavement responses to 445/50R22.5 (wide-base) and 275/80R22.5 (dual) tire loading. The outcome of this task will quantify pavement damage due to various tire and axle loading configurations commonly used in North America and it will be validated using accelerated pavement testing (APT) data. The APT data includes data available to the research team from their previous extensive work in this field as well as from

other studies where APT was conducted as part of the research. The factors to be considered will include the following: axle loads, speed, tire inflation pressure, and tire pressure imbalance within the dual-tire assembly.

Accurate contact stresses will be measured using the Stress-In-Motion (SIM) tire contact stress method. In addition economic, environmental, and safety impacts will be evaluated based on available data. This includes life cycle cost analysis (LCCA) considering pavement and truck operation costs, as well as a framework for environmental life cycle assessment (LCA). A methodology that allows states to assess the impact of using wide-base tires will be presented.

A detailed research plan has been prepared for this project, including the modeling approach, contact stress measurement, and material characterization. In addition, a plan for conducting accelerated testing and using the resulting data has been prepared. The results of the APT data will be used to validate the developed models and to define how the simplified approach will be presented. Life cycle cost analysis (LCCA) and life assessment analysis (LCA) plans will also be introduced.

This report provides a synthesis of the literature review in Chapter 2, and a detailed literature review is attached as an appendix. Chapter 3 describes the numerical approach that will be followed during this project, as well as the material characterization procedures and the approach for the measurement of the tire-pavement contact stresses. The method that will be followed to validate the numerical model will be described in Chapter 4, which includes the description of the proposed pavement sections and a description of the available data. After that, Chapter 5 will illustrate how the results of the numerical model will be used to evaluate the pavement damage. Finally, Chapter 6 will present the methodology that will be followed to develop the analysis tool. A flowchart describing the proposed plan is shown in Figure 1.

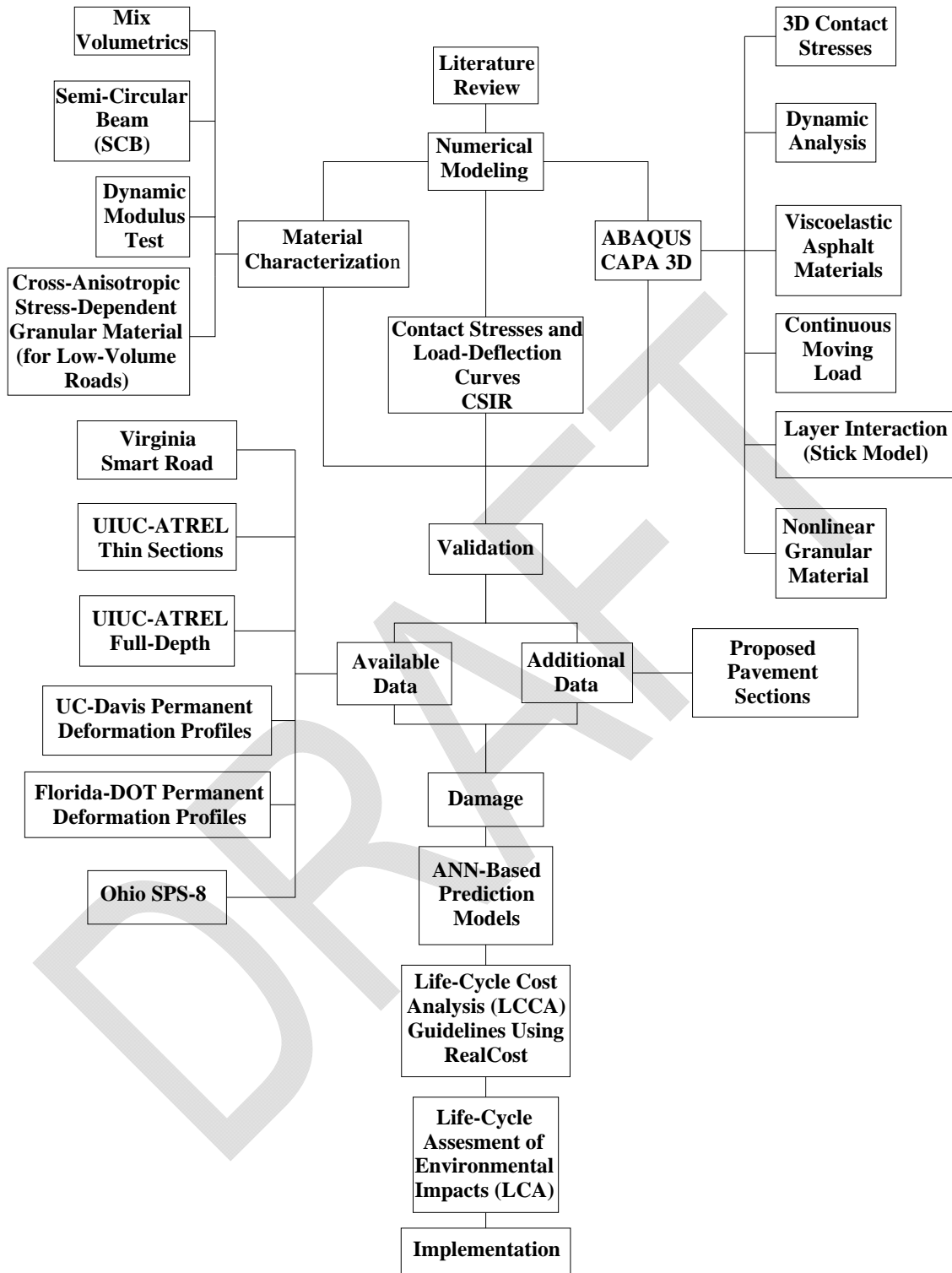


Figure 1. Flowchart of the Work-Plan

2. SYNTHESIS OF THE LITERATURE REVIEW

The research to date regarding wide-base tires (WBT) can be divided in two periods. The first period focused on the first-generation of wide-base tires (FG-WBT) and spanned from early 1980s to 2000. The second period started in early 2000 with the introduction of the new-generation wide-base tire (NG-WBT) after it was evident that FG-WBTs were more damaging to the pavement infrastructure than the conventional dual-tire assembly.

Studies of WBT may be divided into four categories: impact on road infrastructure, impact on dynamic tire loading, impact on trucking operations, and impact on the environment. To investigate the effect of WBT on road infrastructure, researchers have utilized three main approaches: accelerated pavement testing, numerical modeling and analytical methods, and evaluation of in-service field data.

Accelerated pavement testing was used in Finland to study the effect of tire type and axle configurations (Huhtala 1986; Huhtala et al. 1989). Flexible pavements with thicknesses of 2, 3, and 6 inches were instrumented and subjected to various axle configurations and tire types. The study concluded that FG-WBT was more damaging than dual-tire assembly; the difference of the amount of damage caused by these two types of tires decreased as the thickness of the AC layer increased (Huhtala 1986). Furthermore, FG-WBT caused between 1.2 and 4 times more damage than the dual-tire assembly (Huhtala et al. 1989).

In 1992, findings regarding FG-WBT were reported in two states: Virginia and Pennsylvania. Dual-tire assembly and FG-WBT were compared by FHWA in Virginia through performance and response analysis (Bonaquist 1992). Twelve pavement sections were tested at different environmental conditions, axle loads, and tire inflation pressures. Once more, FG-WBT was found to be more damaging than the dual-tire assembly: as much as two times more permanent deformation and 25% less fatigue life than the dual-tire assembly were reported. On the other hand, the Pennsylvania State University test track used trucks traveling at 40 mph with various tire inflation pressures, tire types, axle loads, and axle configurations in its study. The study showed that the damage caused by FG-WBT was between 50 and 70% greater than the dual-tire assembly (Sebaaly and Tabatabaee 1992).

FG-WBT was also evaluated in overlay systems. A study in California compared the performance of dense-graded AC and asphalt-rubber hot-mix gap-graded (ARHM-GG). The accelerated pavement testing was carried out at high temperature and included aircraft tires. The number of repetitions to failure (excessive rutting) of FG-WBT was between 10 and 60% of the dual-tire assembly (Harvey and Popescu 2000).

Several different countries in Europe also studied WBT at the beginning of the previous decade (COST 334 2001). The study included WBT 495/45R22.5, which was referenced as the new generation of WBT. In the United Kingdom, the comparison between WBT-385 and WBT-495 concluded that WBT-385 produced 70 and 50% more rutting in medium-thick and thin flexible pavements, respectively. Thick pavements were tested in Germany, and the ratio between the rutting generated by WBT-495 and dual-tire assembly (315/80R22.5) was around 1.3. Very thick and stiff pavement structures were built and tested in France. No significant difference was found between measurements from both tires at the bottom of the AC. Finally, the difference in dynamic loading between various types of tires was investigated in Finland. Measurements were taken when a truck traveled at 50 mph. The WBT-495 originated a greater response (COST 334 2001).

Twelve different pavement sections were built, heavily instrumented, and tested in Virginia a decade ago. The testing program included various tire types, loading configurations, and speeds (Al-Qadi et al. 2004; Al-Qadi et al. 2005a; Al-Qadi et al. 2005b; Elseifi et al. 2005). Transfer functions were used to link pavement response to damage. The comparison between the combined damage ratio of NG-WBT and dual-tire assembly showed that NG-WBT is, in general, less damaging.

Research regarding WBT has been also performed in Canada (Pierre et al. 2003). Strains near the surface of a flexible pavement with a 4-in AC layer were measured and compared considering different tire types, speeds, loads, and tire inflation pressures. The damage of NG-WBT and dual-tire assembly was found to be dependent on the environmental conditions and location. For instance, strains at the base resulted from NG-WBT and dual-tire assembly loading during summer are close in magnitude. However, during spring NG-WBT produced higher strains (Pierre et al. 2003). NCAT also reported that the horizontal strains at the bottom of the AC and the stresses on top of the subgrade produced by NG-WBT and dual-tire assembly are comparable (Priest and Timm 2006).

The effect of dual-tire assembly, FG-WBT, and NG-WBT on full-depth pavements were compared in a study at the University of Illinois at Urbana-Champaign (Al-Qadi and Wang 2009a; Al-Qadi and Wang 2009b). The thickness of the flexible pavements varied between 6 and 16.5 in. After testing at different tire-inflation pressures, axle loads, and temperatures, it was observed that WBT-425 (FG-WBT) is more damaging than WBT-455 (NG-WBT). Similar tests carried out on low-volume road test sections showed that NG-WBT is more damaging to this type of pavement (Al-Qadi and Wang 2009c).

Finally, a study performed in Florida that focused on permanent deformation compared WBT-445, WBT-455, WBT-425, and dual-tire assembly. Foil strain gauges close to the surface were installed, and the pavement was tested at high temperatures (Greene et al. 2009). Dual-tire assembly had the highest number of passes to reach a 0.5 in rutting, and WBT-425 needed the least number of passes.

Numerical models have also been used to evaluate the effect of WBT. BISAR was utilized to compare radial, bias-ply and FG-WBT in thin (2 in) and thick (8 in) flexible pavements (Sebaaly and Tabatabaee 1989). The study concluded that FG-WBT (15R22.5 and 18R22.5) generated the greatest strain at the bottom of the AC and stress on top of the subgrade. VESYS-DYN was used to assess fatigue damage and rutting. It was reported that FG-WBT caused wider and shallower rut depth than dual-tire assembly (Gillespie et al. 1992). In addition, no influence of the tire-inflation pressure on rutting was observed. CYRCLY, software that considers shear contact stresses and friction between layers, was used to observe that FG-WBT produced between 15 and 40% higher critical strain (Perdomo and Nokes 1993). The relevance of the shear contact stresses was highlighted in the study.

A continuum-based finite-layer method was used to show that for FG-WBT traveling at high speed, the transverse tensile strain was more critical when predicting fatigue life (Siddharthan et al. 1998). The study also mentioned the importance of non-uniform three-dimensional contact stresses. ABAQUS was used to conclude that the contact stresses between the tire and the pavement did not depend on the material of the layer in contact with the tire (Myers et al. 1999). Once more, BISAR was used to highlight the importance of the lateral contact stresses and how they influenced the surface cracking and near-surface rutting. Finally, the software 3D-MOVE was utilized to evaluate the shape of the contact area for different types of tires on the pavement

response (Siddharthan et al. 2002). FG-WBT with circular contact area provided the highest longitudinal strain at the bottom of AC and vertical strain on top of the subgrade. The study also found that lateral contact stresses were relevant only close to the surface.

The general purpose software ABAQUS has been continuously improved to address details in the modeling of the response of flexible pavements. The software was used to included viscoelastic material characteristics (Elseifi et al. 2006), dynamic analysis (Yoo and Al-Qadi 2007), three-dimensional contact stresses (Al-Qadi and Yoo 2007), continuous moving loading and layer interaction (Yoo et al. 2006), and nonlinear granular material (Al-Qadi et al. 2010; Kim et al. 2009). All these effects have been proven as relevant when evaluating the response on flexible pavements.

The impact NG-WBT on trucking operations has also been evaluated. The fuel economy improved when WBT is used. WBT reduced the rolling resistance coefficient to 0.005, which is translated in fuel efficiency of 10% higher than that of dual-tire assembly according to a fuel consumption model (Muster 2000). In addition, the combination of aerodynamic devices and WBT improved the fuel economy by 18% for a truck traveling on a highway at 65 mph according to field testing (Bachman et al. 2005). Moreover, through collection of data from hauling companies, the use of WBT translated into fuel savings between 3.5 and 12% (Genivar 2005). More recently, the improvement of fuel economy resulting from the use of NG-WBT was proven to be around 10% (Franzese et al. 2010).

Other benefits from using WBT have been reported. Since a WBT is lighter than dual-tire assembly, the hauling capacities of trucks equipped with WBT increases (Markstaller et al. 2000). WBT is easier to inspect, repair, and maintain (Genivar 2005); it uses less rubber material, and decreases materials to dispose (Environmental Protection Agency 2004). Furthermore, WBT has similar or slightly better performance than dual-tire assembly regarding safety and comfort (Markstaller et al. 2000).

WBT is more environmentally friendly than dual-tire assembly, and since the gas consumption is reduced with WBT, gas-emission also decreases. Moreover, since the amount of materials needed to produce a WBT is less than that for dual-tire assembly, the material disposed at the end of the life-cycle of the tire is less (Genivar 2005). It is also worth mentioning that WBT produces slightly less noise (Markstaller et al. 2000).

Details of the literature review are provided in Appendix A.

3. NUMERICAL MODELING

The current design method for flexible pavements is based on the structural response that uses inappropriate assumptions. Static analysis of multilayer elastic systems where the tire load is applied on a circular contact area under constant pressure equal to the tire inflation pressure does not accurately represent the actual problem of a flexible pavement subjected to truck loading. Furthermore, the interface between two layers is not characterized by a full continuity of stresses and strains.

Therefore, to accurately predict the response of the system composed by a flexible pavement subjected to moving load, a powerful tool able to capture its actual complex characteristics is needed. The research team will use the Finite Element Method (FEM), which is the foundation of the software ABAQUS and CAPA 3D. The FEM offers the capabilities needed to address, in a successful manner, the response of the mentioned system. This system is a multilayer viscoelastic structure, where there is no full continuity between layers. In addition, it is subjected to dynamic loading with three-dimensional nonuniform contact stresses.

3.1. THE FINITE ELEMENT METHOD

ABAQUS will be used for low-volume pavement response prediction, as this allows the use of nonlinear anisotropic granular material behavior; while *CAPA 3D will be used for the pavement response of high traffic volume pavements*. To ensure the compatibility of both approaches, linear elastic cases under static loading will be tested. Both software are expected to give the same results. This allows checking the validity of using both software in this study and developing a framework that shall be independent of the used software. Then the improvement will be applied to both software. Continuous checking and comparison between the two software is planned throughout the project.

Following is a description of each of the improvements that will be implemented in this study in the FEM and how the improvements compared to multilayer linear elastic analysis. In addition, a brief explanation of how each assumption of the simplified theory affects the response of the system is included.

3.1.1. Viscoelastic Asphalt Material

One of the main weaknesses of the conventional models to analyze flexible pavements is the assumption that asphalt behaves as a linear elastic material. It is well known that the mechanical response of AC depends not only on the rate of loading but also on the temperature, and that these characteristics cannot be captured by a linear elastic model. The effect of the viscoelastic nature of AC is even more important at high temperatures. The *viscoelastic characteristics of the AC will be used in this study* and will be further discussed under the section on Material Characterizations.

3.1.2. Dynamic Analysis

Three methodologies are usually used to describe the applied load in a flexible pavement: static, quasi-static, and dynamic. The static load does not change its magnitude or position during the analysis. On the other hand, in a quasi-static analysis, the load changes its position, but the inertial and damping forces are not considered. Finally, the dynamic analysis accounts not only

for the change in magnitude and position but also for the inertia and damping forces. The conventional analysis of flexible pavement assumes the applied load as static.

It is evident that the nature of moving loads, such as the ones applied by moving trucks, is dynamic. As a consequence, the assumption of static load is incorrect and hence results will be inaccurate. Quasi-static analysis underestimates the response of the pavement and therefore predicts a higher number of repetitions to failure than the pavement can actually withstand. Therefore, ***dynamic analysis will be used in this research to simulate actual loading.***

3.1.3. Three-dimensional Contact Stresses

Another inaccurate assumption used in the conventional analysis of pavements deals with the shape of the contact area and the magnitude and distribution of contact stresses. Currently, the design is based on circular contact area between the pavement and the tire. In addition, it is assumed that the contact stresses are applied only in the vertical direction and are equal to the tire inflation pressure.

Measurements of contact stresses showed that a tire actually applies three-dimensional stresses on pavement surfaces. The distribution of these contact stresses are far from being uniform and equal to the tire inflation pressure. In fact, the peak vertical contact stress can be between 50 and 70% higher than the tire inflation pressure. Hence, actual tire-pavement contact stress distributions greatly influence the response of flexible pavements close to the surface, and they diminish with depth. As a result, in order to obtain an accurate prediction of the distresses associated with the stresses and strains close to the surface (near-surface cracking and primary rutting), ***tire contact stresses in three dimensions will be included in the analysis using actual measured 3D stresses*** as presented in Section 3.3.

3.1.4. Continuous Moving Load

When the tire load is not considered static, two methodologies can be used to define the variation of the amplitude: impulsive loading (e.g. trapezoidal shape) and continuous moving loading. For the impulse assumption, the loading amplitude in the contact area is constant during each step, and it suddenly changes from one to zero for the next step. This method of loading underestimates the pavement response and the difference is increased as temperature increase. On the other hand, the continuous moving loading assumes that the amplitude linearly changes from the value in the current step to the new value in the next step. This allows for the consideration of the variation between the entrance and the exit of the tire, as measurements of tire contact stresses show. Hence, ***continuous moving load, which better simulates better vehicle loading, will be used in this modeling.***

3.1.5. Layer Interaction

Regarding the interaction between layers, it was already mentioned that the conventional analysis assumes full continuity of stresses and strains at layer interfaces. However, this is not a proper consideration, mainly at the interface between AC and granular materials. In addition, numerical modeling suggests that the characterization of the interface is relevant when evaluating the response of flexible pavements. The research team compared the simple friction model and the elastic stick model using FEM. The simple friction model assumes that the stresses along the interface are proportional to the normal stresses at the interface. On the other hand, the elastic stick model assumes a linear relationship between the shear force and the shear displacement up to a point where the interface “fails.” When the interface crosses this point, the behavior at the

interface is governed by the simple friction model. When comparing the FEM results with the experimental measurements, the research team found that simple friction model brings closer results in the case of WBT and stick friction model in the case of dual-tire assembly. The research team suggests the use of *elastic stick model at the interface between AC layers and simple friction model between other layers including AC-granular layer*.

3.1.6. Nonlinear Granular Material

Granular materials are usually assumed as linear in the conventional analysis of flexible pavements. This can be an acceptable assumption if the pavement structure is thick enough so that the stress levels transmitted to the granular layer are low. In this case, the response of the mentioned layer is close to that predicted by the linear behavior. However, if the AC thickness is relatively low, as in the case of low volume roads, the difference between the linear and nonlinear models becomes significant.

The research team will consider the granular material as linear elastic in the heavy traffic pavements and as a stress-dependent for low-volume roads. A user-defined material model, developed by the research team, that takes into account the cross-anisotropy and stress-dependence of the elastic properties of granular materials will be used in ABAQUS. The research team feels that this would be an appropriate tool to model the response of low-volume pavement subjected to a moving load.

As presented above, fully bonded multilayer elastic analysis using a static circular contact area with vertical uniform contact stresses is far from being the most appropriate methodology to predict the response of flexible pavements and most importantly incapable of predicting the impact of various tire characteristics on pavements. *This study will include the following features in its modeling to better predict pavement responses to be used in transfer functions: dynamic analysis, three-dimensional contact stresses, continuous moving load, viscoelastic asphalt material, nonlinear granular materials for low volume roads, and friction between layers.*

3.2. MATERIAL CHARACTERIZATION

Material characteristics are needed as inputs for pavement modeling. The following tests are suggested.

3.2.1. Complex (Dynamic) Modulus

The axial complex modulus is defined as the ration between sinusoidal axial loading and the resulting strain. On the other hand, dynamic modulus is given by the ratio between the amplitude of the applied sinusoidal strain and amplitude of the resulting strain (Kim 2009). The amplitude of the dynamic load is defined by a haversine pulse, and it is applied so that the deformation of the AC specimen is kept in the viscoelastic range. Time-temperature dependent dynamic modulus of AC is used by MEPDG to calculate critical response of the pavement structure (ARA 2004b).

The viscoelastic properties of AC will be measured using frequency-sweep dynamic modulus tests at various temperatures as described by AASHTO TP-62. The measured complex modulus data and constructed master curves will be used as the base of inter-conversion to other viscoelastic properties (relaxation modulus or creep compliance). Particularly, core specimens collected from the field, specimens prepared in the laboratory from field samples, and laboratory prepared-mix specimens will be tested. Figure 2 presents the experimental configuration of the

dynamic modulus test. As described by AASHTO TP-62, *the test will be performed at five temperatures (14, 40, 70, 100, and 130 °F), each temperature being tested at five frequencies (0.1, 0.5, 1, 2, 10, and 25 Hz).*



Figure 2. Dynamic modulus test set-up

3.2.2. Semi-Circular Beam (SCB)

SCB is a controlled displacement test usually performed at low temperature that is used to obtain measurements for fracture energy, fracture toughness, and stiffness. The applied load will generate a constant crack mouth opening displacement rate. The load-displacement variation will be plotted, and the work of fracture will be obtained as the area under this curve. The fracture energy will be calculated as the ratio between the work of fracture and the ligament area.

In order *to characterize the fracture behavior at low temperature of AC used in the field, the semi-circular beam (SCB) test will be performed.* The test will be applied to field cores, and samples prepared in the lab using both a mixture sampled in the field and one mixed in the lab. Figure 3 shows the set-up of the SCB test. SCB test will help to provide a failure criterion for low temperature cracking



Figure 3. SCB test configuration

3.2.3. Cross-Anisotropic Characterization of Granular Materials

In order to model the variation of the elastic properties of granular material with direction and stress level, *the procedure presented by AASHTO T307 will be followed*. In this test, a cyclic loading is applied to the specimen. This cyclic loading is composed of a period of loading and a period of unloading. This will allow the computation of the resilient deformation, which will be used to calculate the resilient modulus.

A total of 16 stress levels will be applied to the specimen: one for conditioning and 15 for the actual calculation. The magnitude of the confining pressure and applied cyclic axial load will depend on the type of granular material. The measured resilient moduli will be used to fit the generalized model adopted by MEPDG for unbound granular material. *The cross-anisotropic characterization will be done for granular material only.*

3.2.4. Volumetric Properties of Asphalt Mixtures

Volumetrics establish the relationship between mass and volume, and it can be used as indication of durability and performance. *In addition to basic properties and proportions of the mixture components, bulk specific gravity and theoretical maximum specific gravity are needed to determine all the volumetric properties of the mix* (Asphalt Institute 2007).

Bulk Specific Gravity (G_{mb}) will be obtained following AASHTO T166. In this procedure, three different weights of the compacted samples are recorded: the air-dry weight, submerged weight, and saturated surface-dry weight. The submerged weight is measured after the sample has been under water for at least three minutes. Based on these measurements, not only G_{mb} is obtained but also the percentage of water absorbed by volume.

AASHTO T209 will be used to find the theoretical Maximum Specific Gravity (G_{mm}). As described by the mentioned standard, the sample used to calculate G_{mm} is not compacted. Instead, the two-hour-aged mixture is broken down into particles of size 0.25 in or smaller. Once the mixture is broken down into small pieces, it will be weighted. After that, the sample will be covered with water, and it will be subjected to a vacuum in order to fill all the voids with water.

The explained procedure, as in the case of dynamic modulus test, will be applied to field and laboratory prepared-mix samples.

3.3. TIRE CONTACT STRESS MEASUREMENTS

Accurate pavement response prediction can only be achieved using a modeling approach that simulates realistic tire-pavement interaction and allows incorporation of appropriate pavement material characteristics. It is evident from field measurements that tires induce non-uniform vertical and tangential shear stresses on the pavement surface. Because the complex 3D contact stresses increase the potential of various pavement damage mechanisms including top-down or “near-surface” cracking and AC rutting, *measured tire-pavement contact stresses will be used in the modeling*. Because tire-contact stress measurements are costly and time consuming, the contact stresses of two sets of tires will be measured: 445/50R22.5 (wide) and 275/80R22.5 (dual).

In this task, a database of 3D tire-pavement contact stresses for the tires *445/50R22.5 (wide) and 275/80R22.5 (dual)* will be developed in accordance with test plan presented in Table 1. The tires

will be provided by Michelin. However, other manufacturers will provide contact stresses for the same tire types. Contact stresses as measured by Michelin will be checked against the values obtained from this study using the Vehicle-Road Surface Pressure Transducer Array (VRSPTA) or Stress-In-Motion (SIM) (Figure 4) under Heavy Vehicle Simulator loading. If the difference between the measured tire contact stresses by Michelin and VRSPTA are small, contact stresses from other manufacturers will be adopted in the study. Otherwise, the VRSPTA data will be used in the study and the variation will be reported.

Table 1. Test Matrix for SIM testing in South Africa

Tire Type	Inflation Pressure (psi)	Tire Loading (kips)+			
NG-WBT and Dual	80	6	8	10	14
NG-WBT and Dual	100	6	8	10	14
NG-WBT and Dual	110	6	8	10	14
NG-WBT and Dual	125	6	8	10	14
Dual Only	60/110*	6	8	10	14
Dual Only	80/110*	6	8	10	14

Note: NG-WBT = New generation of wide-base tire (445/50R22.5); Dual = Dual-tire assembly (Conventional 2 x 275/80R22.5 tires, max. size to fit on HVS); + maximum load is 14kps per panel; * indicates pressure differential in dual tires.



Figure 4. Measurement of tire contact stress using SIM

Because the measurement of tire-pavement contact stresses is expensive and time-consuming, *a realistic 3D air-inflated tire model may be developed for additional simulations of tire-pavement interaction* (Figure 5). Because the tire industry does not make the exact material properties and structural design of tires available to the general public, a relatively simple but effective tire-pavement interaction model that shows the comparative interface stress distributions under various tire loading conditions will be developed and checked against the manufacturers' measured tire contact stresses. This model will be used to predict the tire-pavement contact stresses for conditions not tested at VRSPTA after being calibrated/validated for measured conditions.

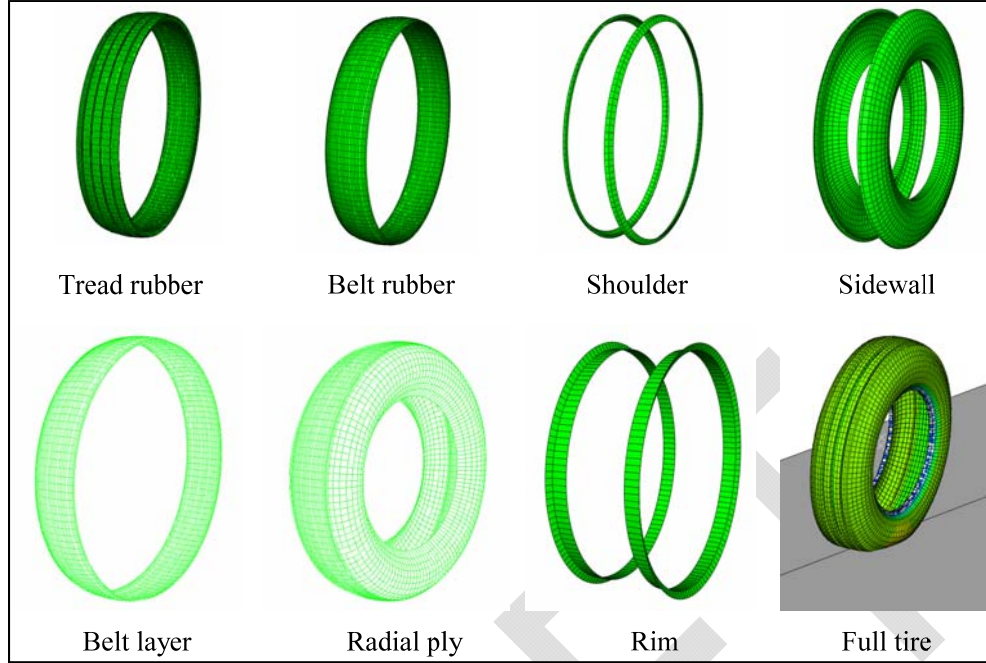


Figure 5. 3D air-inflated tire model for tire-pavement interaction simulation as developed by the research team

3.4. LOAD-DEFLECTION CURVES

As mentioned before, tire-pavement contact stresses are costly and time consuming. As a consequence, a 3D air-inflated tire model will be used to predict the contact stresses for the tire inflation pressure and load that will not be tested. However, in order to guarantee the accuracy of the predictions, the model needs to be calibrated/validated not only with the measured contact stresses, but also with the load-deflection curves of each testing scenario. In other words, ***a load-deflection curve will be measured for each tire type and tire inflation pressure presented in Table 1.*** Measured and predicted contact stresses will form a complete and accurate loading input for the various scenarios of FE analysis.

4. VALIDATION OF NUMERICAL MODELING

4.1. PROPOSED PAVEMENT STRUCTURES

4.1.1. Pavement Sections at UIUC

The pavement section(s) at UIUC will consist of a granular base layer on top of a subgrade at an approximately 6% CBR. The thickness of the base layer will be determined at the project technical panel meeting on October 26. The AC layer thickness will also be determined at that meeting. Strain gauges will be installed at the bottom of the AC layer in both traffic direction and perpendicular to that direction. Pressure cells will be installed at the bottom of the granular base layer.

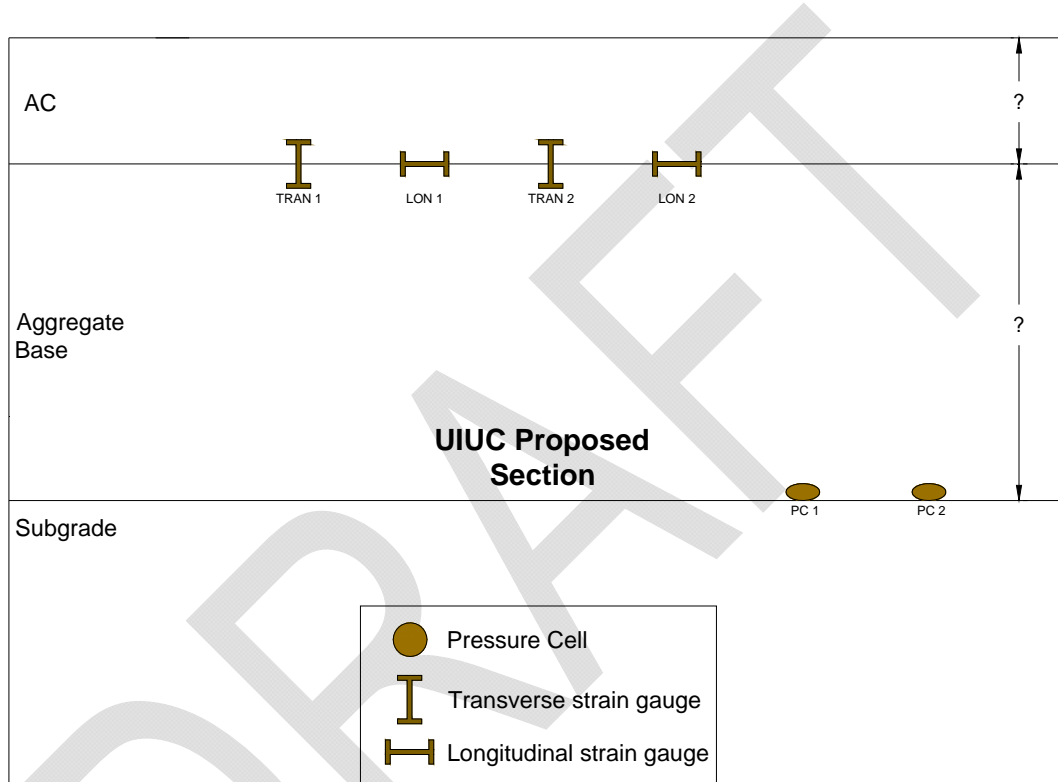


Figure 6. Plan and profile view of possible pavement structure and instrumentation of proposed section at UIUC

4.1.2. New Test Sections in UC-Davis

Pavement structures using high amounts of recycled asphalt pavement will be built and instrumented in UC-Davis. Six test sections, 165 ft-long and 16.4 ft-wide, will use various 16in of granular base layer on top of clayey subgrade. 5in of granular recycled asphalt layer will be placed on top of the base layer, and overlaid with 2in AC wearing surface.

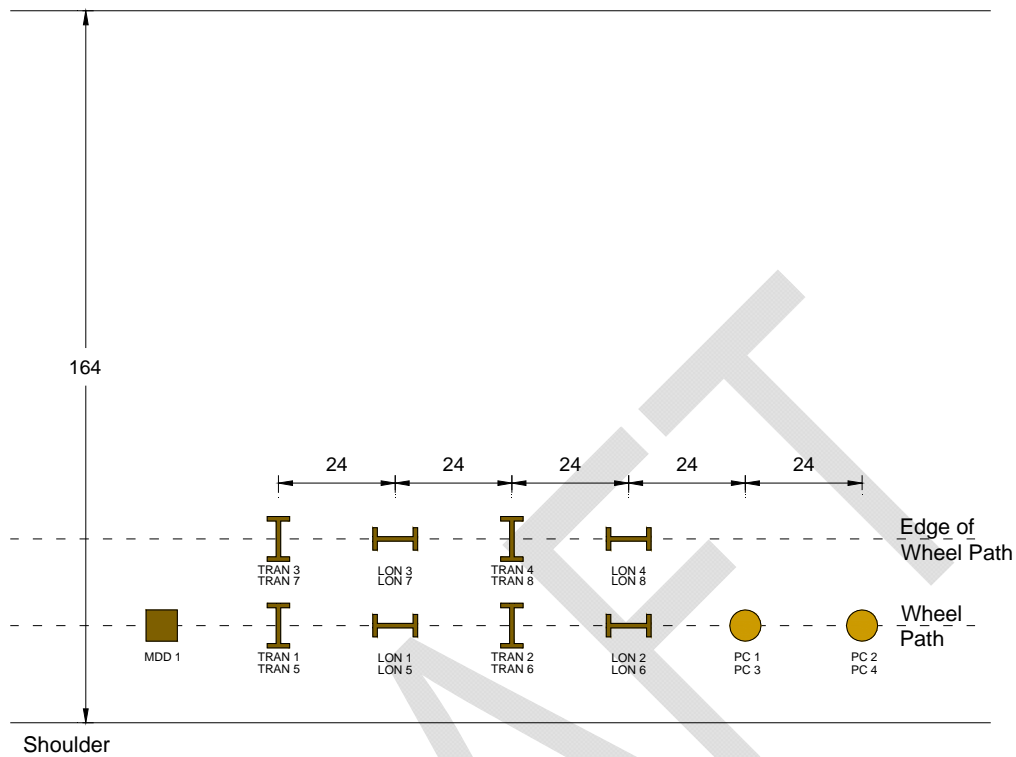
The instrumentation will include strain gauges in both directions under the AC layer lifts; they will be located at the middle and at the edge of the wheel path. Two pressure cells will also be installed at the bottom of the recycled granular layer and the AC wearing surface layer. A multidepth deflectometer will complement the instrumentation, in order to measure the deflection at different depths in the pavement structure. Figure 7 presents details regarding the typical pavement structure and instrumentation of the section proposed by UC-Davis.

4.1.3. New Test Sections in Florida

The AC layers to be built and instrumented by Florida DOT will be supported by 10.5 in of limerock base and 12 in of natural subgrade mixed with limerock. The thickness of the AC layers will be 4 and 6 in. A set of 6 strain gauges (three longitudinal and three transverse) will be installed at the bottom of the AC layer. Furthermore, the strain on the surface of the pavement will be measured using foil gauges installed at different offsets (between 0 and 15 in with a separation of 3 in). Stresses will also be measured using pressure cells installed at the bottom of the AC layer. However, it is important to mention that the installation of pressure cells depends on the availability of test pits. Figure 8 shows the pavement structure for the case of 6-in AC layer and the instrumentation.

DRAFT

PLAN VIEW



PROFILE VIEW

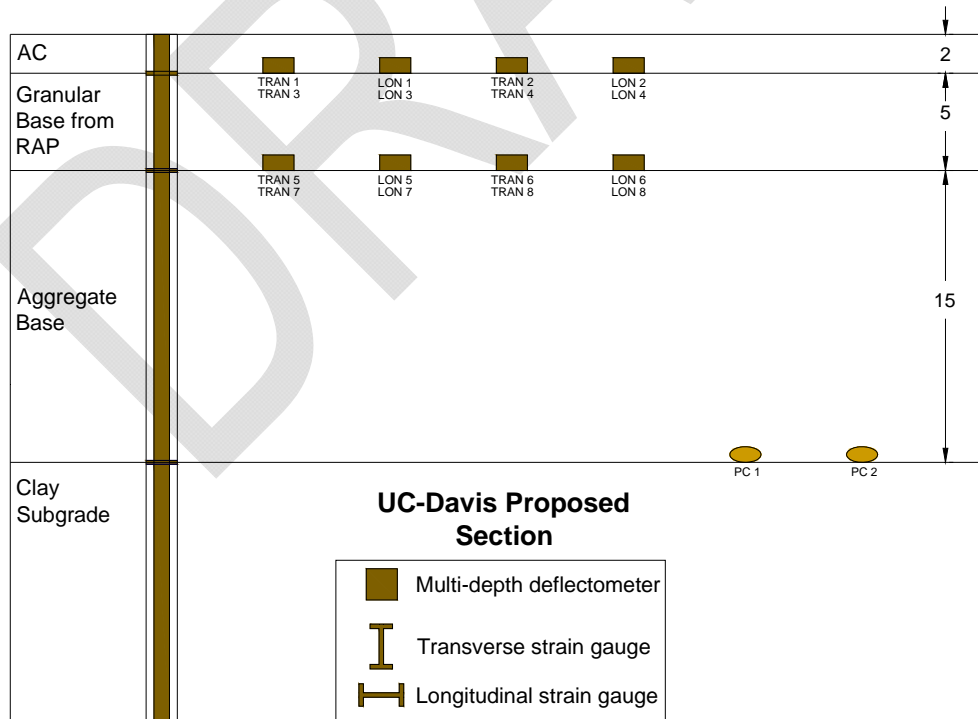


Figure 7. Plan and profile view of typical pavement structure and instrumentation of proposed section at UC-Davis

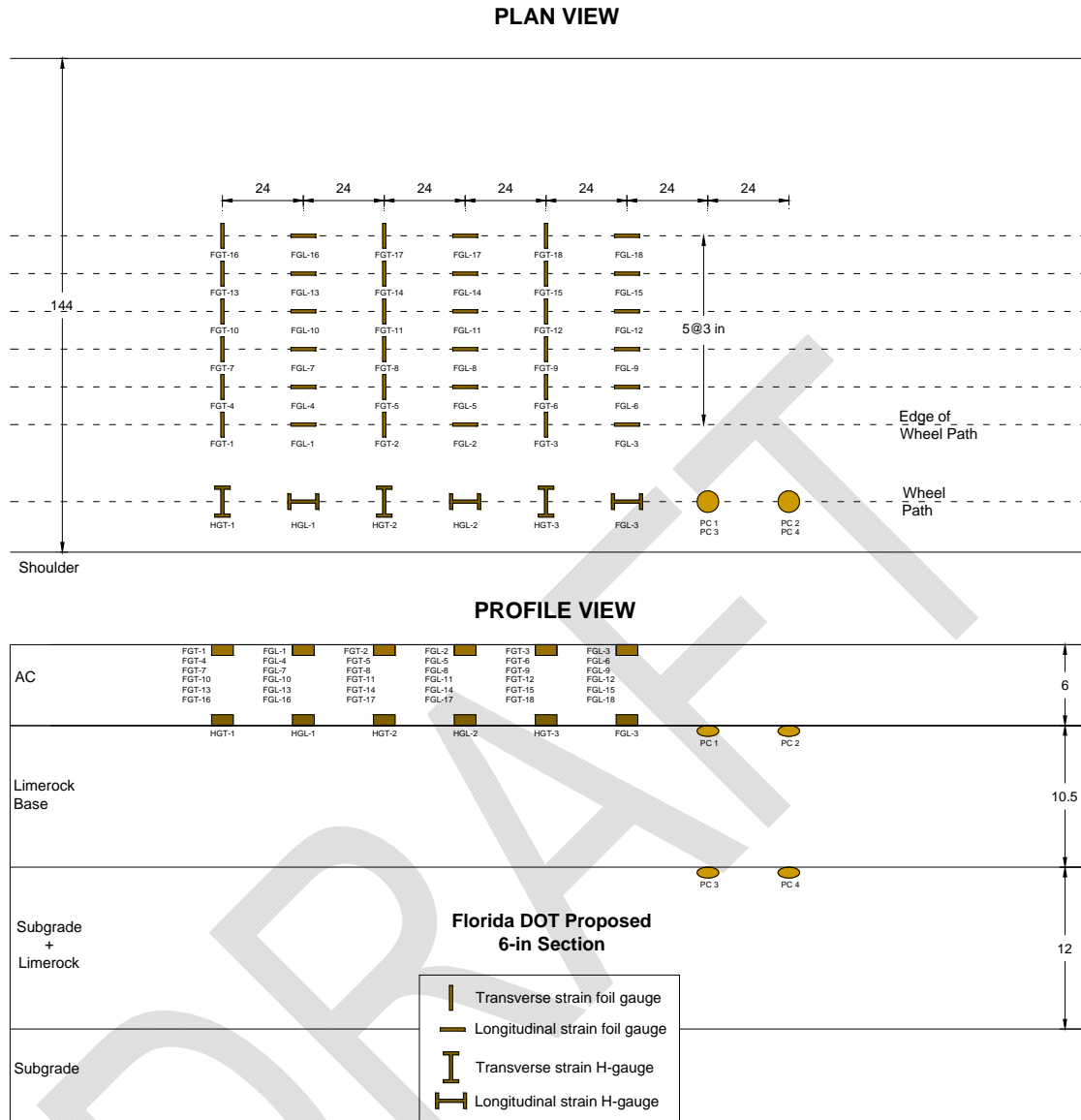


Figure 8. Plan and profile view of typical pavement structure and instrumentation of proposed section at Florida DOT

4.2. OVERVIEW OF AVAILABLE DATA

The research team has access to a wealth of databases that could be available to this project including data from the Virginia Smart Road, thin and full-depth pavement sections at UIUC-ATREL, Ohio SPS-8, UC-Davis, and Florida DOT.

4.2.1. Virginia Smart Road

The Smart Road is a full-scale research facility located in southwest Virginia. It is comprised of 12 different pavement sections that are instrumented with load and environment-associated sensors such as strain gauges, pressure cells, thermocouples, and time domain reflectometry probes.

The twelve pavement structures, labeled from Section A to Section L (see Figure B- 1to Figure B- 12, Appendix B), combined seven wearing surface mixes, one intermediate AC layer (BM-25.0) at various thicknesses, and a fine mix (SM-9.5A) underneath some sections. In addition, nine sections include an open-graded drainage layer (OGDL) with a thickness of 3 in, and ten sections have a 6 in-thick cement stabilized layer (21-A). Finally, a subbase layer (21-B) was placed on top of the subgrade; this layer has different thicknesses and may or may not comprise geosynthetic.

From Section A to Section D, the pavement structure is very similar: wearing surface with a thickness of 1.5in is placed over a 6 in-thick base layer on top of the OGDL. The thickness of the subbase (21-B) in these four sections is 7 in, which results in a total pavement thickness of 23.5 in. The differences between these sections is the type of wearing surface mix (SM-12.5D, SM-9.5D, SM-9.5E, SM-9.5A in accordance with the Virginia DOT specifications) and the presence of geosynthetic between the subbase and the subgrade in Sections B, C, and D.

Sections E, F, G, and H have the same wearing surface (SM-9.5D) and the same thickness for the cement stabilized base (21-A) as in the sections described in the previous paragraph. The BM-25.0 base layer is the same in Sections F and G (4 in-thick), but the thickness changes to 9 and 6 in in Section E and F, respectively. In addition, Sections E and F do not possess SM-9.5A base, while the thickness of this layer in sections G and H is 2 in. Out of these four sections, the only one that includes OGDL in its pavement structure is Section H, with a thickness of 3 in. The thickness of the 21-B subbase is 3 in in Sections E and H and 6 in in Sections F and G.

The remaining sections (Sections I, J, K, and L) have different wearing surfaces: SM-9.5A in Section I, SM-9.5D in Section J, OGFC+SM-9.5D in Section K, and SMA-12.5 in Section L. The OGDL layer in Sections K and L was stabilized with Portland cement; it has the same thickness (3 in). The thickness of the 21A base layer is the same in Sections I and L (6 in), and Sections J and K do not include this layer. Furthermore, the 21B subbase layer has two values of thickness in these sections, 6 in in Sections J and K, and 3 in in Sections I and L. The intermediate AC layer configuration varies for each section: 4 in with reinforcement mesh in Section I, 9 in in Section J, 9 in in Section K with stress relief geosynthetic, and 6 in with reinforcement mesh in Section L. The details of the pavement structure can be found in Figure B- 9 to Figure B- 12.

The described sections were heavily instrumented with load-associated and environmental sensors. The load-associated sensor included strain gauges and pressure cells; they were mainly placed at the bottom of each layer of the pavement structure. Furthermore, they were not only placed along the wheel path, but also at two different offset from the tire edge (20, and 40 in). The strain gauges were installed in the longitudinal and transverse directions, and some of them were placed with an inclination of 45° in the plan view. The location and distribution of sensors for each section are presented in Figure B- 1to Figure B- 12.

The testing using WBT was grouped in 22 conditions: Condition 1 to 14 were tested in May 2000, Condition 15 to 18 in November 2000, and Condition 19 to 22 in July 2001. Each of these 22 conditions is defined by the tire configuration, the magnitude of the axle load, and the speed of the truck. Condition 1 to 6 used dual-tire assembly in both axles; two of these conditions (3 and 4) used differential tire pressure. On the other hand, Conditions 7 to 14 used WBT. For the other two scenarios, November 2000 and July 2001, each axle of the tandem configuration combined WBT and dual-tire assembly. Conditions 15 and 16 used the first axle with dual-tire assembly and the second one with WBT, while in Condition 17 and 18 this configuration was inverted (first axle WBT and second with dual-tire assembly). Furthermore, the testing of the third scenario

used dual-tire assembly in the first axle and WBT in the second. It is worthwhile to mention that the inflation pressure of the WBT was kept constant and equal to 105 psi. Regarding the axle load, two different magnitudes were used in the 22 testing conditions: 17 kip in Conditions 1 to 4 and Conditions 11 to 22, and 8.5 kip in Conditions 5 to 10. Testing was also conducted at various speeds, 5 to 45 mph. Each test was performed at five different lateral positions.

4.2.2.UIUC-ATREL Thin Pavement Sections

Nine low-volume flexible pavement sections were constructed at the Advanced Transportation Engineering Laboratory (ATREL) of University of Illinois at Urbana-Champaign in order to evaluate and quantify the effect of geogrid in this type of pavement. Three base-layers with a thickness of 8, 12, and 18 in were built on top a subgrade whose CBR is 4%. In addition, two different thicknesses of AC layers (3 and 5 in) were constructed. See Figure C- 1to Figure C- 6 (Appendix C) for details related to pavement structure.

The load-associated instrumentation is comprised of strain gauges, pressure cells, and LVDTs. Longitudinal and transverse strain gauges were placed at the bottom of the AC layers, while the pressure cells were installed at the interface between the granular base and the subgrade. A total of 12 strain gauges and 18 pressure cells (2 per section) were placed. Each cell has 4 strain gauges, three in the transverse direction and one in the longitudinal. A total of 49 LVDTs were used to measure deflection in three directions.

The Accelerated Testing Loading Assembly (ATLAS) was used to load the described sections. Dual-tire assembly and WBT were used at two different speeds (5 and 10 mph). In addition, three different offsets were used during testing. Inflation pressure was another factor accounted for in this study: cell A was tested with tires at 80 and 100 psi; while in the other cells an extra inflation pressure was added (110 psi). Finally, axle loads between 6 and 14 kips with an increment of 2 kips were tested. In addition to the response measurements, all the sections were tested until failure subjected to a dual-tire assembly with an axle load of 10 kips traveling at 5 mph and an inflation pressure of 100 psi.

4.2.3.UIUC-ATREL Full Depth Sections

Full depth pavements were also tested at ATREL-UIUC. Four pavement sections were built on top of lime modified subgrade with three different AC thicknesses: 6 in (Section F), 10 in (Section D), and 16.5 in (Section A and B). All sections have a 2 in-thick wearing surface: DG surface for section D, B, and F, and SMA for section A. Details of the sections are presented in Figure D- 1 and Figure D- 2 (Appendix D) schematics.

The instrumentation of this project is relatively simple. It is composed of three strain gauges in each section, for a total of 12. In each section, two strain gauges were placed in the transverse direction and the other one in the longitudinal direction. All the sensors were located at the bottom of the AC layer. The details are given in Figure D- 1 and Figure D- 2.

The accelerated pavement testing was carried out using ATLAS with three different tires: wide-base 455, wide-base 425, and 11R22.5 dual-tire assembly. In the case of WBT, the applied load varied between 6 and 14 kips with increments of 2 kips. On the other hand, the dual-tire assembly was loaded with three loadings: 6, 10, and 14 kips. Regarding the inflation pressure, the WBT were tested at 80, 100, and 110 psi. Differential pressure was also taken into account for the dual tire: The inflation pressure of one tire was fixed at 110 psi, and it was varied for the other between 30 and 110 psi with an increment of 20 psi.

4.2.4. Ohio SPS-8 Sections

Two pavement structures were built in Ohio to validate the existing rutting models. Each pavement structure is composed of an AC layer built on top of 6 in of dense-graded aggregate base. The thickness of each AC layer is 4 and 8 in.

The thin section was instrumented with 12 strain gauges: six close to the pavement surface and the other six at the bottom of the AC layer. Out of these six sensors at each location, three measured longitudinal strain and three measured transverse strains. The strain gauges were distributed in a similar manner in the thick section; however, three additional strain gauges were installed at the middle of the AC layer, for a total of 15 gauges. Furthermore, eight Canadian strain gauges were also placed: four close to the surface and four at the bottom of the AC (two longitudinal and two transverse). In addition, a total of eight rosettes, four in each section, were placed. Details of the pavement structure and instrumentation are presented in Figure E- 1 to Figure E- 2 (appendix E).

The testing program consisted of four different tires (WBT 66R22.5, WBT 45R22.5, Dual-tire assembly 75R22.5, and Dual-tire assembly 80R22.5) inflated at three different pressures (70, 100, and 120 psi). Each tire at each inflation pressure was tested at three different speeds (5, 25, and 55 mph). The load applied by each tire varied according to the type of tire: 9.65 kip for WBTs, 4.2 kip for dual-tire assembly 75R22.5, and 5.05 kip for dual-tire assembly 80R22.5, respectively.

4.2.5. UC-Davis Permanent Deformation Profiles

To evaluate the rutting performance of two types of overlays, accelerated pavement testing at high temperature was performed at the University of California at Davis (UC-Davis). The overlays were placed on existing flexible pavements.

Two types of overlay mixes were used: asphalt-rubber hot-mix gap-graded (ARHM-GG) and dense-graded asphalt concrete (DGAC). In addition, two design thicknesses were used for each overlay: 1.5 and 2.5 in for the case of ARGH-GG, and 2.5 and 3 in for DGAC. The existing flexible pavement was composed of two types of structures: 6 in of AC layer placed on top of 3 in of asphalt treated permeable base (ATPB) on untreated base with a thickness of 10.8 in, while the thickness of the aggregate subbase was 9 in. The details of the pavement structures are illustrated in Figure F- 1 (Appendix F). The permanent deformation profile was measured using laser profilometer at 16 locations in each section.

Four kinds of tires were used in the accelerated pavement testing (each applied to a different pavement section): bias-ply dual (Goodyear 10.00-20), radial duals (Goodyear G159A, 11R22.5), WBT (Goodyear G286, 425/65R22.5), and aircraft single (BF Goodrich TSO C62C, 46x16). The target temperature for the testing was 122°F at 2 in under the surface of the pavement. For all the tires, but aircraft single, the applied load was 9 kip. In the case of bias-ply duals, the tire inflation pressure was 90 psi; while for radial duals it was 105 psi. Regarding WBT, the mentioned pressure was 110 psi. The single aircraft tire transmitted a load of 44.8 kip to the pavement, and its tire inflation pressure was 150 psi.

4.2.6. Florida DOT

Five-inch full depth flexible pavement was instrumented by the Florida Department of Transportation (FL-DOT) with longitudinal and transverse strain gauges on the surface of the pavement.

The pavement structure is composed of 5.1 in of AC placed on top of 10.5 in of limerock base. Under the base, a 12 in granular subbase was placed on top of the subgrade. The instrumentation of this pavement section is composed of 12 strain gauges placed on the surface in three locations. For each location, one of the sensor lines was on the wheel path (middle of the dual tires) and the other two were located 2 and 5 in from the dual-tire assembly edge.

Four types of tire were used during the testing program: dual (Goodyear Unisteel G149 RSA, 11R22.5), WBT (Goodyear G286 A SS, 425/65R22.5), WBT-445 (Michelin X One XDA-HT Plus, 445/50R22.5), and WBT-455 (Michelin X One XDA-HT Plus, 455/55R22.5). The load applied to each tire was 12 kip, and the speed of the moving load was 2 and 5 mph. In addition, the temperature of the pave was $78\pm 2^{\circ}\text{F}$. A total of five deformation profiles were measured for each combination of tire and speed.

4.3. TESTING PROGRAM

The testing program is intended to cover the most common and representative scenarios that an APT configuration allows. The objective is to measure the pavements' responses to specific loading configurations including axle loading, tire pressure, and tire type. Stresses and strains at certain locations in the pavement sections will be measured with appropriate instrumentation. It is important to recall that the instrumented pavement sections are located in different geographic areas.

4.3.1. Accelerated Pavement Testing

The accelerated pavement testing will be performed at a speed of 5 mph. 100 cycles are proposed to be run on each of the proposed pavement structures. In addition, the same tire type, applied load, and tire inflation pressure as the ones used to measure the tire-pavement contact stresses will be used during APT (see Table 1). The loading will start with the lowest load and lowest tire pressure and then increase the tire pressure for each load.

4.3.2. Pavement Response

The pavement response of the APT pavement sections will be measured using in-situ instrumentation. The instrumentation includes strain gauges and pressure cells. The pavement responses will be used to calibrate and validate the numerical models. The instrumentation will be installed at critical location including, but not limited to, strain gauges at the bottom of the AC layer and pressure cells on top of the granular layer and possibly on top of subgrade. Redundancy and reliability of instrumentation will be considered.

5. EVALUATION OF PAVEMENT DAMAGE

The pavement damage caused by WBT will be evaluated using the transfer functions recommended by the mechanistic-empirical pavement design guide (ARA 2004a). Five distresses will be considered when evaluating pavement damage: fatigue cracking, including bottom-up cracking and surface/near surface cracking (caused by surface tensile and shear strains), AC rutting, and subgrade rutting. Each one of these distresses is related to a variable of the pavement response through a transfer function.

5.1. FATIGUE CRACKING (BOTTOM-UP AND TOP-DOWN)

Fatigue cracking is mainly caused by the effect of repeated loading on the tensile strain at the bottom of the AC layer in thin AC pavements. Traffic loading bends the pavement structure, generating tensile strains and stresses that create cracks at the bottom of the AC and then propagate to the surface (ARA 2004a).

In opposition to bottom-up cracking, top-down fatigue cracking generates at the surface (or near surface) of the pavement and propagates downwards. It is believed that top-down cracking is caused by load-associated tensile strains and stresses on the surface of the pavement, shear stresses close to the edge of the tire, and over-aging of the AC (ARA 2004a). In addition, shear stresses in the upper part of the AC pavements can cause near surface cracking.

The formula recommended by MEPDG to calculate the number of repetition to fatigue cracking and that will be used in this project is the following:

$$N_f = 0.00432 \cdot k'_1 \cdot C \cdot \left(\frac{1}{\varepsilon_t}\right)^{3.942} \left(\frac{1}{E}\right)^{0.854} \quad (1)$$

$$C = 10^M \quad (2)$$

$$M = 4.84 \left(\frac{V_b}{V_a + V_b} - 0.69 \right) \quad (3)$$

where: N_f = number of repetitions to fatigue cracking;

ε_t = tensile strain at the critical location;

E = stiffness of the material;

C = laboratory to field adjustment factor;

V_b = effective binder content (%); and

V_a = air voids (%).

The value of the parameter k'_1 depends on the type of distress. For bottom-up cracking:

$$k'_1 = \frac{1}{0.000398 + \frac{0.003601}{1 + e^{11.02 - 3.49h_{ac}}}} \quad (4)$$

And for top-down cracking:

$$k'_1 = \frac{1}{0.01 + \frac{12.00}{1 + e^{15.676 - 2.8186h_{ac}}}} \quad (5)$$

where: h_{ac} = total thickness of the asphalt layer.

Even though the formula for top-down cracking is based on tensile strain on the surface, it will be also used the maximum shear strain in the AC instead of the tensile strain on the surface. This will take into account the effect of shear strain.

5.2. AC RUTTING

AC rutting is defined as permanent deformation (inelastic or plastic) that results from densification or compression, or lateral movement of the AC (ARA 2004a). MEPDG offers two expressions to evaluate rutting. The first one is based on laboratory repeated load test, and it is given by the following:

$$\frac{\varepsilon_p}{\varepsilon_r} = 10^{-3.15552T^{1.734}N^{0.39937}} \quad (6)$$

where: ε_p = accumulated plastic strain at N repetitions of load;

ε_r = resilient strain of asphalt material;

N = number of load repetitions; and

T = temperature (°F).

The second expression is based on national field calibration:

$$\frac{\varepsilon_p}{\varepsilon_r} = k_1 \cdot 10^{-3.4488T^{1.5606}N^{0.479244}} \quad (7)$$

$$k_1 = (C_1 + C_2 \cdot \text{depth}) \cdot 0.328196^{\text{depth}} \quad (8)$$

$$C_1 = -0.1039 \cdot h_{ac}^2 + 2.4868 \cdot h_{ac} - 17.342 \quad (9)$$

$$C_2 = 0.0172 \cdot h_{ac}^2 - 1.7331 \cdot h_{ac} + 27.428 \quad (10)$$

5.3. SUBGRADE RUTTING

Another type of rutting is observed when the elastic limit of the subgrade is exceeded; it is associated with the repetitive shear strain in the subgrade. The subgrade rutting will be evaluated using the expression recommended by the Asphalt Institute:

$$N_f = 1.365 \cdot 10^{-9} \varepsilon_v^{-4.477} \quad (11)$$

where: N_f = allowable load repetitions for subgrade rutting failure; and

ε_v = maximum vertical strain on top of the subgrade.

5.4. COMBINED DAMAGE RATIO

A total of five distresses will be considered in this study: i) bottom-up fatigue cracking; ii) top-down fatigue cracking caused by tensile strain on the surface; iii) top-down fatigue cracking caused by shear strain in AC layer; iv) AC rutting; and v) subgrade rutting. Each distress will allow the calculation of a damage ratio, which is defined as the quotient between number of repetitions to failure for reference load and the allowable number of repetitions for specific tire, or:

$$DR = \frac{N_{ref}}{N} \quad (12)$$

where: DR = damage ratio;

N_{ref} = allowable number of loading repetitions for a reference load; and

N = allowable number of load repetitions for specific load.

In order to combine the considered failure mechanisms, a logarithmic damage distribution factor will be used. Logarithmic distribution is chosen because the variables to be integrated spread over several orders of magnitude; as a result, linear transfer function becomes inappropriate. The expression that will be used to calculate the combined damage ratio is the following:

$$CDR = a_1 DR_{bu} + a_2 DR_{tds} + a_3 DR_{tdt} + a_4 DR_{rs} + a_5 DR_{rh} \quad (13)$$

$$a_i = \frac{\frac{1}{\log(N_i)}}{\sum_{j=1}^n \frac{1}{\log(N_j)}} \quad (14)$$

where: CDR = combined damage ratio;

DR_{bu} = damage ratio for bottom-up fatigue cracking;

DR_{tds} = damage ratio for top-down fatigue cracking caused by shear strain;
 DR_{tdt} = damage ratio for top-down fatigue cracking caused by tensile strain on surface;
 DR_{rs} = damage ratio for rutting in the subgrade;
 DR_{rh} = damage ratio for rutting in the AC; and
 n = total number of failure mechanisms considered (it depends on the road type).

DRAFT

6. USE OF MODELING RESULTS IN ANALYSIS TOOL

6.1. ARTIFICIAL NEURAL NETWORK (ANN) BASED PREDICTION MODEL FOR PAVEMENT DAMAGE BASED ON FINITE ELEMENT ANALYSES

To accurately assess the economic, safety and environmental effects of increased use of wide-base tires, the results of the measurement and modeling efforts to assess pavement damage in other sub-tasks must be incorporated into a calculation engine that will permit computation for economic and environmental analyses. This calculation engine must be robust, accurate, and rapid. The calculation engine must make use of the finite element (FE) model, and the limited number of tire/stress measurements and accelerated test sections to be used to validate the model. It cannot rely on the finite element analysis engine itself because of the computation time needed to perform accurate modeling.

In order to achieve this, a factorial of FE analysis cases will be developed to calculate the relative damage ratios between different tire configurations under various scenarios, such as different pavement structures, axle configurations, load and pressure levels (including extreme values), and environmental conditions. A soft computing model based on Artificial Neural Networks (ANN) will be developed to predict the relative damage ratios based on the factorial of FE analyses for low volume roads. The primary advantage of ANN is the ability to develop complex linear/non-linear models under minimum assumption about the underlying data distribution. Dataset obtained from the FE factorial will provide training for the ANN model in order to improve the accuracy of the output. The input layer in the ANN model will include the following:

- Loading factors (axle load and configuration, tire pressure, speed);
- Tire factors (tread width, tire contact length, aspect ratio, peak and average contact stress);
- Pavement factors (asphalt and base layers' characteristics and subgrade support); and
- Environmental factors (temperature).

6.2. LIFE CYCLE COST ANALYSIS RESULTS AND ENVIRONMENTAL LIFE CYCLE ASSESSMENT FRAMEWORK

6.2.1. Life Cycle Cost Analysis

An LCCA tool for agency costs and road user delay associated with pavement maintenance and rehabilitation exists in the FHWA software RealCost and its associated documentation. This software has been used by many states and has been further customized to facilitate more widespread use by states such as California (customized by the UCPRC for Caltrans). Guidelines for using RealCost to assess the change in life cycle cost (LCC) for a pavement structure due to increased use of WBT will be developed. The guidelines will be outlined as follows:

- Identify RealCost inputs and assumptions other than those identified here based on standard state practice.
- Calculate low volume road pavement damage for current traffic using ANN damage sub-module. Reconcile any differences between state assumptions and damage calculations. This is the control case.
- Calculate pavement damage for traffic with expected use of WBT.
- Run RealCost for the control case and WBT case following standard state practice and input values.
- Compare difference in LCC.

- *Conduct only simple comparison for dual-tire assembly and WBT for typical interstate highway design.*

Using this approach, this project will perform an assessment of the impacts of tire type on pavement's life and associated traffic delay impacts using RealCost for a factorial of typical U.S. scenarios, which will be documented as examples in the guidelines. The set of examples in the guidelines will be used to develop a decision tree that will permit users to assess the potential effect on LCC of WBT use. The study will primarily look at examples that will help the development of a framework and provide a first look at the effects of WBT on costs. RealCost has been used for factorial experiments of this type, such as an assessment of long-life pavement rehabilitation versus conventional rehabilitation performed for the California Department of Transportation.

This project will not provide a comprehensive evaluation covering a large number of cases that might occur due to project cost limitations.

6.2.2. Life Cycle Assessment (LCA)

To evaluate environmental effects, the most comprehensive and robust methodology appears to be the life cycle assessment (LCA) approach. The UCPRC has developed a framework for performing the LCA for pavement systems. The framework is shown in Figure 9. Based on the framework, and the critique from an industry/government/academia held in May, 2010, UCPRC has established a common practice for conducting LCA for pavements, which is laid out in the *UCPRC Pavement LCA Guideline*. The mentioned guideline will serve as high-level guidance for the LCA work for this project (the three documents in the Pavement LCA Guideline area available at <http://www.ucprc.ucdavis.edu/P-LCA/>).

The focus of the LCA for this project will be on energy use and greenhouse gas emissions.

The basic trade-offs in LCA for increased use of WBT will be between the increment in pavement damage which will cause more emissions from increased materials use and construction, and improved fuel economy in the Use phase. The energy savings from decreased tires produced and wasted will be considered based on calculations of tire use for current tires and WBT and tire LCA models available in the literature.

A literature survey was performed by UCPRC that focused on the energy consumption during the Use phase of pavement, because the deterioration of pavement will increase the vehicle rolling resistance and thus fuel consumption. This literature survey was incorporated into MIRIAM Project SP1 report. Previous studies have reached a consensus that for conventional vehicles, a 10% reduction in rolling resistance can lead to a 1% to 2% improvement in fuel economy, but the trade-offs between tire rolling resistance and other tire characteristics are sometimes significant. Lower rolling resistance can reduce wet traction. Less tread depth can reduce rolling resistance (lowering fuel expense), but this comes with the risk of higher lifetime tire expenses and increased waste generation. It is also concluded that that IRI (International Roughness Index) and MPD (Mean Profile Depth) are the two main factors in pavements that are currently identified to affect the vehicle fuel economy. Considering that rolling resistance is still a relatively small influence on fuel consumption, the major impact accumulates through traffic volumes.

The basic approach to be used for this project will involve analyzing the environmental impacts from the entire highway network as the ultimate goal; however, considering the various situations in the highway network, it will be inaccurate to create an "average" highway scenario for the entire network. Therefore, the approach for this project will follow these steps:

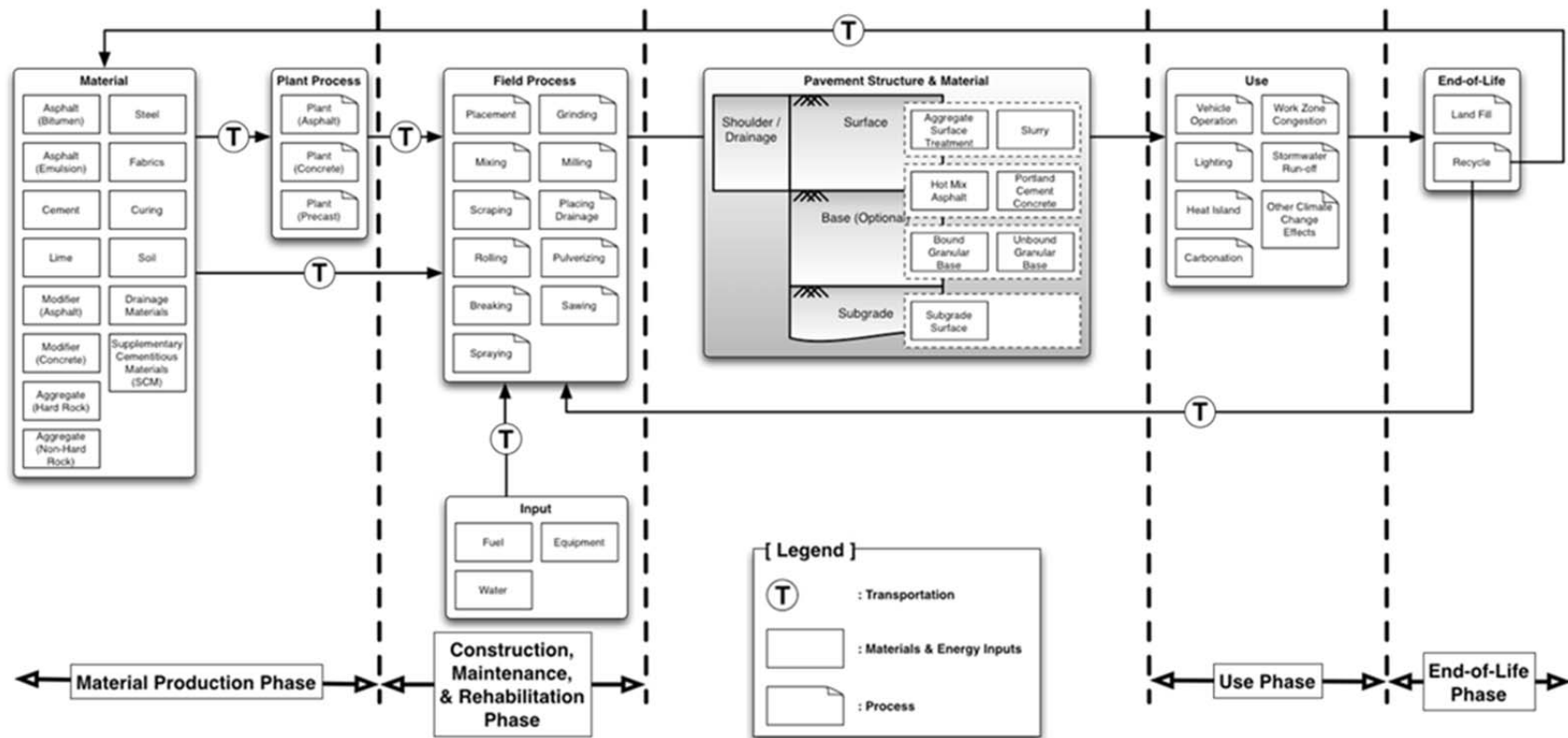


Figure 9. Proposed framework for pavement LCA¹

¹ The list in this figure is not intended to be comprehensive or exhaustive

- Divide the national highway network into categories based on a factorial analysis case design.
- For each category, perform a case study. Each case study includes all life cycle phases of a pavement segment.
- Apply results from the categorical case studies to the network with additional sensitivity analyses, including:
 - Range of smoothness or rolling resistance and surface characteristics: IRI, MPD, materials (including type, producing method, etc.);
 - Hauling distance;
 - Traffic levels and congestion;
 - Traffic closure during construction;
 - Fleet composition (new vehicle technologies);
 - Others.

Two main factors are considered in constructing the factorial analysis: traffic condition and pavement condition. Traffic condition includes road type, road gradient, road access type, and traffic level. These factors affect the final result from the traffic perspective. Pavement condition includes surface characteristics. The combination of these factorials constructs a 7-dimensional matrix, which bases the factorial analysis. These factorials and their possible values are explained as follows.

- Road type: urban road or rural road. This factor mostly affects the speed profile of vehicles. Studies have shown that vehicles running on an urban road and rural roads may represent different driving behaviors.
- Road access type: restricted access or unrestricted access. This factor affects the speed profile of vehicles. For restricted access, vehicles will not present a large speed fluctuation, while in unrestricted access, road vehicles could encounter frequent cycles of accelerate, decelerate, and stop. The effect from this factor is more significant for urban roads.
- Road grade: mountainous road or flat road. This factor affects the engine power because on mountainous roads, a vehicle's engine needs to overcome extra resistance when going uphill or saves energy when going downhill.
- Traffic level: a list of AADT and AADTT categories. This factor essentially determines how much fuel consumption the change in damage from use of WBT will cause.
- Pavement surface characteristics: a list of IRI and MPD categories based on predicted pavement damage. This factor affects the fuel consumption by changing the rolling resistance that the vehicle engine needs to overcome.
- Treatment: a list of pavement treatment options, such as overlay. This factor provides the options for possible rehabilitation and maintenance strategies when the condition of a road has reached a certain level. Each of these options includes a set of material production in the upstream, the construction process, and its effect on the pavement surface characteristics.

The factorial will initially be built around an initial factorial being analyzed for the California Department of Transportation. This factorial will be expanded to consider other national scenarios. Guidance from the Technical Panel will be needed to finalize the factorial, while remaining within budget for the project.

For each life cycle phase of a pavement segment, including material production, construction, use, maintenance and rehabilitation (M&R), and end-of-life treatment, the energy consumption

and pollutant emission will be assessed. Sensitivity analysis will be performed on variables with high uncertainty.

For the Construction phase, the basic principle of evaluating fuel use and emissions can be formulated as in the following equations:

$$Fuel\ use = \sum Fuel_factor * Activity * Population \quad (15)$$

$$Total\ Emission = \sum Emission_factor * Activity * Population \quad (16)$$

where *Fuel_factor* and *Emission_factor*: represents the fuel use factor and emission factor of pollutants (e.g., SO₂ or NO_x) of one type of equipment under unit amount of activity (such as an hour), respectively. *Activity* represents the amount of work (such as the total hours needed in this construction event); and *Population* represents the total number of this equipment.

A construction schedule analysis tool is used to model the equipment activities and equipment population needed during a construction event. The CA4PRS (Construction Analysis for Pavement Rehabilitation Strategies) model, licensed by FHWA to all states, will be used to achieve this goal. CA4PRS can quantify the total operation hours of construction equipment based on its schedule estimate output based on engine and operation information.

Figure 10 shows the procedures to be considered. First, the time progression of pavement surface characteristics of a road segment, which affects maintenance and rehabilitation scenarios, is generated from a pavement condition survey. With a rolling resistance model, the rolling resistance based on these surface characteristics can be calculated, and these rolling resistance values can be used to update the relevant parameters in a vehicle emission model. This vehicle emission model should be capable of analyzing the emission on a microscopic level, which is simulating the engine running status.

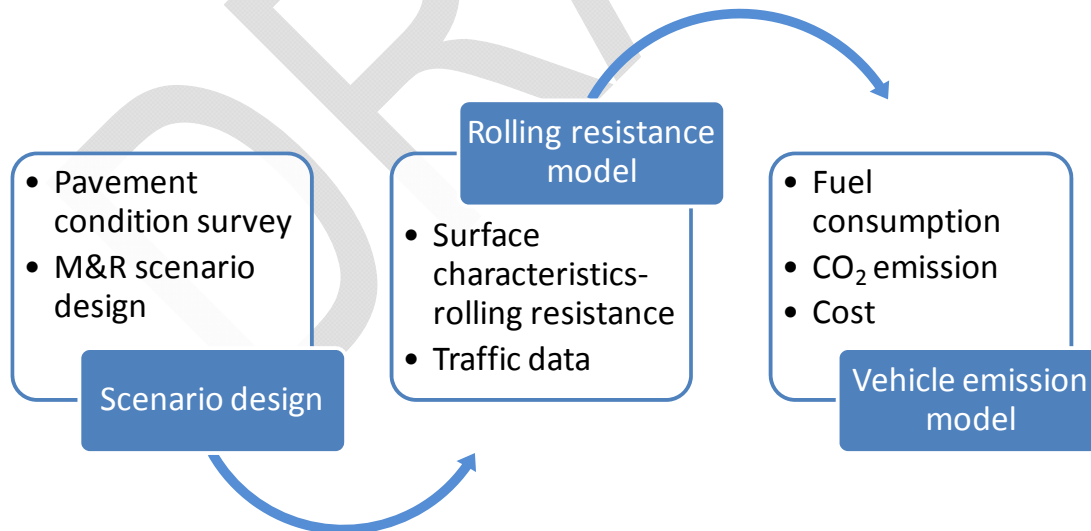


Figure 10. Procedure to address additional fuel consumption adopted by UCPRC.

Depending on the specific vehicle emission model, the method to update this rolling resistance parameter can be different. The traffic data on a road segment can be extracted from the traffic database. With the traffic data and rolling resistance parameter updated, the fuel consumption and emissions can be modeled through the vehicle emission model, and the net difference between

different M&R strategies can be evaluated. MOVES, (Motor Vehicle Emission Simulator) is the official highway vehicle emission model developed by U.S. Environmental Protection Agency (U.S. EPA), will be considered in this study.

A process and framework to analyze the environmental effects of a change to WBT will be developed in this project. The results of the sensitivity analysis will be organized into a look-up table for those agencies that do not want to perform their own analyses. In addition, available data and analysis will be summarized regarding the potential impacts of WBT use on safety. Other factors such as waste tire generation will be considered.

6.3. SUGGESTED OPTIONS FOR UTILIZATION OF MODELING RESULTS

As indicated earlier, the results of the FE models would be used to calculate a combined damage ratio for the various pavement-loading scenarios. The scenarios parameters include layer thicknesses, material properties of each layer, pavement structure, type of tire, applied load, and inflation pressure. The total number of cases can be divided by the number of possible pavement structures and loading cases.

Table 2 presents the total number of possible loading combinations. It is important to notice that at least 40 cases will be considered for each APT pavement testing section.

Table 2. Total number of loading combinations

	Wide Base Tire	Dual-Tire Assembly
Applied Load	4	4
Inflation Pressure	4	6
Loading Cases	16	24

In order to obtain results for all the cases in the FE matrix, considerably more time than the duration of the project will be required. In order to address this issue, three options are proposed for discussion at the panel meeting:

6.3.1. Consider Analysis of Full Factorial Pavement System

Table 3 shows the total number of possible pavement structures. As can be seen, the amount of cases to be run if all possible pavement structures are considered is extremely high (Table 3 excludes the loading configuration presented in Table 2)

Table 3. Possible structures for Interstate pavement design

Thick Pavement Structure		
	Different Materials	Thicknesses
Wearing Surface	3	2
Intermediate Layer	3	2
Binder Layer	3	2
Base Granular	3	3

Base Treated	3	3
Subbase Treated	3	3
Subbase Granular	3	3
Subgrade	3	--
Possible Combinations	4,251,528	
(with Loading Conf.)	102,036,672	

Advantages:

- A comprehensive set of pavement damaged values for multiple pavement structures will be obtained.
- No additional FE runs will be required

Disadvantages:

- Significant additional efforts (time and budget).

6.3.2. ANN on Specific Scenarios

Limit the scenarios for the application of ANN. In this case, selective type of pavements will be considered to build ANN. This approach will facilitate the prediction of combined damage of cases not analyzed with the FE for the selected type of pavement. Table 4 presents the total number of cases in the hypothetical scenario that the ANN is developed for the low volume road pavements.

Table 4. Total cases for low-volume road pavements

Thin Pavement Structure		
	Different Materials	Thicknesses
AC Layer	2	2
Base	3	2
Subgrade	3	--
Possible Combinations	72	
(with Loading Conf.)	1728	

Advantages:

- This approach and the final product can serve as a standard to be followed by future studies to expand it to other pavement sections.
- The panel can select a scenario with higher priority.

Disadvantages:

- Minimum changes to the timeline and budget of the research.

6.3.3. Postpone ANN for a Future Work

In this option the focus will be on conducting the pavement analysis and postpone the ANN work for a future study. If this alternative is adopted, a different approach will be suggested to present the outcomes of this research instead of the Analysis Tool.

Advantages:

- A future or independent study focused on ANN can cover all possible scenarios.
- Comprehensive analysis tool.

7. IMPLEMENTATION

A plan for implementing and disseminating the study's findings and results will include presentations at state and national levels, establishing a website to post online briefs, documents (after FHWA approval), and self-directed presentations, to target state transportation agencies, local government agencies, and other policy makers. The results of the project will be publicized through various road agency and trucking industry oriented publications and other communications (email updates, technical brief items in electronic updates, etc.). These will also be made available to technology transfer organizations in each interested state for further dissemination through their regular technology transmissions (electronic newsletters, mailbag items, etc.). Different versions of the information developed in the project will be targeted for audiences with different technical backgrounds and interests in the results. The research team will coordinate webinars for transportation agencies and engineers.

DRAFT

8. REFERENCES

- Akram, T., Scullion, T., Smith, R. E., Fernando, E. G. (1992). "Estimating Damage Effects of Dual Versus Wide Base Tires with Multidepth Deflectometers." *Transportation Research Record: Journal of the Transportation Research Board*, 1355, 59-66.
- Al-Qadi, I. L., Wang, H., Tutumluer, E. (2010). "Dynamic Analysis of Thin Asphalt Pavement by using Cross-Anisotropic Stress-Dependent Properties for Granular Layer." *Transportation Research Record: Journal of the Transportation Research Board*, 2154, 156-163.
- Al-Qadi, I. L., and Wang, H. (2009a). "Full-Depth Pavement Responses Under various Tire Configurations: Accelerated Pavement Testing and Finite Element Modeling." *Journal of the Association of Asphalt Paving Technologists*, 78, 645-680.
- Al-Qadi, I. L., and Wang, H. (2009b). *Evaluation of Pavement Damage due to New Tire Design*, Illinois Center for Transportation, Rantoul, IL.
- Al-Qadi, I. L., and Wang, H. (2009c). *Pavement Damage due to Different Tire and Loading Configurations on Secondary Roads*, NEXTRANS University Transportation Center, West Lafayette, Indiana.
- Al-Qadi, I. L., Wang, H., Yoo, P. J., Dessouky, S. H. (2008). "Dynamic Analysis and in-Situ Validation of Perpetual Pavement Response to Vehicular Loading." *Transportation Research Record: Journal of the Transportation Research Board*, 2087, 29-39.
- Al-Qadi, I. L., and Yoo, P. J. (2007). "Effect of Surface Tangential Contact Stresses on Flexible Pavement Response." *Journal of the Association of Asphalt Paving Technologists*, 76, 663-692.
- Al-Qadi, I. L., Elseifi, M. A., Yoo, P. J., Janajreh, I. (2005a). "Pavement Damage due to Conventional and New Generation of Wide-Base Super Single Tires." *Tire Science and Technology*, 33(4), 210-226.
- Al-Qadi, I. L., Yoo, P. J., Elseifi, M. A., Janajreh, I. (2005b). "Effects of Tire Configurations on Pavement Damage." *Journal of the Association of Asphalt Paving Technologists*, 84, 921-962.
- Al-Qadi, I. L., Elseifi, M. A., Yoo, P. J. (2004). *Pavement Damage due to Different Tires and Vehicle Configurations*, Virginia Tech Transportation Institute, Blacksburg, Virginia.
- Al-Qadi, I. L., Loulizi, A., Janajreh, I., Freeman, T. E. (2002). "Pavement Response to Dual Tires and New Wide-Base Tires at Same Tire Pressure." *Transportation Research Record: Journal of the Transportation Research Board*, 1806, 125-135.
- Ang-Olson, J., and Schroeder, W. (2002). "Energy Efficiency Strategies for Freight Trucking: Potential Impact on Fuel use and Greenhouse Gas Emissions." *Transportation Research Record: Journal of the Transportation Research Board*, 1815, 11-18.
- ARA, I. (2004a). *Guide for Mechanistic-Empirical Design of New and Rehabilitated Pavement Structures, Part 3: Design Analysis, Chapter 3: Design of New and Reconstructed Flexible Pavements*, NCHRP, Champaign, IL.
- ARA, I. (2004b). *Guide for Mechanistic-Empirical Design of New and Rehabilitated Pavement Structures, Part 2: Design Inputs; Chapter 2: Material Characterization*, NCHRP, Champaign, IL.
- Asphalt Institute. (2007). *The Asphalt Handbook*, 7th Ed., Asphalt Institute, Lexington, Kentucky.
- Bachman, L. J., Erb, A., Bynum, C. L. (2005). "Effect of Single Wide Tires and Trailer Aerodynamics on Fuel Economy and NOx Emissions of Class 8 Line-Haul Tractor-Trailers." *Society of Automotive Engineers*, 05VC(45), 1-9.

- Bonaquist, R. (1992). "An assessment of the increased damage potential of wide-base single tires." Proc., 7th International Conference on Asphalt Pavements, International Society for Asphalt Pavements, Lino Lake, Minnesota, 1-16.
- COST 334. (2001). Effects of Wide Single Tires and Dual Tires, Final Report of the Action European Cooperation in the Field of Scientific and Technical Research, Brussels, Belgium.
- Elseifi, M. A., Al-Qadi, I. L., Yoo, P. J. (2006). "Viscoelastic Modeling and Field Validation of Flexible Pavements." *Journal of Engineering Mechanics*, 132(2), 172-178.
- Elseifi, M. A., Al-Qadi, I. L., Yoo, P. J., Janajreh, I. (2005). "Quantification of Pavement Damage Caused by Dual and Wide-Base Tires." *Transportation Research Record: Journal of the Transportation Research Board*, 1940, 125-135.
- Emmanuel, G. F., Dilip, M., Dae-Wook, P., Wenting, L. (2006). Evaluation of Effects of Tire Size and Inflation Pressure on Tire Contact Stresses and Pavement Response, Texas Transportation Institute, College Station, Texas.
- Environmental Protection Agency. (2004). A Glance at Clean Freight Strategies: Single Wide-Base Tires, .
- Franzese, O., Knee, H. E., Slezak, L. (2010). "Effect of Wide-Base Single Tires on Fuel Efficiency of Class 8 Combination Trucks." *Transportation Research Record: Journal of the Transportation Research Board*, 2191, 1-7.
- Genivar. (2005). Economic Study: Use of Supersingle Tires by Heavy Vehicles Operating in Québec, GENIVAR Consulting Groups, Montreal, QC.
- Gillespie, T. D., Karamihas, S. M., Sayers, M. W., Nasim, M. A., Hansen, W., Ehsan, N., Cebon, D. (1992). Effect of Heavy-Vehicle Characteristics on Pavement Response and Performance, Transportation Research Board, Washington, D.C.
- Greene, J., Toros, U., Kim, S., Byron, T., Choubane, B. (2009). Impact of Wide-Base Single Tires on Pavement Damage, Florida Department of Transportation, .
- Hallin, J. P., Sharma, J., Mhoney, J. P. (1983). "Development of Rigid and Flexible Pavement Load Equivalency Factors for various Widths of Single Tires." *TRB*, 949, 4-13.
- Harvey, J., and Popescu, L. (2000). "Accelerated Pavement Testing of Rutting Performance of Two CALTRANS Overlay Strategies." *Transportation Research Record: Journal of the Transportation Research Board*, 1716, 116-125.
- Huhtala, M., Philajamaki, J., Pienimaki, M. (1989). "Effects of Tires and Tire Pressures on Road Pavements." *Transportation Research Record: Journal of the Transportation Research Board*, 1227, 107-114.
- Huhtala, M. (1986). "The effect of different trucks on road pavements." Proc., International Symposium on Heavy Vehicle Weights and Dimensions, Kelowna, British Columbia.
- Kim, D., Salgado, R., Altschaeffl, E. G. (2005). "Effects of Super-Single Tire Loadings on Pavements." *Journal of Transportation Engineering*, 131(10), 732-743.
- Kim, M., Tutumluer, E., Kwon, J. (2009). "Nonlinear Pavement Foundation Modeling for Three-Dimensional Finite-Element Analysis of Flexible Pavements." *International Journal of Geomechanics - ASCE*, 9(5), 195-208.
- Kim, Y. R. (2009). Modeling of Asphalt Concrete, First Ed., McGraw-Hill, .
- Loulizi, A., Al-Qadi, I. L., Lahouar, S., Freeman, T. E. (2001). "Data Collection and Management of the Instrumented Smart Road Flexible Pavement Sections." *Transportation Research Record: Journal of the Transportation Research Board*, 1769(2668), 142-151.
- Markstaller, M., Pearson, A., Janajreh, I. (2000). "On vehicle testing of michelin new wide base tire." Proc., SAE International Conference, .
- Muster, T. (2000). Fuel Savings Potential and Costs Considerations for US Class 8 Heavy Duty Trucks through Resistance Reductions and Improved Propulsion Technologies Until 2020, Energy Laboratory Massachusetts Institute of Technology, Cambridge, Massachusetts.

- Myers, L. A., Roque, R., Ruth, B. E., Drakos, C. (1999). "Measurement of Contact Stresses for Different Truck Tire Types to Evaluate their Influence on Near-Surface Cracking and Rutting." *Transportation Research Record: Journal of the Transportation Research Board*, 1655, 175-184.
- Nylund, N. (2006). *Fuel Savings for Heavy-Duty Vehicles, Summary Report 2003-2005*, VTT, Helsinki, Finland.
- Perdomo, D., and Nokes, B. (1993). "Theoretical Analysis of the Effects of Wide-Base Tires on Flexible Pavements using CIRCLY." *Transportation Research Record: Journal of the Transportation Research Board*, 1388, 108-119.
- Pierre, P., Dore, G., Vagile, L. (2003). *Characterization and Evaluation of Tire-Roadway Interface Stresses*, Ministry of Transport, University of Laval, Quebec, Canada.
- Priest, A. L., and Timm, D. H. (2006). "Mechanistic Comparison of Wide-Base Single Versus Standard Dual Tire Configurations." *Transportation Research Record: Journal of the Transportation Research Board*, 1949(155), 163.
- Reisman, J. I. (1997). *Air Emissions from Scrap Tire Combustion*, Office of Air Quality and Standards, U.S. Environmental Protection Agency, .
- Sebaaly, P. E., and Tabatabaee, N. (1992). "Effect of Tire Parameters on Pavement Damage and Load-Equivalency Factors." *Journal of Transportation Engineering*, 118(6), 805-819.
- Sebaaly, P. E., and Tabatabaee, N. (1989). "Effect of Tire Pressure and Type on Response of Flexible Pavement." *Transportation Research Record: Journal of the Transportation Research Board*, 1227, 115-127.
- Siddharthan, R. V., Krishnamenon, N., El-Mously, M., Sebaaly, P. E. (2002). "Investigation of Tire Contact Stress Distributions on Pavement Response." *Journal of Transportation Engineering*, 128(2), 136-144.
- Siddharthan, R. V., and Sebaaly, P. E. (1999). "Investigation of Asphalt Concrete Layer Strains from Wide-Base Tires." *Transportation Research Record: Journal of the Transportation Research Board*, 1655, 168-174.
- Siddharthan, R. V., Yao, J., Sebaaly, P. E. (1998). "Pavement Strain from Moving Dynamic 3D Load Distribution." *Journal of Engineering Mechanics*, 124(6), 557-566.
- Streit, D. A., Kulakowski, B. T., Sebaaly, P. E., Wollyung, R. J. (1998). *Road Simulator Study of Heavy Vehicle Wheel Forces*, Federal Highway Administration, U.S. Department of Transportation, Washington, D.C.
- Tielking, J. T. (1994). "Force Transmissibility of Heavy Truck Tires." *Tire Science and Technology*, 22(1), 60-74.
- Yoo, P. J., and Al-Qadi, I. L. (2007). "Effect of Transient Dynamic Loading on Flexible Pavements." *Transportation Research Record: Journal of the Transportation Research Board*, 1990, 129-140.
- Yoo, P. J., Al-Qadi, I. L., Elseifi, M. A., Janajreh, I. (2006). "Flexible Pavement Responses to Different Loading Amplitudes Considering Layer Interface Condition and Lateral Shear Forces." *International Journal of Pavement Engineering*, 7(1), 73-86.

9. APPENDIX A: DETAILED LITERATURE REVIEW

The wide-base tire (WBT) technology was introduced as an alternative for the truck and hauling industry to increase assets by reducing operational and energy costs. The wide-base tire (WBT) studies related to pavement infrastructure can be divided into two periods. The first period corresponds to the time between the appearances of the first generation of wide-base tires (FG-WBT) in the early 1980s until the end of the previous century, although WBT was introduced earlier than that date. In the year 2000, the new generation of wide-base tires (NG-WBT) entered the market, and a new era of research regarding WBT started and continues today.

9.1. IMPACT ON ROAD INFRASTRUCTURE

Most of the findings related to the effect of FG-WBT on the pavement structure generally agree with one fact: FG-WBT are more damaging than dual-tire assemblies. The studies included accelerated testing, modeling, and in-service pavement testing.

9.1.1. Accelerated Pavement Testing

In 1986, instrumented test sections in Finland were used to investigate the effect of different axle configurations and type of tires on pavements (Huhtala 1986). Strain gauges at the bottom of the asphalt concrete (AC) layer and pressure cells at the base-subbase and subbase-subgrade interface in thin pavements (2-in, 3-in, and 6-in-thick AC layers) were installed. Three axle configurations (single, tandem, and tridem) and three different types of tires (single, tandem, and WBT) were considered in the experimental program. Based on the measurements, fatigue curves were calculated for various axle configurations. It was concluded that WBT caused more damage to the pavement than the dual-tire assembly. Furthermore, the tridem axle with WBT produced an amount of damage similar to the tandem with dual-tire assembly. In addition, the difference between the damage caused by WBT and dual-tire assembly decreased as pavement depth increased. Additional test using the same experimental setting were reported in 1989 (Huhtala et al. 1989). In this part of the investigation, two dual-tire assembly (11-22.5 bias and 11R22.5) and WBT (385/65R22.5 and 350/75R22.5) with three applied loads (16, 20, and 24 kip) and three inflation pressures (the recommended by the manufacturer and $\pm 20\%$) were employed. Uneven load distribution in the dual-tire assembly was also considered. The study concluded that WBT caused more damage than dual-tire assembly: WBT caused between 2.3 and 4.0 times more damage than dual-tire assembly when using equal inflation pressure, and from 1.2 to 1.9 with uneven inflation pressure in the dual-tire assembly. The study also reported that the wider WBT (385/65R22.5) generated less damage than the 350/75R22.5.

Bonaquist (1992) presented results of accelerated pavement testing (APT) by the FHWA in Virginia. The aim of the experimental configuration was to compare a dual-tire assembly (11R22.5) with a WBT (425/65R22.5). Twelve flexible pavement sections were built and distributed in three lanes (four sections per lane). Two out of the three lanes were used for WBT testing: one for response analysis and the other one for performance analysis. Two different AC thicknesses (3.5 and 7 in) were constructed on top of 12.0 in-crushed aggregate. All the section were tested during three various seasons (spring, winter, summer), four loads (9.2, 12.1, 14.4, and 16.6 kip), and three tire inflation pressures (75.4, 103, and 139 psi). Horizontal strain at the bottom of AC, average vertical strain at different locations, and temperature profile were measured using strain gauges, differential deflectometer, and thermocouples, respectively. Six strain gauges per section were installed (three in traffic direction and three perpendicular to traffic direction). The differential deflectometers were located in the AC layer, crushed aggregate base,

and the top 6.0 in of the subgrade. For each combination of applied load and tire inflation pressure, the footprint area was recorded. The instrument measurements were used to predict the response for various loading at different temperatures and inflation pressures using multi-linear regression analysis. The study found that WBT produced greater horizontal strain and average vertical strain in all layers (the average vertical strain was defined as the difference between the deflection of two differential deflectometers and its separation). Moreover, for 12.5-kip-load and 104-psi-tire pressure, WBT produced between 3.5 and 4.3 times more fatigue damage than dual-tire assembly and between 1.1 and 1.5 more rutting, using the measured AC strain and the average vertical strain. In general, WBT produced more permanent deformation in all pavement layers (two times as much as dual-tire assembly) and lower fatigue life (25% of dual-tire assembly).

Instrumented flexible pavement sections subjected to traffic loads traveling at 40 mph at Pennsylvania State University test track were studied by Sebaaly and Tabatabaee (1992). The study focused on the pavement response and the load equivalent factor created by various tire inflation pressures, tire types, axle loads, and axle configurations. Surface deflection, strain, and temperature were measured in two flexible pavement sections: 6 in (thin) and 10 in (thick). In addition to single and tandem axles having different loads and tire inflation pressures, four different tires were analyzed: two dual-tire assembly (11R22.5 and 245/75R22.5) and two WBT (425/65R22.5 and 385/65R22.5). In the case of thin pavement, it was found that the damage caused by single WBTs is between 50 and 70% greater than the damage caused by a single-axle with dual-tire assembly 11R22.5. In general, WBT loading (at the same load and tire pressure) resulted in greater strain and deflection than dual-tire assembly. Also, the wider the WBT, the less the damage: 385/65R22.5 resulted in greater strain and deflection than 425/65R22.5.

A study focused on rutting performance of two overlay systems was presented by Harvey and Popescu (2000). The two overlays analyzed are dense-graded asphalt concrete (DGAC) and asphalt-rubber hot mix gap-graded (ARHM-GG). Accelerated pavement testing was performed at high temperatures (104°F and 122°F) with four different types of tires: bias ply (Goodyear 10.00-20), radial (Goodyear G159A, 11R22.5), WBT (Goodyear G286, 425/65R22.5), and aircraft (BF Goodrich TSO, 46x16). The measurement of the rut depth showed that the worst performance was resulted from the aircraft tire followed by the WBT for DGAC at 122°F. The WBT resulted in greater rutting when compared to dual/radial in ARHM-GG. The number of repetitions to rutting failure of WBT varied between 10 and 60% of the value for radial dual-tire assembly. As a general conclusion, the study reported that WBT increased the rutting in highways.

The effects of WBT as compared to a dual-tire assembly were also investigated by COST 334 in Europe (COST 334 2001). Seventeen different tire types were considered in the study, eight of them dual-tire assembly, and nine of them WBT. It is worth noting that the new generation of wide-base tires (NG-WBT) in this study refers to the 495/45R22.5, while the proposed NG-WBT in North America corresponds to 445/50R22.5 (2000), and subsequently the 455/55R22.5 (2002). This discrepancy is due to the difference in axle configurations and load regulations between Europe and North America. The following field pavement tests were conducted in the study:

- British TRL Pavement Test:

Testing at the British Pavement Testing Facility compared a conventional wide-base tire (385/45R22.5) at a load of 10 kip and a tire pressure of 145 psi to a NG-WBT (495/45R22.5) at a load of 10 kip and a tire pressure of 116 psi. Two pavement designs were considered; one with an AC thickness of 4 in, and the other with an AC thickness of 8 in. Pavement responses were measured for six tire types at several wheel loads and tire inflation pressures. The average rutting

ratio of the conventional WBT (385/65R22.5) relative to the new WBT (495/45R22.5), was 1.7 for the medium thickness pavement (8 in) and 1.5 for the thin pavement (4 in).

- Dutch Lintrack Pavement Test

Full scale accelerated pavement tests were conducted at the Dutch Lintrack for four different tire assemblies. Tests were conducted at four pavement sections with the same pavement design (thick pavement with 10.6 in AC layer). After the tests were completed on the first design, the two top layers of AC were changed with the same mix design, but using a stiffer binder. Pavement temperature was maintained at 104°F using infrared heaters. The study concluded that the average rutting ratio of the conventional WBT (385/65R22.5) to the conventional dual-tire assembly (315/80R22.5) ranged from 1.94 to 2.73, whereas the average rutting ratio of NG-WBT (495/45R22.5) to the conventional dual-tire assembly (315/80R22.5) varied between 1.32 and 1.34.

- French LCPC Pavement Test

The accelerated pavement testing of the Laboratoire Central des Ponts et Chaussées (LCPC) in France conducted a study on various tires and wheel load configurations to evaluate rutting and fatigue performance of flexible pavements. The experimental program was conducted on a very stiff pavement structure consisting of 3.2 in wearing surface, on top of a 16 in AC base layer, 16 in granular base, and 12 in coarse subbase on a sandy clay subgrade. Due to the very thick and stiff pavement structure, the measured longitudinal and transverse strain amplitudes were very low, between 10 and 20 microstrains at the bottom of the AC, and the vertical strains at the top of the granular base were 40 to 70 microstrains. To eliminate the influence of temperature variation in pavement responses, a second analysis was performed using linear elastic multilayer software, “Alize,” which was developed by the LCPC. After the model was successfully calibrated based on measured pavement responses, relative comparisons were made between the various tire configurations at a reference temperature of 59°F. For the WBT, the vertical and longitudinal strains induced by the conventional WBT (385/65R22.5) were very close to the responses exerted by the NG-WBT (495/45R22.5). In the case of dual-tire assembly, the 315/80R22.5 resulted in a 6.2% lower strain than the 95/60R22.5. This pattern of results could be attributed to the use of linear elastic theory, which does not consider nonuniform contact stresses or variation in the loading contact area. In addition, the impact of the tire contact area, uniformity, and pressure diminish with depth. Measurements in this study were taken at relatively deep locations within the pavements.

- Finnish Pavement Test

Accelerated pavement testing at the VTT Transportation Research Center in Finland measured pavement responses under two tire assemblies using pavement instrumentations. The primary objective of the study was to investigate the differences in dynamic loading between different tire types. A dual-tire assembly (315/70R22.5) and a WBT (495/45R22.5) were tested at inflation pressures of 110 and 130 psi, respectively. Testing was conducted at two different speeds (28 and 50 mph) on a pavement system consisting of 6 in of AC, 6 in crushed rock base, and 16 in granular subbase on sandy subgrade. Longitudinal strains at 50 mph indicated that the wide-base tire induced about 17% greater strain at the bottom of the AC than the dual-tire assembly. Vertical pressure at pavement interfaces indicated that the wide-base tire produces about 21% greater stresses on top of the base layer, and 14% greater stresses on top of the subbase layer than the dual-tire assembly, while vertical pressure on top of the subgrade were nearly equal between the tires.

Results of COST Action 334 (COST 334 2001) were formulated through the concept of tire configuration factor (TCF). The tire configuration factor is “a factor describing the pavement wear attributable to different tire types and sizes, when compared with an arbitrarily selected reference tire, at equal load” The selected reference tire with a TCF of 1.0 was the dual-tire assembly 295/80R22.5 under maximum recommended loading conditions. To evaluate the

damage of the new generation of wide-base tires used in North America (i.e., 445/50R22.5 and 455/55R22.5) to the most equivalent dual-tire assembly in the tractor drive position (275/80R22.5), the following model developed during the COST study was used:

$$TCF = \left(\frac{width}{470}\right)^{-1.68} \left(\frac{length}{198}\right)^{-0.85} (pres.ration)^{0.81}$$

where: TCF = tire configuration factor;

$width$ = contact area width;

$length$ = length of the contact area; and

$pres.ratio$ = pressure ratio compared to the manufacturer recommended pressure (i.e., 1.0 means inflated as recommended).

Similar models were developed for fatigue and subgrade rutting. A correction factor is also used to account for real-world operating conditions (i.e., possible imbalance in load distribution in case of dual-tire assemblies, roughness of the road, and dynamic effects). These correction factors were 1.01 and 0.97 for dual-tire assembly and WBT tires, respectively. Table 2 illustrates the calculation of the TCF for the dual-tire assembly and WBT. As presented in this table, NG-WBT would cause approximately the same primary rutting damage as a dual-tire assembly on primary roads. In secondary roads, a weighted average was used, which assumes 20% primary rutting, 40% secondary rutting, and 40% fatigue cracking. Surface-initiated top-down cracking was not considered in the study. Based on this distribution, the new generation of wide-base tires (445/50R22.5 and 455/55R22.5) would be 44% and 52% more damaging than the equivalent dual-tire assembly.

Table 2. Damage Ratios between the NG-WBT and a Dual-Tire Assembly Based on the COST TCF Models.

Tire Type	W (mm)	D (mm)	Primary Roads		Secondary Roads	
			TCF	Wide-base vs. dual	TCF	Wide-base vs. dual
Dual (275/80R22.5)	368	1054	1.52	NA	1.51	NA
Wide (445/50R22.5)	380	947	1.56	2.7%	2.29	52.4%
Wide (455/55R22.5)	380	998	1.47	-3.1%	2.17	44.1%

1 mm=0.0394 in

COST 334 also estimated the relative damage between the steering axle and a reference dual-tire assembly axle. Assuming the same axle load, the steering axle, on average, was three to four times as aggressive as the reference axle on primary roads, and five to eight times as aggressive as the reference axle on secondary roads. Nevertheless, even under smaller loads, it is still expected a steering axle with 20 kip on two single tires to be much more detrimental than the reference axle. This agrees with the findings of Smart Road studies by Al-Qadi and his coworkers with respect to the steering axle (Al-Qadi et al. 2004).

Major research was conducted at Virginia Tech to assess the pavement damage caused by different tire types and axle configurations (Al-Qadi et al. 2004; Al-Qadi et al. 2005a; Al-Qadi et

al. 2005b; Elseifi et al. 2005). Twelve pavement structures were built combining different types of wearing surfaces, intermediate layer with different thicknesses, asphalt layer under the intermediate layer, drainage layer, cement stabilized subbase, and subbase. In addition to sensor to determine moisture and frost penetration, each section was heavily instrumented with strain gauges, pressure cells, and thermocouples (Al-Qadi et al. 2004; Al-Qadi et al. 2005b). Four damage mechanisms were considered in this study: fatigue cracking, surface and subgrade rutting, and top-down cracking. Each of these mechanisms was linked to a pavement response by the use of transfer functions. The experimental program considered two types of tires: dual-tire assembly (275/80R22.5) and NG-WBT (445/50R22.5). The built sections were subjected to truck load during May and November 2000 and July 2001 with two load configurations: 17 and 8.5 kip per tandem axle. The speed of the moving load was 45 and 5 mph for both tires, and two different speeds were incorporated in May 2000 for WBT: 15 and 25 mph. During the other two testing sessions, the dual and WBT were combined in the tandem axle. In addition to the program described above, the dual-tire assembly was tested at three tire inflation pressures (80, 95, and 105 psi) and four speeds (5, 15, 25, and 45 mph). A third loading condition was introduced, in which barrier walls were not used (Loulizi et al. 2001). Dual-tire assembly was also tested at different axle loads, tire-inflation pressures, environmental conditions, and speeds.

This NG-WBT were compared with dual-tire assembly at Section A of the Virginia Smart Road test (Al-Qadi et al. 2002). The study highlights the differences between the NG-WBT and conventional WBT: NG-WBT has greater loading carry capacity, has lower contact stresses, and requires less inflation pressure to carry the same load. The experimental program subjected the pavement to truck load traveling at different speed (5, 15, 25, and 45 mph) and two values of tandem axle load (17 and 8.5 kip per axle). The whole testing program consisted of three sessions at different seasons: May 2000, November 2000, and July 2001. During the first test session (May 2000) and based on strain at the bottom of AC, NG-WBT produced almost the same fatigue damage as dual-tire assembly. Regarding vertical compressive stress, the difference between dual and NG-WBT decreases with depth, even though it is higher for NG-WBT near the surface. Similar results were obtained during November 2000 and July 2001.

The effect of different tire types has also been studied in Canada (Pierre et al. 2003). An experimental section with a thickness of 4 in was built in Laval University, Quebec, and it was instrumented to measure longitudinal and transverse strains at different levels as well as vertical strain. The strains near the surface were measured using a slab built and instrumented in the laboratory, and attached later to the pavement structure. Diverse testing scenarios were created based on tire type, applied load, and tire inflation pressure. Four tire types (11R22.5, 12R22.5, 385/65R22.5, and 455/55R22.5) moving at a speed of 30 mph, five loads (13.3, 17.6, 22.0, 26.4, and 30.9 kip per axle), and three inflation pressures (81, 106, and 130 psi) comprise the experimental program. It was found that at an inflation pressure of 106 psi, dual-tire assembly produce less strain at the base than the WBT, and 455/55R22.5 produced less strain than 385/65R22.5. In general, all tests showed that 385/65R22.5 is more damaging than the other tires. In addition, the strains created by 455/55R22.5 and dual-tire assembly at the pavement's base during summer are comparable in magnitude. This situation changes during spring, when strains from 455/55R22.5 were greater than dual-tire assembly. A similar trend is shown for fatigue cracking. On the other hand, when the tire inflation pressure was increased to 130 psi, 385/65R22.5 and 455/55R22.5 produced lower vertical strain than the dual-tire assembly. Regarding rutting, WBT gave a better performance; they produced less permanent strain than the other two type of dual tire assembly, with 455/55R22.5 giving the lowest values. Finally, the deflection produced by dual-tire assembly is less than WBT.

Dual and WBT were mechanically compared by NCAT in 2006 (Priest and Timm 2006). A pavement section 6.73 in-thick was subjected to accelerated pavement testing using two types of tires: 275/80R22.5 and 445/50R22.5. The mentioned section was instrumented with longitudinal and transverse strain gauges at the bottom of the AC layer and pressure cell on top of the base and subgrade. The readings from the instrumentation were compared to analytical results calculated using WESLEA. The study concluded that there is insignificant difference in the horizontal strain at the bottom of the AC layer and the stress on top of the subgrade between WBT and standard dual-tire assembly.

Dual and WBT have been also compared in pavements with different thicknesses regarding response and damage (Al-Qadi and Wang 2009a; Al-Qadi and Wang 2009b). Flexible pavement sections with thicknesses varying between 6 and 16.5 in were instrumented and tested at the Advanced Transportation Research Engineering Laboratory (ATREL) of University of Illinois at Urbana-Champaign. Thermocouples and strain gauges (two longitudinal and one transverse) were installed in order to monitor the response on the three types of pavement: interstate (16.5 in-thick), primary road (10 in-thick), local road (6 in-thick). These three types of pavements were subjected to moving load (5 and 10 mph) using conventional dual-tire assembly (11R22.5), NG-WBT (455/55R22.5) and FG-WBT (425/65R22.5). All tires were inflated at three different pressures (80, 100, and 110 psi). The applied load was varied between 6 and 14 kips, with 2 kips increments. Pressure differential in dual-tire assembly was also considered. The measurements showed that the lowest longitudinal strain at the bottom of the AC is created by dual-tire assembly. Also, WBT-425 presented a higher response than WBT 455 for all testing condition. As previously noted by other researchers, the difference between WBT and dual-tire assembly is relevant close to the surface, but it becomes negligible as the depth increases. As a general trend, a linear increment of the longitudinal strain with the applied load was seen, and this strain is not significantly affected by the inflation pressure. Based on the experimental measurements, it was possible to conclude that WBT-425 is the most damaging tire regarding fatigue cracking followed by WBT-455.

A similar study focused on the damage caused by dual-tire assembly and WBT-455 on roads with low traffic volume was conducted by Al-Qadi and Wang (Al-Qadi and Wang 2009c). Three sections having the same surface layer (3-in-thick) but different base thickness (8, 12, and 18 in) were instrumented and modeled. The instrumentation included strain gauges at bottom of AC, linear variable differential transformers in granular layer in three directions and subgrade in vertical direction, and thermocouples at different depths. The investigation found that, in opposition to the case interstate highway, WBT caused more damage to the low-traffic volume when compared to dual-tire assembly.

One additional study regarding WBT and pavement damage was presented in 2009 by Greene et al. (Greene et al. 2009). The focus of this project was to evaluate rutting prediction. Two types of pavement were subjected to accelerated loading until a rut depth of 0.5 in was reached. The two pavements differ from each other in the kind of surface used: dense graded and open graded. The load applied on each of the four tires considered (445/50R22.5, 455/55R22.5, 425/65R22.5, and 11R22.5) was 9.0 kips, at 122°F traveling at 8 mph with different offset. A numerical model was also developed using ADINA; this model did not include all the details given by other researchers (Al-Qadi et al. 2008; Yoo et al. 2006). It assumed constant vertical contact stresses, and elastic materials. The type of tire with the greatest number of passes to create 0.5 in rut-depth was the dual-tire assembly, while WBT-425 needed the least. In addition, WBT-455 required similar number of repetitions as dual-tire assembly on open-graded surface and slightly less on dense-graded. Based on the readings of two surface sensors installed 5 in from the edge of the tire, it was concluded that WBT-425 generated the highest transverse strain. WBT-455 produced the

lowest shear strain under the edge of the tire while the result for dual-tire assembly and WBT-445 were similar. Regarding tensile strain at the bottom of AC, WBT-445 generated slightly higher values, while WBT-455 and dual-tire assembly were similar. Finally, WBT-445 was found to be more damaging than dual-tire assembly and WBT-455; while WBT-455 and dual-tire assembly were similar. The numerical model proved that elastic material properties are not suitable to predict rutting.

9.1.2.Numerical Modeling and Analytical Methods

The influence of the tire-width on the equivalent loading factor was studied by Hallin et al. (1983) based on an analytical study. Flexible and rigid pavement subjected to dual-tire assembly and single tire-loading were analyzed using the finite element method (ILLI-SLAB for rigid pavement, developed by University of Illinois and PSAD2A from University of Berkeley). The width of the single tire was varied in a range that included WBT (from 10 to 18 in). In the case of rigid pavement, the applied load contact area was assumed rectangular with uniform contact pressure and located at four different points. Not only the width of the tire varied but also the contact pressure and the joint spacing. It was found that, for rigid pavement, the maximum tensile strain decreases as the width of the tire increases. On the other hand, the flexible pavement was assumed as composed by one elastic layer with the load applied through a circular contact area. The reported load equivalent factor was based on the average of two different contact-area assumptions: two circles with constant radius but different contact pressure and one circle. Fatigue analysis based on warping and load stresses (concrete pavement) and strain at the bottom the AC layer (flexible pavement) allowed the calculation of the equivalent loading factor. The authors showed a reduction of the difference in the equivalent loading factor as the tire width is increased for different values of AC thickness. Furthermore, in the case of rigid pavement, this difference is almost constant as the tire width changes from 10 to 18 in

A modified version of the linear elastic program BISAR was used to assess the influence of tire inflation pressure and tire type on the response of flexible pavement (Sebaaly and Tabatabaee 1989). Radial (11R22.5) and bias (11-22.5) tires and WBT were used in the study. Each tire class was subjected to values of load and pressure that covers behaviors such as under and over-loaded and under and over-inflated tire. The resulting footprint and vertical contact pressures were measured in order to obtain the input required by BISAR. The analyzed flexible pavement, whose thickness was varied from 2 to 8 in, was assumed to be placed on top of 8 in granular base. The study concluded that if the pavement is 2 in-thick, the longitudinal strain at the bottom of the AC is 40% greater when the tire inflation pressure changes from 130 to 145 psi for an applied load of 20 kips. In addition, if the thickness of the AC is 6 or 8 in and the load changes from 10 to 17 kip, the change in the mentioned strain is less than 10%. Regarding the deflection at the surface, all three tires showed similar values with bias tire producing the greatest ones. The authors not only concluded that WBT generates the greatest strain at the bottom of the AC, but also the largest stress on top of the subgrade. In addition, it was found that WBT with high applied load were more critical in thin pavements.

A major effort was made in 1992 by the University of Michigan Transportation Research Institute to establish a relationship between truck characteristics and pavement response and performance (Gillespie et al. 1992). The characteristics of heavy-vehicles considered in this study are weight, axle load, axle configuration, suspension properties, tire types, tire pressure, tire contact area, tire configuration, and operating conditions. In addition, flexible and rigid pavements were built with different surface condition (smooth, rough, and joined surface). The analytical tool used depended on the type of pavement: VESYS-DYN for flexible pavement and ILLI-SLAB for rigid. Fatigue damage was assessed in both flexible and rigid pavement, and rutting was included

in flexible pavement. Different tires were considered: dual-tire assembly (11R22.5), and WBT (15R22.5 and 18R22.5). In relation to the WBT, this study concluded that WBT produced between 2 and 9% more peak tensile stress in the rigid pavement than the dual-tire assembly. Moreover, WBT were more damaging than dual-tire assembly for the typical major highway pavement design if the axle load is 18 kip, and the damage of the WBT increased from 22 to 52% when compared to the damage caused by a 20 kip axle. The authors also observed that WBT caused wider but shallower rut depth than single and dual-tire assembly. If rut depth is considered as the variable in defining rut damage, conventional single tire and WBT are more harmful; however, this is not the case if rut volume is taken into account. The research also found that for WBT 15R22.5, the fatigue damage increases 9 times when the tire inflation pressure changes from 75 to 120 psi. In the case of dual-tire assembly with 11R22.5, the increment is 2.8 times for the same change in tire inflation pressure. In addition, it was concluded that changes in the inflation pressure do not affect rutting, no matter the type of tire used. As a final and general conclusion, it was recommended to use dual-tire assembly instead of WBT.

The software CYRCLY was used to assess the effect of WBT on the response of flexible pavements in 1993 (Perdomo and Nokes). This software accounts for shear contact stresses on a circular contact area, nonuniform contact stresses, and gradient of temperature in surface layers. In addition, it is able to consider the pavement structure as a multilayered elastic anisotropic system whose layers can be fully bonded or frictionless. The analyses considered thick flexible pavement with nonuniform vertical contact stresses and with and without shear contact stresses. In addition, temperature gradient and different axle configuration (single, tandem, and tridem) were included. Based on these analytical results, it was concluded that WBT produce between 15 and 40% higher critical strain and between 30 and 115% higher strain energy of distortion. The authors also claimed that the shear contact stresses increase the tensile strain between 6.0 and 6.7 times when compared to the case when they were ignored. Moreover, the inclusion of shear contact stresses increased the strain energy between 5.5 and 5.8 times. However, it is noticed that the shear contact stresses used by the authors are unreasonably high.

In order to measure the dynamic wheel force applied by a truck to the pavement, a new wheel load transducer was introduced by Streit et al. (1998). The experimental program included two types of suspension (steel lead spring and air bag), three different types of tires (two dual: one low profile (295/75R22.5) and one radial (11R22.5), and one WBT (425/65R22.5)), and four values of axle static load (16, 20, 24, and 30 kip). In addition, different values of speed (15, 30, 45, and 60 mph), tire inflation pressure (70, 95, and 120 psi), and road roughness were analyzed. Gross contact area, net contact area, load-deflection curves, and contact pressure distribution were measured for each tire, inflation pressure and applied load. Based on linear regression, a relationship was established between the net contact area, applied load, and inflation pressure. Similarly, equations to determine the tire stiffness as a function of inflation pressure were given. The authors found that the maximum contact stress is 1.6 or 1.7 times the inflation pressure for both types of tires (WBT and dual-tire assembly), and that speed has negligible effect on the contact stress distribution. The authors also proposed equations to calculate the dynamic load coefficient (DLC) as a linear function of road roughness, speed, wheel load, and inflation pressure. The experimental results showed that WBT has a DLC between 10 and 12% lower than dual-tire assembly. This difference, according to the researchers of this study, is caused by the mismatch in stiffness (WBT are 30% softer than dual-tire assembly). In addition, DLC for the three types of tires analyzed is very similar if they are in the front axle. However, based on the Eisenmann's stress factor, WBT have 85% more potential damage than dual-tire assembly.

Siddharthan et al. (1998) and Siddharthan and Sebaaly (1999) introduced an analytical method to calculate the response of flexible pavement. This continuum-based finite-layer approach consists

of multiple layers with the same properties, and it accounts for moving load, contact area of any shape, elastic and viscoelastic materials, and three-dimensional contact stresses implemented using Fourier series. Siddharthan et al. (1998) used this method to compare the response of thin and thick asphalt pavement subjected to a moving tandem-axle load with both dual-tire assembly and WBT traveling at 44.7 mph. It was found that the strain at the bottom of the AC layer is 33% higher for WBT than dual-tire assembly in thin pavements and 16% in thick pavements. This same analytical procedure was used to develop a parametric study when the load is applied by a WBT 425/65R22.5 in thin and thick flexible pavement (Siddharthan and Sebaaly 1999). The parametric study showed that for WBT at high speed, transverse normal strain should be used when predicting fatigue life. The authors also affirmed that the contact stresses between the pavement and WBT are nonuniform and the loaded area is not circular.

In 1999, the effect of tire structure, applied load, and inflation pressure on pavement performance was assessed by Myers et al. (1999). Contact stresses were measured for three different types of tires: bias ply (General Ameri Freight), radial (Bridgestone R299), and wide-base (Bridgestone M844); three inflation pressures (90, 115, and 140 psi); and different applied loads. These laboratory measurements showed that WBT have the highest vertical and transverse contact stresses. Based on a finite element model created in ABAQUS, it was concluded that the contact stress distribution was not dependent of the material at which the tire was applying the load. The measured contact stresses were used in the software BISAR to determine the pavement response, and it was found that the vertical and transverse contact stresses of WBT at high values of applied load and inflation pressure can create considerably more damage than dual-tire assembly considering surface rutting and cracking. It was also reported that surface cracking and near-surface rutting were mainly influenced by lateral stresses, and the main difference between WBT and bias ply dual-tire assembly was due to lateral contact stresses.

Siddharthan et al. (2002) used the software 3D-MOVE to carry out an analytical study to determine the effect of the contact stress distribution on pavement response. 3D-MOVE is based on the continuum-based finite-layer approach (Siddharthan et al. 1998; Siddharthan and Sebaaly 1999). Two AC pavement thicknesses (5.9 and 9.8 in) were analyzed under tandem axle load with dual-tire assembly and WBT. Different contact conditions were assumed according to the tire. For the tandem axle with dual-tire assembly, circular and rectangular contact area with constant and nonuniform stress distributions were considered. On the other hand, for the tandem with WBT, circular contact area with uniform and constant stresses and non-uniform distribution represented the contact stresses. Three-dimensional contact stresses for WBT (425/65R22.5) were also included. For WBT, circular contact area brought greater longitudinal strain at the bottom of the AC and greater vertical strain at the top of the subgrade. In addition, the shear stresses and strains at 2 in from the surface for both thin and thick pavement were also higher in magnitude for WBT with circular contact area when compared to the other contact assumptions. The authors also concluded that the effect of shear contact stresses for WBT is not relevant unless the response near the surface is being studied.

Finite Element Modeling (FEM) is another important aspect of the Virginia Smart Road study (Al-Qadi et al. 2005a; Elseifi et al. 2005). The developed model included exact contact area between the tire and the pavement and vertical nonuniform contact stress distributions. The AC layers were assumed viscoelastic, while subgrade and granular materials were assumed linear with its elastic modulus determined from in-site FWD measurements. The viscoelastic characterization of AC was based on the indirect creep compliance test and variable creep loading test (time hardening model) (Al-Qadi et al. 2005a; Elseifi et al. 2005). This FEM was validated with the experimental measurements of the instrumented sections, and it was used to quantify the

damage. This allowed the comparison of dual-tire assembly and two sizes of NG-WBT: 445/50R22.5 and 445/55R22.5.

Based on the experimental measurements and the numerical model, the authors concluded that WBT 445/50R22.5 produced more subgrade rutting than dual-tire assembly. Regarding surface rutting, 445/50R22.5 was found to be more damaging than dual-tire assembly, but 455/55R22.5 caused as much damage as dual-tire assembly at low speed. In general, 455/55R22.5 tires were less damaging than 445/50R22.5 tires from the surface rutting perspective. In the case of top-down cracking, both sizes of NG-WBT were considerably less harmful than dual-tire assembly. Finally, WBT caused more fatigue cracking than dual-tire assembly, but NG-WBT showed a better performance than the first generation of WBT for this type of distress.

A direct comparison between 385/65R22.5 and 445/50R22.5 reasserts that the first generation of WBT is more harmful for the pavement than NG-WBT (Al-Qadi et al. 2005a). The experimental data also evidenced a reduction in the strain at the bottom of the AC layer as the speed increases. The rate at which these strains were reduced was greater for dual-tire assembly than for WBT. After all the damage mechanisms were combined, it was concluded that 385/65R22.5 tire is the most deteriorating type among the tires considered in this study, followed by 445/50R22.5 tires and dual-tire assembly.

In 2005, the impact of WBT on the subgrade was study using FEM (Kim et al. 2005). The mentioned model considered a 425/65R22.5 tire with inflation pressure of 125 psi and applied load of 11.4 kip. In the numerical model, the contact area was assumed to be rectangular with no treads and without longitudinal or transverse contact stresses. In addition, two types of models were compared: plain strain 2D and 3D. The pavement structure was composed by 6 in of asphalt on top of 6.75 in-thick base, 24 in-thick compacted clay, and 240 in-thick clay or sand subgrade. After comparing different assumptions, uniform contact stress distribution equal to the maximum vertical stress was selected for being more conservative. The material properties for all layers were obtained from the literature, and the subgrade was assumed to be governed by the Druvker-Prager model. Furthermore, three tire configurations were analyzed: conventional dual-tire assembly at 18 kip axle load, conventional dual-tire assembly at 22.8 kip axle load, and WBT (425/65R22.5) at 22.8 kip axle load. The FEM results indicated that WBT produced the highest vertical stress on top of the subgrade, and that WBT induced four times more permanent strain than dual-tire assembly. Moreover, single axle with WBT resulted in the largest vertical plastic strain on top of the subgrade when compared to the other axle configurations.

An analytical study was presented by Yoo et al. (2006) using FEM of flexible pavements to assess the validity of different assumptions commonly used to model such as layer interaction, amplitude of applied load, and tire contact stresses. The asphalt material was considered as viscoelastic with its parameter determined from the creep compliance test; while base and subbase were assumed linear with their modulus of elasticity given by FWD test. WBT and dual-tire assembly were modeled considering 3D contact stresses. In addition, two friction models (simple friction (Coulomb) and Stick model) and two load amplitude assumptions (trapezoidal and continuous) were investigated. Experimental measurements from Section B of the Virginia Smart Road project (Al-Qadi et al. 2004) were used to validate the numerical predictions. It was concluded, in general, that continuous amplitude loading and non-uniform 3D contact stresses improve the accuracy of the FEM and should be considered in any future study. In particular, it was found that results of the simple friction model for WBT are closer to the experimental measurements.

Three-dimensional contact stresses were measured for a variety of tires (WBT included), inflation pressures, and applied load in Texas (Emmanuel et al. 2006). In order to measure these contact stresses, the Stress-in-Motion system was used. In the case of WBT (425/65R22.5), measurements were taken at four inflation pressures (73, 102, 131, and 145 psi) and five applied loads (5.86, 10.4, 12.6, 14.9, 19.4, and 23.9 kip). Based on these readings, expressions to predict the contact area as a linear function of tire load and inflation pressure were proposed. The entire experimental results were compiled in software called TireView; this software can be used to predict the 3D contact stresses at any load and inflation pressure. This is done by interpolation between the experimental values. The authors also used the measured contact stresses to calculate the pavement response analytically. Three analytical calculations were included: 3D FE with 3D measured contact stresses, layered linear elastic with contact area equivalent to the measured one, and layered linear elastic with the contact area based on the load and inflation pressure. It was concluded that the 3D contact stresses and uniform circular pressure assumptions bring “quite comparable” results. It was also noted by the authors that WBT experimental values provided the worst repeatability.

The experimental readings obtained by NCAT in 2006 were compared to analytical results calculated using WESLEA (Priest and Timm 2006). This software uses the layered elastic theory and assumes circular contact area with uniform pressure. The elastic properties of each layer used as input in this program were backcalculated using EVERCALC 5.0. The testing program, where the only different parameter was the type of load used, showed that the strain and stresses of WBT and dual-tire assembly are virtually the same. On the other hand, the analytical result presented higher strains and pressures in the case of WBT. In addition, the difference between both tires decreased as the depth increased. Based on the numerical results, the fatigue life was found to be 69% less if the pavement is subjected to moving load using WBT. It was also noted that the difference in WESLEA’s results was higher for WBT.

In addition to the experimental program described in the previous section, a detailed finite element model was developed during the investigation carried out by University of Illinois (Al-Qadi et al. 2008; Al-Qadi and Wang 2009a; Al-Qadi and Wang 2009b). This model included advanced characteristics such as dynamic implicit analysis, continuous loading amplitude, Coulomb friction between layers, three dimensional contact stresses, and viscoelastic asphalt materials. The aforementioned model was proved to predict the response of the pavement structure, since it brought good agreement with experimental readings of the peak strain and time history. The study showed that NG-WBT produced higher longitudinal strain at the bottom of the AC layer and higher stresses on top of the subgrade than dual-tire assembly. On the other hand, it resulted in less compressive and vertical shear strain close to the surface of the pavement. As in studies by other authors, the difference in the response of the pavement between both types of tires decreased as the depth increased.

The effect of the offset was also documented: as the offset was increased, the longitudinal strain at the bottom of AC for NG-WBT decreased at a higher rate. The numerical model was used to assess other failure mechanism (rutting and near-surface cracking). NG-WBT-445 resulted in higher strain damage at the bottom of AC (fatigue cracking) and compressive strain at top of the subgrade (secondary rutting), but less near the surface damage (primary rutting, top-down cracking, and near-surface cracking). The researcher of the study concluded that, based on combined damage, NG-WBT-445 caused less damage on interstate highways, but it is more harmful on local roads. Based on cost analysis, it was also affirmed that NG-WBT-445 could be more cost-effective for an interstate highway, but it is slightly more expensive for primary roads.

Al-Qadi and Wang (2009a; 2009b; 2009c) conducted a study on quantification of the damage caused by dual-tire assembly and NG-WBT-455 on roads with low-volume traffic. The main characteristics of the experimental set-up were presented in the previous section. The numerical model accounted for all the features used by the author in other studies (Al-Qadi et al. 2008). Even though the agreement between measured and predicted values was not strong, the ratio of NG-WBT to dual-tire assembly of the experimental measurements was similar to the FEM ratio. For all base thicknesses, the longitudinal strain at the bottom of AC was greater for the dual-tire assembly, but the transverse strain was very similar. It was also concluded that NG-WBT produced the lowest vertical shear stresses, no matter the thickness of the base layer. On the contrary, WBT-425 resulted in the greatest deviatoric and bulk stresses for all pavement structures analyzed.

The authors noted that the compressive strain and deviator stress on top of the subgrade decreased as the thickness increased. The analysis of the damage performed based on described analysis indicated that NG-WBT-455 was more harmful than dual-tire assembly: from 1.9 to 2.5 times more fatigue damage, from 1.3 to 2.3 times subgrade rutting, and from 1.3 to 1.8 times more AC rutting due to densification. On the other hand, NG-WBT-455 showed less AC rutting due to shear flow and less shear failure potential. The authors reported that after all the damage mechanisms were combined, NG-WBT-455 caused between 1.12 and 1.38 more combined damage than dual-tire assembly on secondary road. NG-WBT-455 was also showed to be more expensive on low-volume traffic.

9.1.3. Sections subjected to real traffic

Multidepth deflectometers were used by Akram et al. (1992) to compare the damage produced by dual-tire assembly (11R22.5) and NG-WBT (425/65R22.5) in two flexible pavement sections open to real traffic. Each pavement section represented a thin and thick structure (1.5 and 7 in-thick respectively), and the speed varied between 4 and 60 mph. Not only was the offset of the tire taken into account, but also the WBT and the dual-tire assembly were switched between the tandem drive trailer axles. The authors found that a lower deflection is caused by the dual-tire assembly when compared to NG-WBT. It was also concluded that the maximum deflection occurred at a different location depending on the type of tire: around the center of the tire for NG-WBT and under one of the tires of the dual-tire assembly. Some important remarks were made regarding WBT: the maximum shear stress occurred at its edge, and its deformation basins were deeper and more concentrated. Moreover, NG-WBT was more damaging based on the vertical strain on top of the subgrade. The vertical strain on top of the subgrade was used to determine the number of repetitions to failure. It was reported that the number of repetitions increased 45% and 39% when the speed changed from 4 to 60 mph for dual-tire assembly and NG-WBT respectively. For thick pavement, the increment was 87% for dual-tire assembly and 26% for NG-WBT for the same change in speed, respectively. When the speed was kept constant at 55 mph, NG-WBT were 2.8 times more damaging on thin pavements and 2.5 times more damaging on thick pavements than dual-tire assembly, respectively.

9.2. IMPACT ON DYNAMIC TIRE LOADING

Since WBT have only two sidewalls, it is much more flexible than a pair of dual-tire assembly, which has four sidewalls. This flexibility means that the tire absorbs more dynamic bouncing of the truck; hence, less dynamic load is transmitted to the pavement. Tielking (1994) compared a single 425/65R22.5 and two 11R22.5 tires on an MTS servo-hydraulic machine. The author found that, except near the resonant frequency, the transmissibility of the WBT was less than that of the dual-tire assembly. At 10Hz, which is near the fundamental vibration frequency of a heavy

highway vehicle, the force transmissibility of the WBT is 35% less than that of the dual-tire assembly. This indicates that the dynamic component of pavement load from a WBT is less than the dynamic component of pavement load from dual-tire assembly. Moreover, the research found that the sensitivity of the force transmissibility was negligible considering the load level, and it was slightly sensible to tire inflation pressure.

Similar results were found in a shaker table study by Streit et al. (1998). Two different types of dual-tire assembly (standard and low profile) were compared with a WBT (425/65R22.5). The magnitudes of the dynamic wheel loads produced by the dual-tire assembly were very similar. The Dynamic Load Coefficient (DLC is equal to standard deviation of tire load divided mean value) values of the standard radial tires were about 2% higher than those produced by the low-profile tire. The WBT produced DLC's from 10 to 12% lower than those of the dual-tire assembly.

9.3. IMPACT ON TRUCKING OPERATIONS

A review of the improvements provided by the NG-WBT was given by Elseifi and Al-Qadi (Elseifi et al. 2005). They mention how this type of tire decreases the rolling resistance, which translates in fuel saving from 2 to 10%. The gross weight of the truck having NG-WBT could be reduced by 744 lb, increasing the hauling capacity. The NG-WBT could have a 50% lower maintenance cost while the cost could be the same as dual-tire assembly. Regarding safety, NG-WBT has a sensor that controls the inflation pressure, so the probability of having a sudden flat tire is reduced. This is confirmed by the satisfactory performance of NG-WBT on the sudden-failure test. In addition, the drivers of trucks with NG-WBT installed noted similar truck handling as with dual-tire assembly.

Overall economic analysis of the use of wide-base tires from COST Action 334 (COST 334 2001) indicated that the benefits of this technology are considerably greater than the additional pavement maintenance costs they may cause. Items considered in the economic analysis included pavement maintenance costs, government tax income, vehicle operating costs, non-pavement related government expenditures (polluting emissions), and trucking operations spending (tires cost and recycling). It was estimated that the use of wide-base tires on the towed axles alone would be associated with a saving of €2,302 million in the European Union. Using wide-base tires on the towed, driven, and steering axles would provide an additional saving of €682 million.

9.3.1. Fuel Economy

In 2000, the Energy Laboratory of the Massachusetts Institute of Technology (MIT) analyzed alternatives to reduce gas consumption and to improve fuel efficiency of class-8 trucks by reducing the rolling resistance and improving propulsion technologies (Muster 2000). A script using Matlab-Simulink was used to predict the fuel economy. The proposed model assumes a vehicle traveling on a flat road, and it considers the rolling resistance coefficient (RRC), aerodynamic drag coefficient (C_d), vehicle mass, frontal vehicle area, engine and transmission performance, and driving cycle (highway and urban). Also, the resistance (internal and external) that the vehicle must overcome in order to move was taken into account. The rolling resistance coefficient was varied between 0.007 and 0.005, 0.005 representing a truck equipped with WBT. The results of the modeling process show that the reduction of the RRC to 0.005 (WBT) increases the fuel efficiency of the truck by 10%.

The effect of reducing the rolling resistance and the aerodynamic drag on the gas consumption and the emission of oxides of nitrogen (NOx) was studied by Bachman et al. (2005). Class-8

trucks on a test track simulating the operating conditions of real traffic were used. The tests included two scenarios: highway conditions at two different speeds (55 and 65 mph) and suburban circumstances. The truck was equipped with aerodynamic devices and WBT, so the rolling resistance and dynamic drag could be varied. It was found that both aerodynamic devices and WBT improved fuel economy by similar values. However, WBT are more efficient in the suburban scenario. WBT improved fuel economy between 3 and 18%: 3% for no WBT in suburban conditions with aerodynamic devices, and 18% for the truck traveling at 65 mph on a highway and equipped with aerodynamic devices.

As explained by Genivar Consulting Groups (Genivar 2005), the energy used by a truck can be sorted in the following categories: 35% for rolling resistance, 50% for aerodynamic resistance, 5% for mechanical resistance (assuming that the truck travels at 60 mph), and 10% is used by auxiliary devices of the truck. The study collected information from hauling companies regarding savings resulting from reduction in fuel consumption when WBT were used. The fuel consumption was found to be reduced between 3.5 to 12%.

Ang-Olson and Schroeder (2002) analyzed the use of WBT as one of eight strategies to improve environmental performance and fuel efficiency in the truck industry. The authors affirmed that the use of WBT improves the fuel economy between 2 and 5% depending on the specific model of the WBT (tire manufacturer). This translates to savings of 424 gal/year for a typical long-haul truck.

Different alternatives to reduce the gas consumption of heavy truck vehicles from different points of view such as vehicle technology and driver skills were analyzed in Finland (Nylund 2006). The report highlights the benefits of WBT regarding weight, space, and reduction of rolling resistance when compared to dual-tire assembly. The fuel consumption was measured using a chassis dynamometer, and it compared WBT and dual-tire assembly. No significant difference was observed. The results obtained using the chassis dynamometer were verified with a test on a straight highway; similar results were reported. The authors affirmed that rolling resistance is a relevant factor that links tire with fuel efficiency. They also point out that the tire system (tire pressure, tire type, tread depth, etc.) can improve the fuel efficiency between 5 and 15%.

Recently, Franzese et al. (2010) analyzed real performance data of class 8 trucks regarding its fuel efficiency when using NG-WBT. Six trucks were instrumented to measure not only instantaneous gas-consumption related data, but also information related to weather, speed, location, and weight among others. Three trucks were equipped with NG-WBT and the other three with conventional dual-tire assembly. Four combinations were used for the installation of the tires: tractor and trailer with dual-tire assembly, tractor and trailer with NG-WBT, tractor with dual-tire assembly and trailer with NG-WBT, and tractor with NG-WBT and trailer with dual-tire assembly. The authors concluded that truck equipped with NG-WBT improved the fuel efficiency by 6%. The data was also analyzed by grouping the truck by weight, and it was found that less fuel was consumed by trucks with NG-WBT in all truck-weight ranges. This increment becomes more important as the number of NG-WBT installed in the truck increases. It reached 10% improvement when all the tires were NG-WBT, and it augmented if the truck weight became higher.

9.3.2. Hauling Capacity

WBTs increase the hauling capacity of trucks by reducing the total weight of the empty truck. As described by Markstaller et al. (2000), WBT are lighter than dual-tire assembly, so the total

weight reduction in a truck with WBT can be as high as 896 lb. This reduction in total weight translates to an increment in hauling capacity of 2%.

9.3.3. Tire Cost and Repair

The use of WBT also allows a reduction in maintenance costs (Genivar 2005). This is due to easier inspection and repair of trucks equipped with WBT. According to the referenced study, the time allotted for maintenance of a truck using WBT can be reduced by 50% when compared to a truck with dual-tire assembly. However, WBT can be retread just once, while dual-tire assembly can be retread as many as three times under particular conditions. Another source of savings is the rim cost. Even though the cost of one dual-tire assembly is as high as one WBT, a single wide-rim cost is cheaper than two rims for a dual-tire assembly (Environmental Protection Agency 2004). Finally, it is easier to inspect the inflation pressure of a WBT when compared to dual-tire assembly, specially the interior tire of the dual set. Differential inflation pressure is a common problem in dual-tire assembly.

9.3.4. Truck Operation and Safety

Concerns have emerged regarding tire inflation pressure controls in WBT; however, incidents have been reduced by enhancing pressure maintenance. Markstaller et al. (2000) conducted rapid air loss tests in trucks with WBT installed. It was found that the most critical situation appears when sudden air loss occurs in the rare drive position on the exterior part of a curve. The traveling speed of the truck was 60 mph, and the radius of the curve was 1200 ft creating a lateral acceleration of 2g. The truck never left the corresponding lane during the test.

9.3.5. Ride and Comfort

The driver's impression was also considered by Markstaller et al. (2000). According to the authors, both types of tires require similar degrees of handling, and the vibration was reduced by installing WBT. Constant-radius understeer test show a linear increase of understeer behavior with lateral acceleration. The steering wheel angle was lower in most of the ranges for WBT than dual-tire assembly.

Vehicle ride tests also showed advantages of WBT over dual-tire assembly. Power spectral density at the base of the seat base was measured using accelerometers showing a reduction in the acceleration level for the truck with WBT.

9.4. IMPACT ON ENVIRONMENT

Al-Qadi and Elseifi (2005) highlight the fact that NG-WBT is more environmentally friendly than dual-tire assembly: it generates less noise and fewer emissions due to less gas consumption. In addition, the amount of rubber needed to fabricate NG-WBT is less, so the disposed material at the end of its service life is reduced. In general, various studies have consistently concluded that NG-WBT causes similar damage to the pavement than dual tires.

9.4.1. Gas Emission

The reduction in the gas consumption of trucks using WBT results in a reduction of the emission of contaminant from the truck to the air. The savings caused by less emission can be calculated based on the amount of contaminant produced by a gallon of gas and the amount of gas not consumed by a truck using WBT (Genivar 2005). Following this procedure, Genivar Consulting Groups calculated environmental savings of \$17.8 million.

In addition, Ang-Olson and Schroeer affirmed that the use of WBT can reduce the gas emission by 1.1 million metric tons of carbon equivalent (MMTCE) in 8 years (Ang-Olson and Schroeer 2002).

The effect of reducing the rolling resistance and the aerodynamic drag on the emission of oxides of nitrogen (NO_x) was studied by Bachman et al. (Bachman et al. 2005). The authors reported a reduction of NO_x emission between 9 and 45% when NG-WBT compared to dual-tire assembly.

9.4.2. Tire Recycling

According to Riesman (1997), landfill and stockpiles in the United States store between 2 and 4 billion of scrap tires. Genivar calculated the amount of savings resulting from the reduction of tire disposal. The calculation was based on the amount of disposed material according to the type of tire (118 lb for a WBT and 160 lb. for conventional dual-tire assembly), the amount of tires disposed, and the cost of disposing used tires (Genivar 2005). The authors calculated savings of \$415,900/year in their study if WBT were disposed instead of conventional dual-tire assembly.

9.4.3. Noise

In a noise test conducted by Markstaller et al. (2000), WBT produce slightly less noise when compared to trucks that use conventional dual-tire assembly.

10.APPENDIX B: AVAILABLE PAVEMENT STRUCTURES AND INSTRUMENTATION – VIRGINIA SMART ROAD

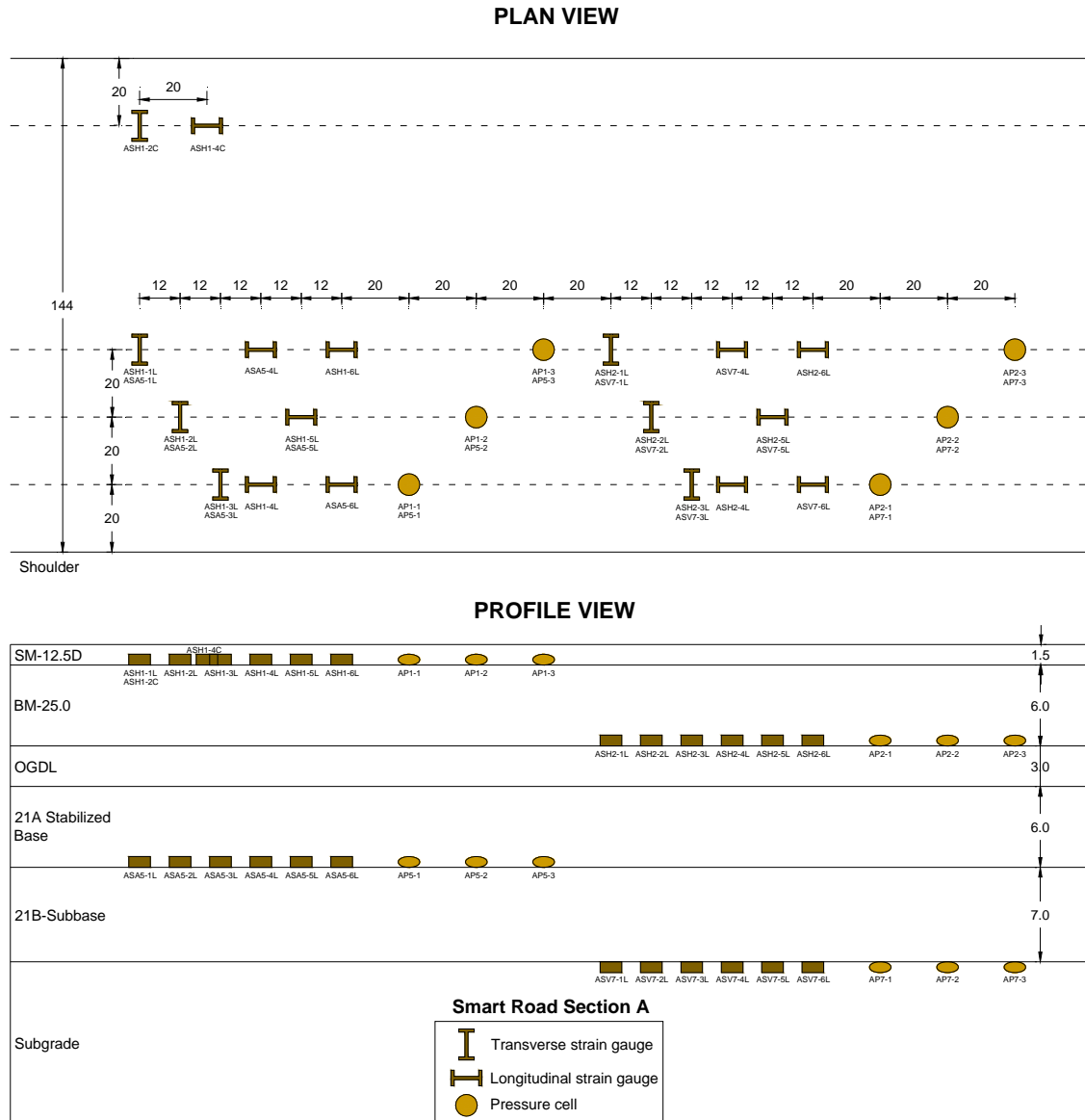


Figure B- 1. Plan and profile view of pavement structure and instrumentation of Section A, Virginia Smart Road

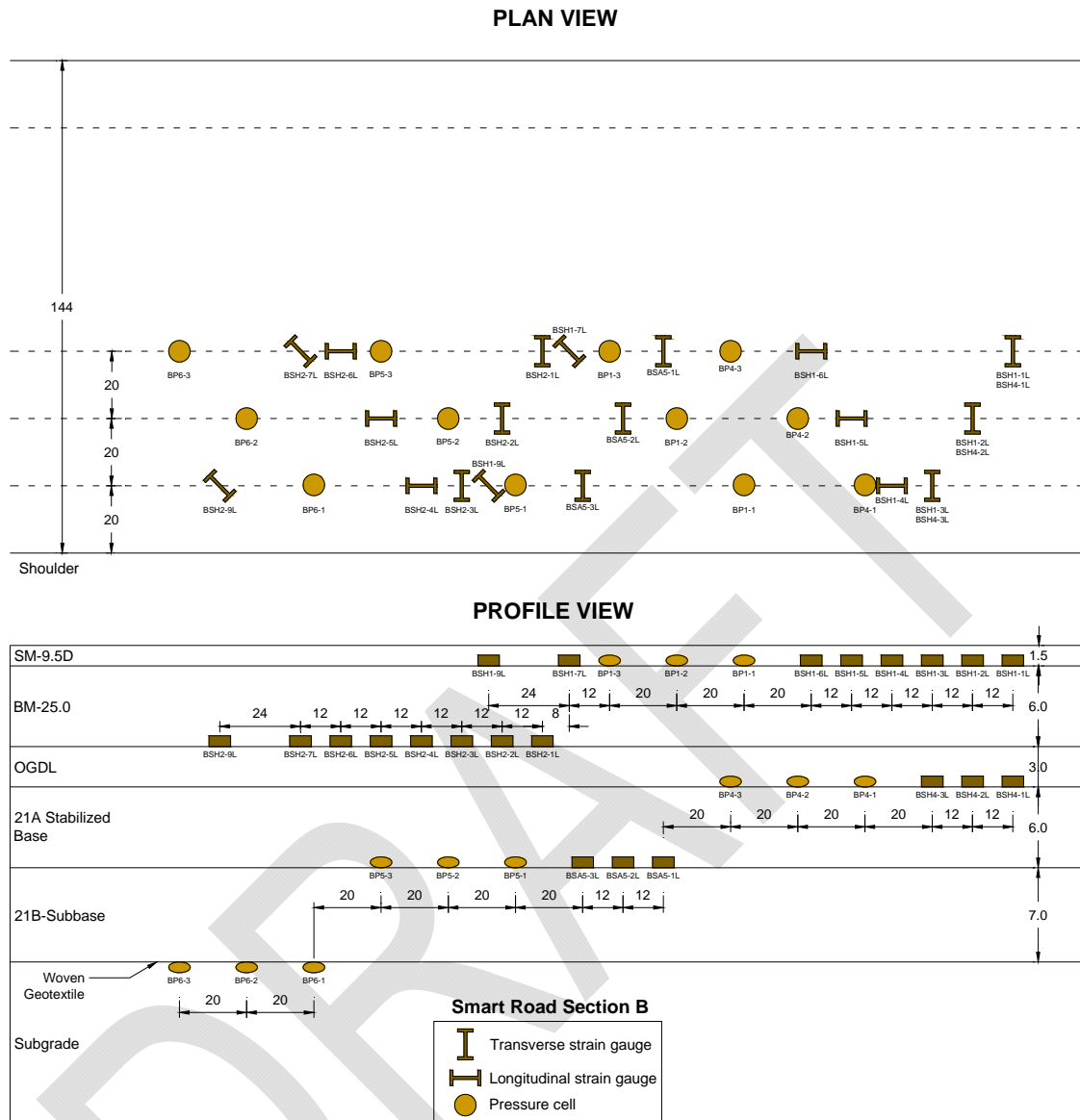


Figure B- 2. Plan and profile view of pavement structure and instrumentation of Section B, Virginia Smart Road

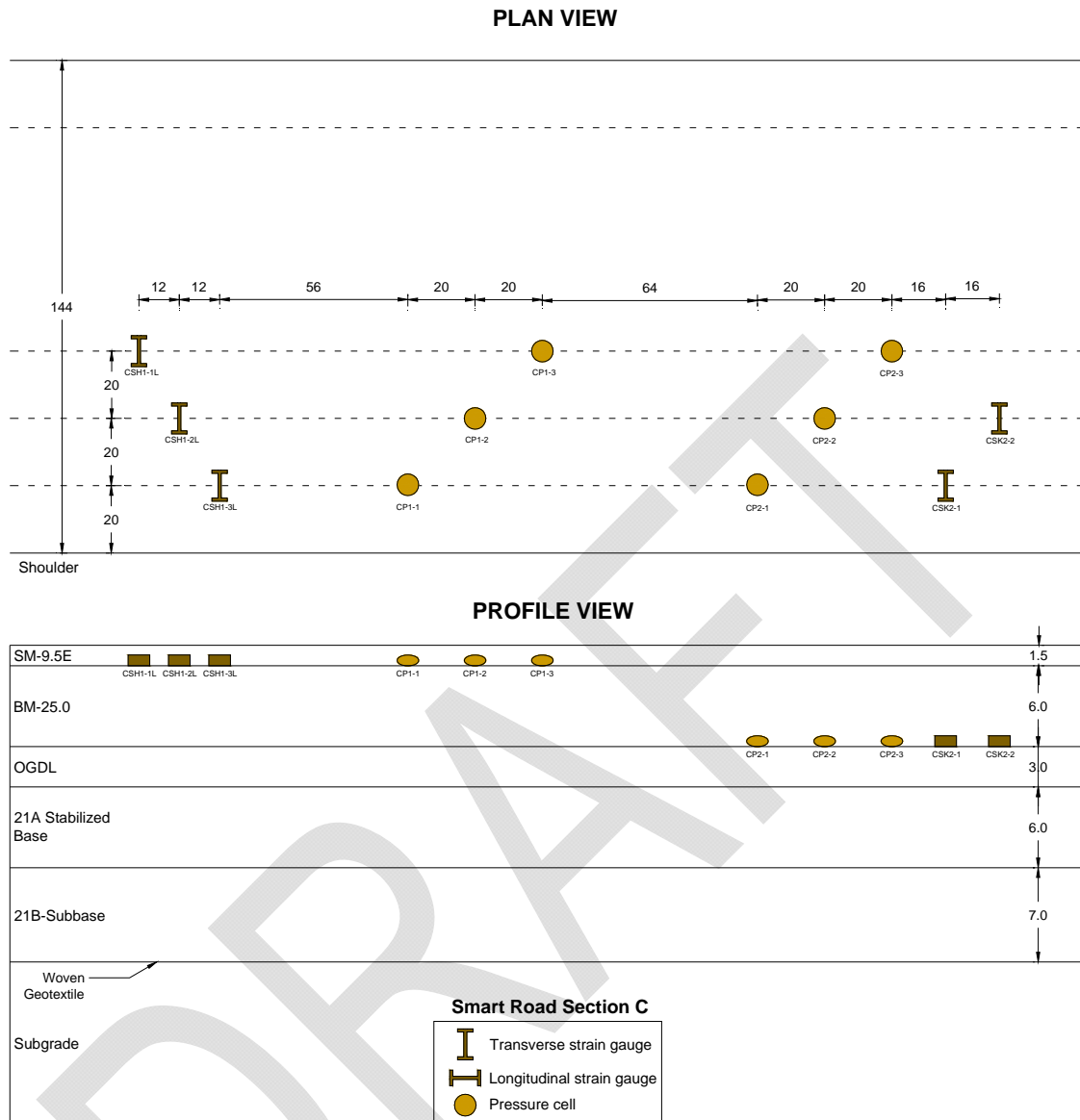


Figure B- 3. Plan and profile view of pavement structure and instrumentation of Section C, Virginia Smart Road

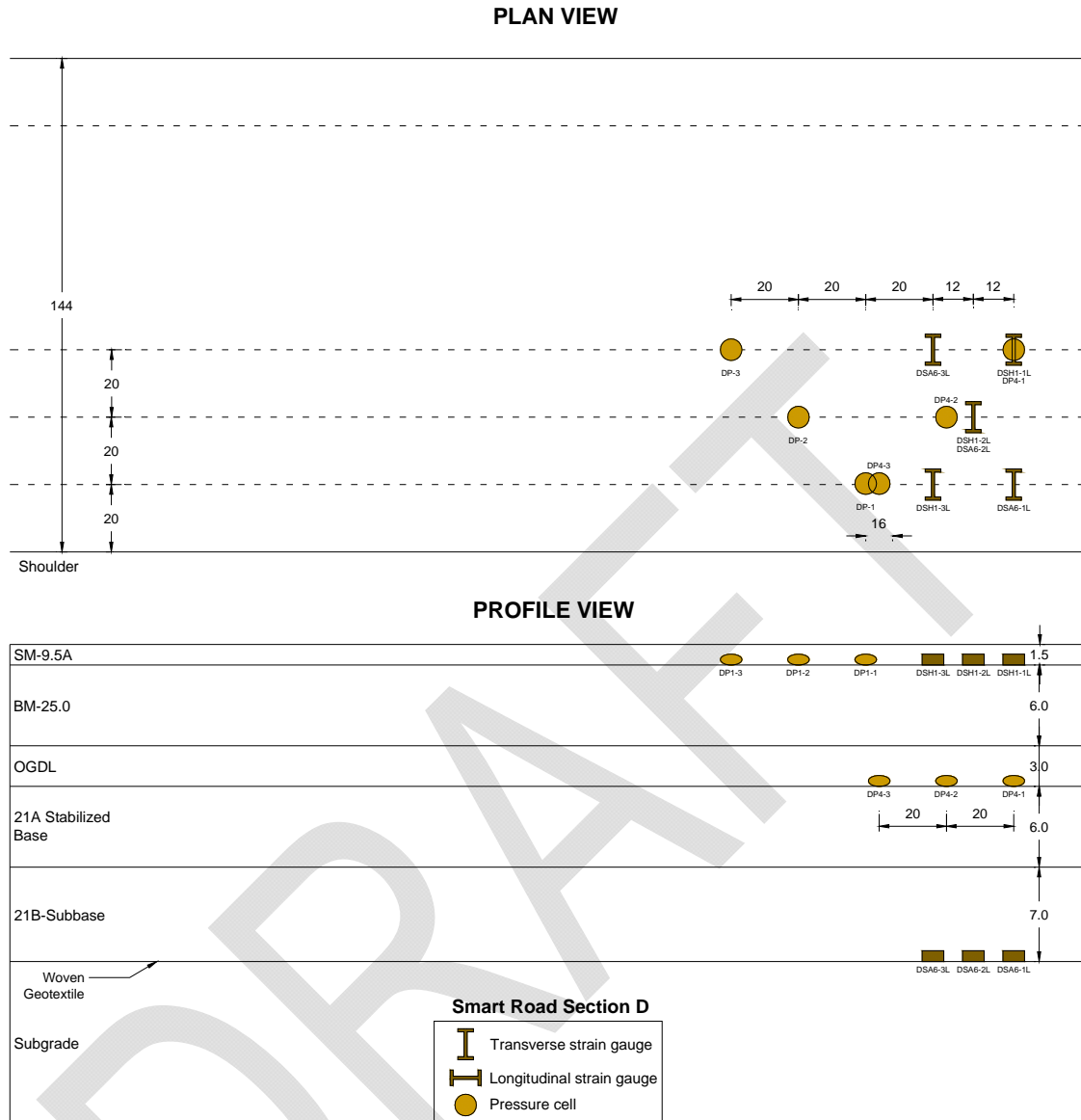


Figure B- 4. Plan and profile view of pavement structure and instrumentation of Section D, Virginia Smart Road

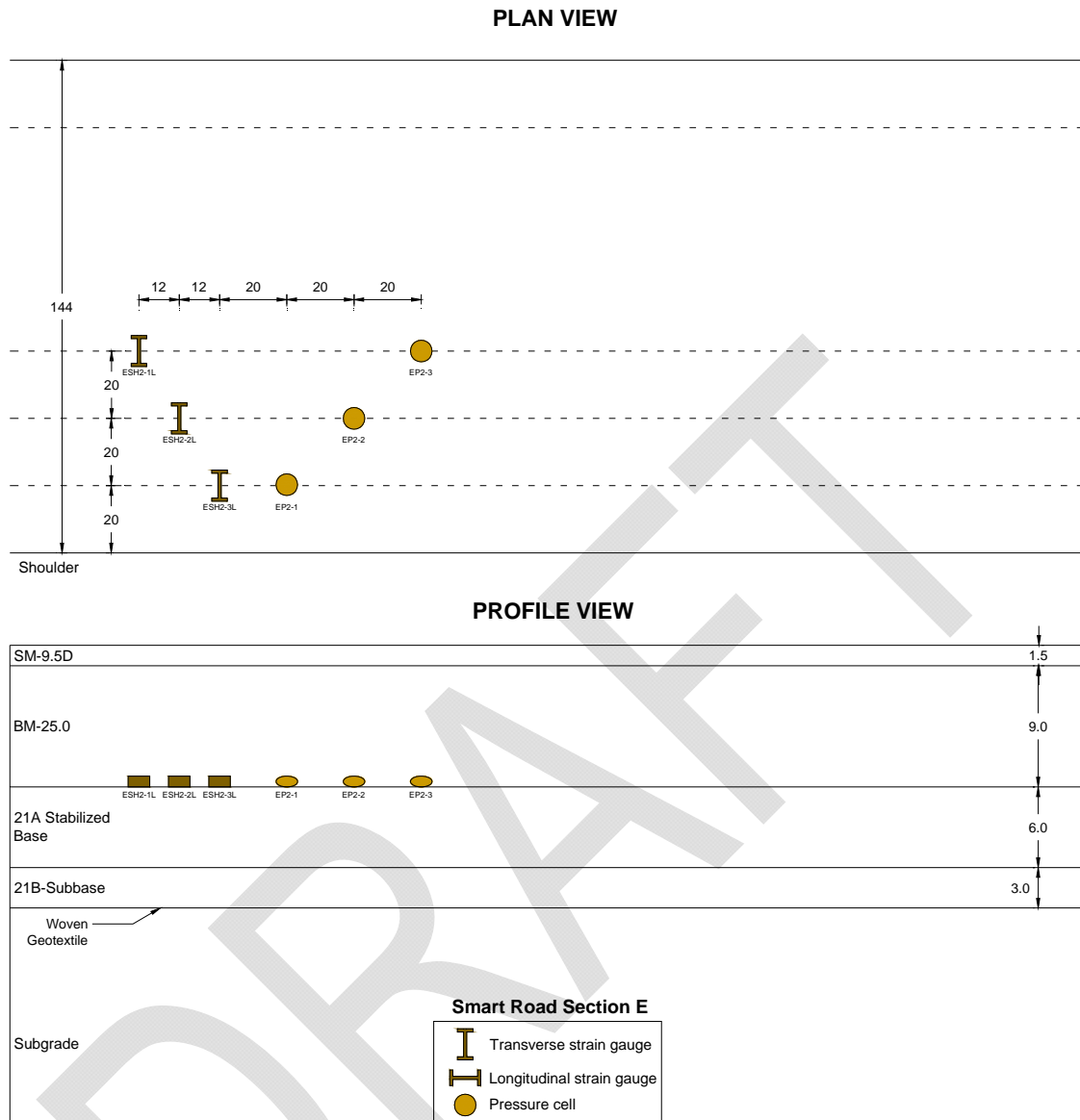


Figure B- 5. Plan and profile view of pavement structure and instrumentation of Section E, Virginia Smart Road

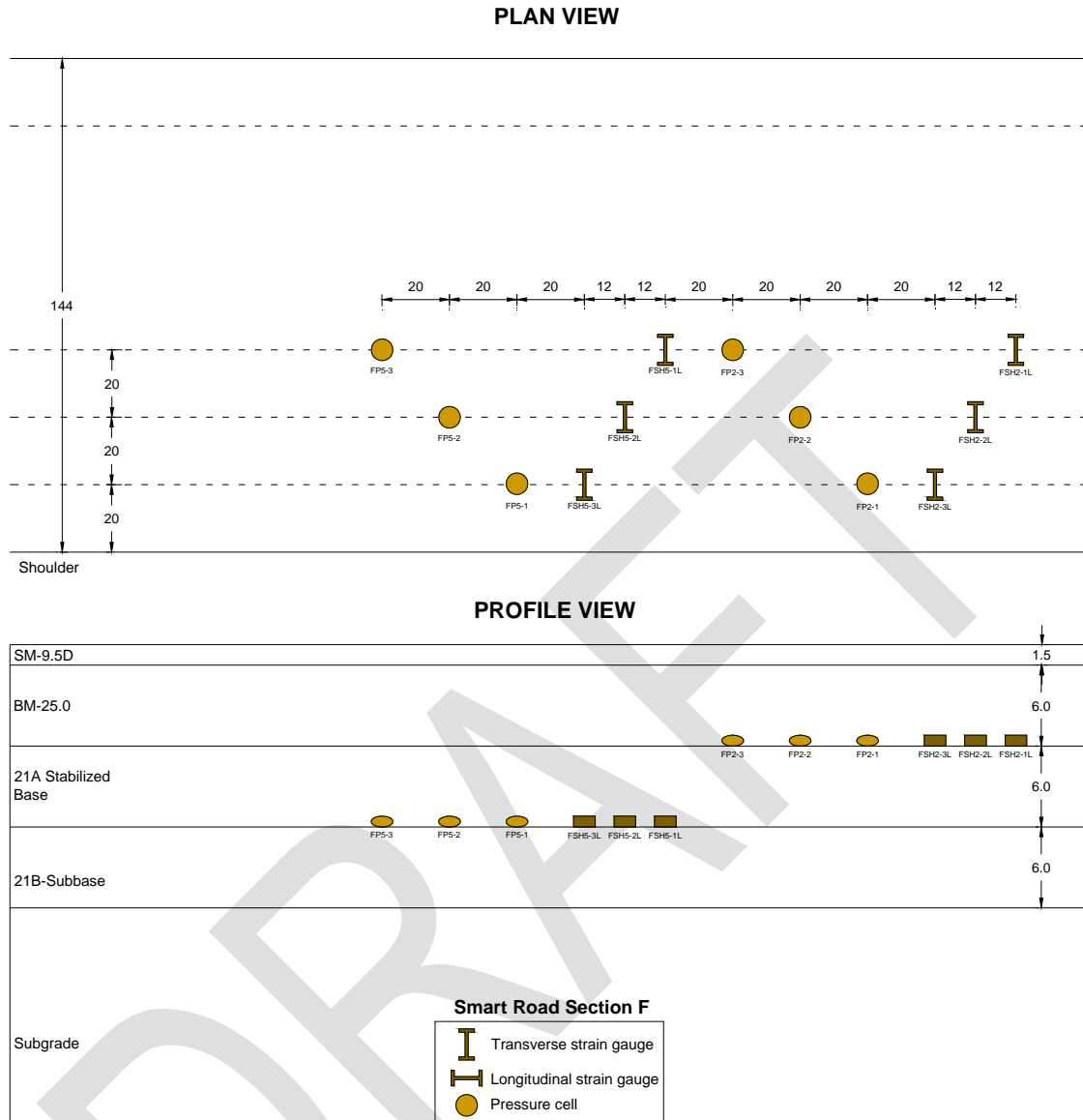


Figure B- 6. Plan and profile view of pavement structure and instrumentation of Section F, Virginia Smart Road

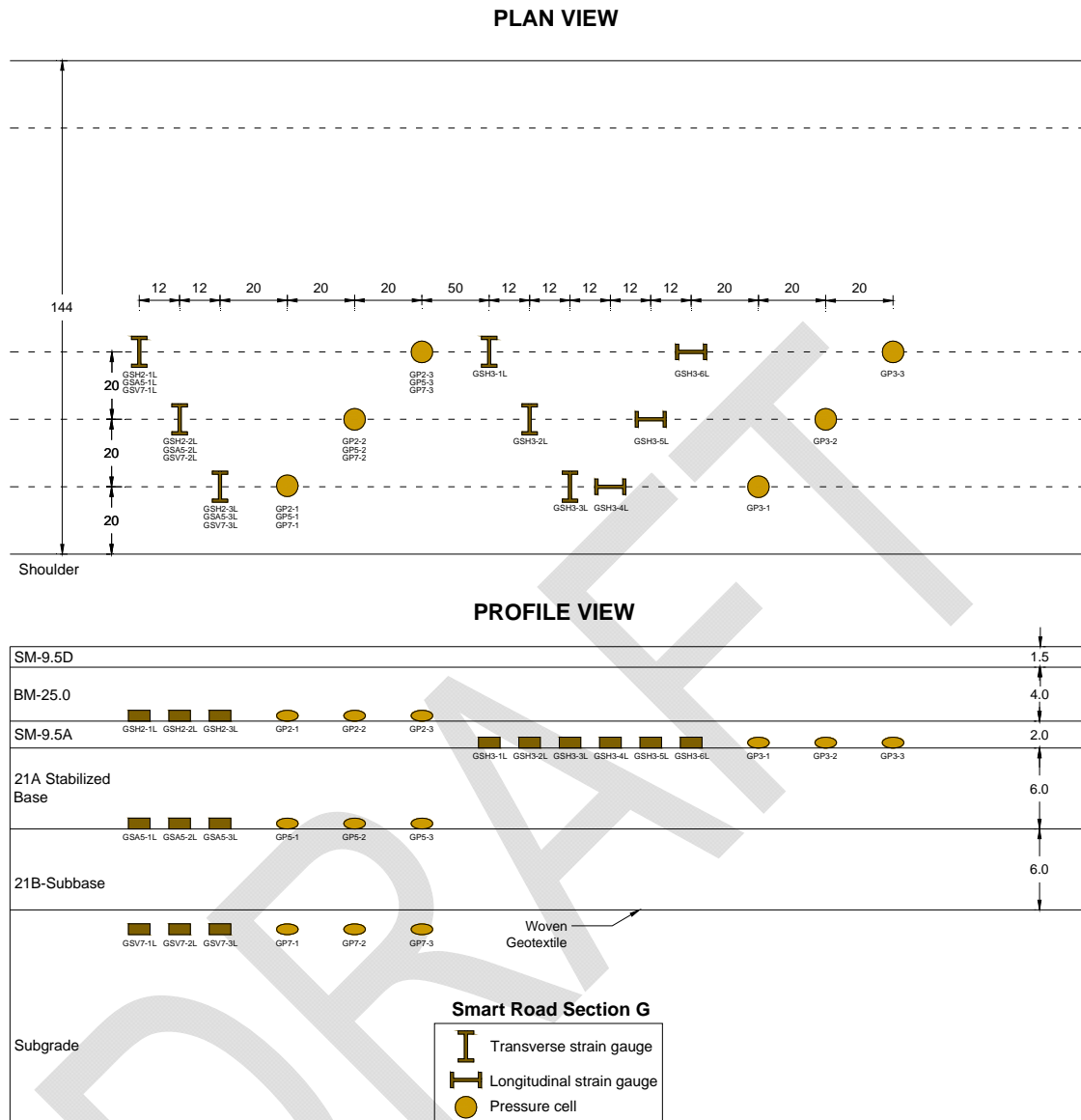


Figure B- 7. Plan and profile view of pavement structure and instrumentation of Section G, Virginia Smart Road

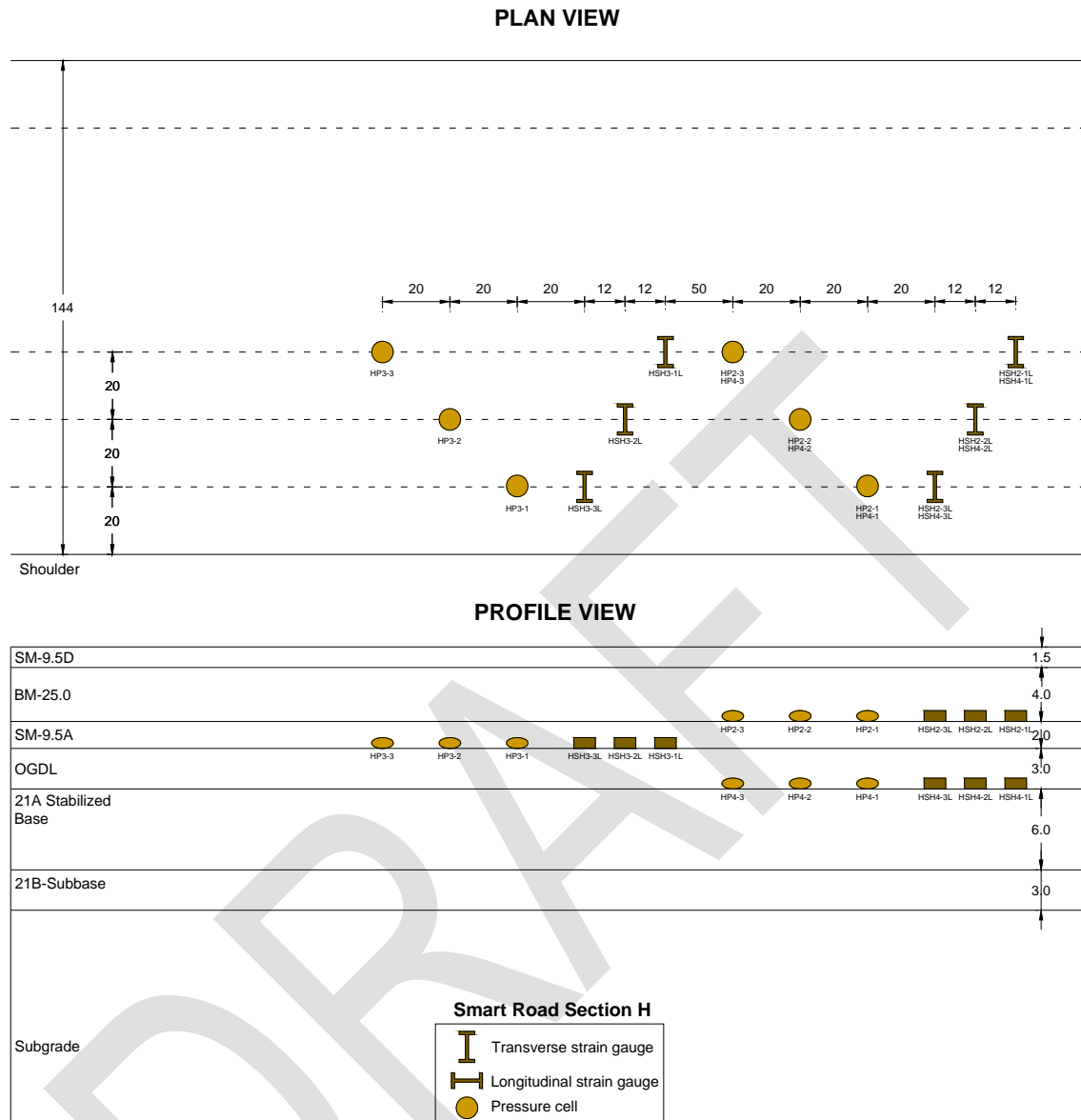


Figure B- 8. Plan and profile view of pavement structure and instrumentation of Section H, Virginia Smart Road

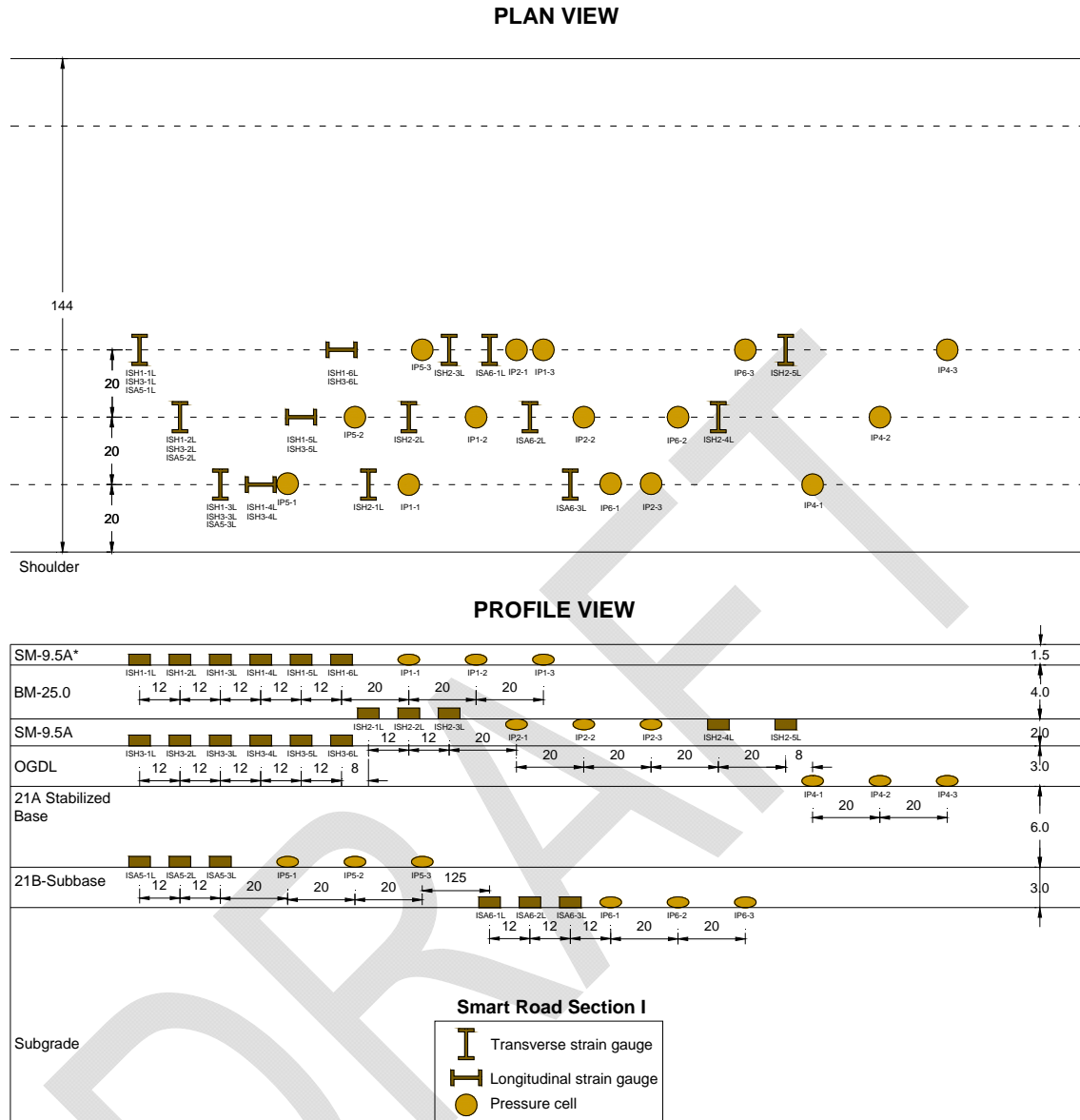


Figure B- 9. Plan and profile view of pavement structure and instrumentation of Section I, Virginia Smart Road

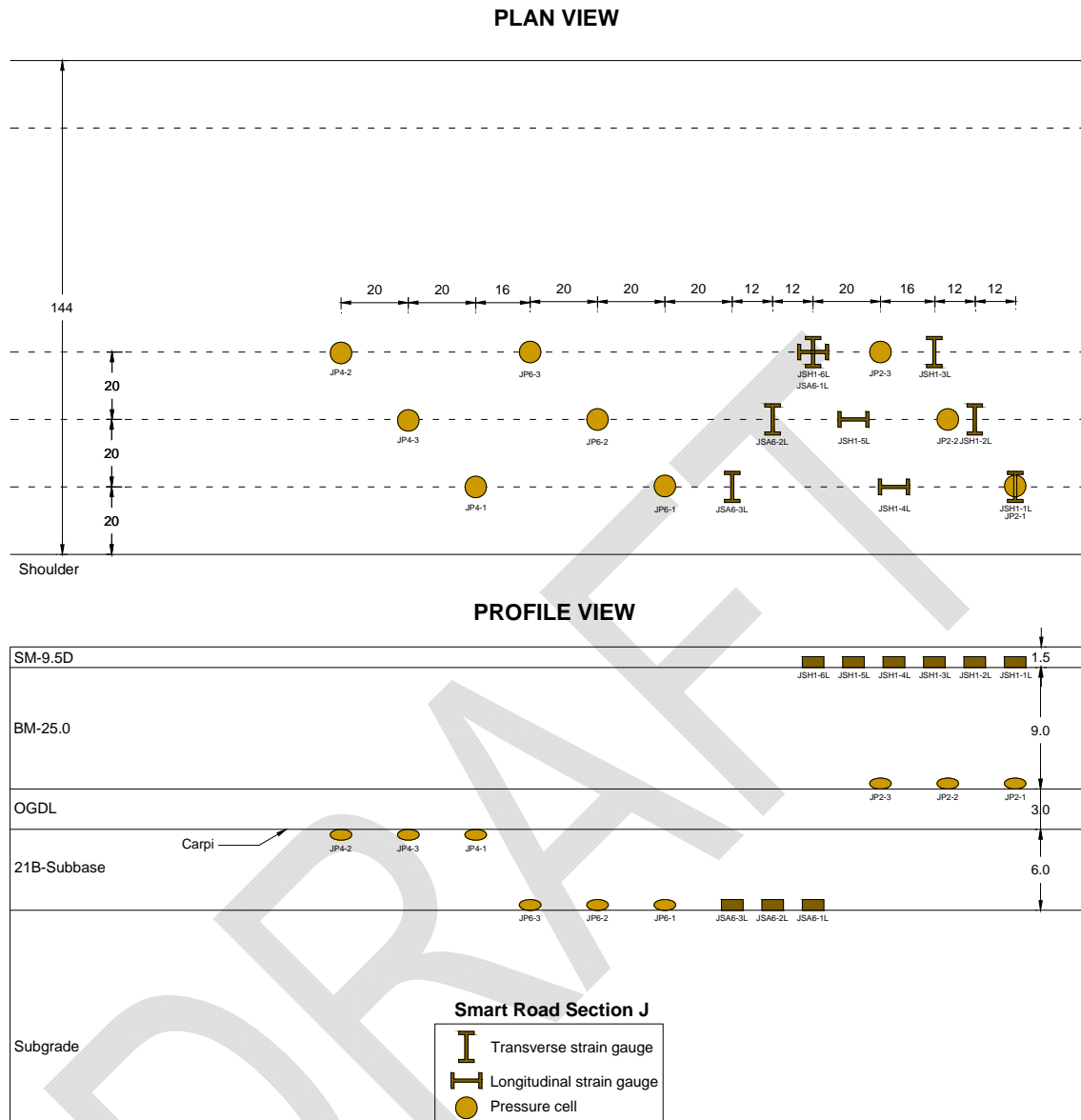


Figure B- 10. Plan and profile view of pavement structure and instrumentation of Section J, Virginia Smart Road

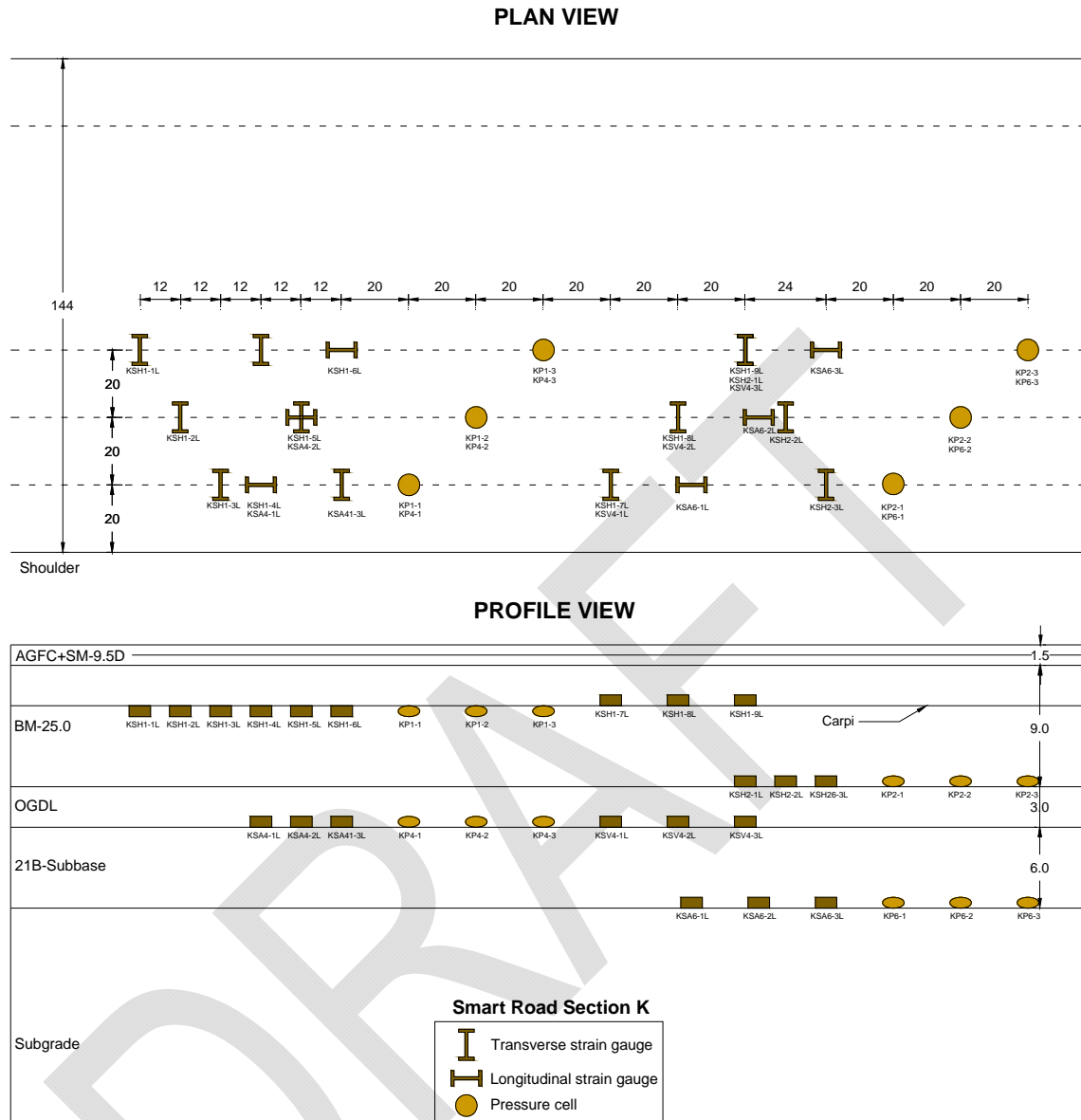


Figure B- 11. Plan and profile view of pavement structure and instrumentation of Section K, Virginia Smart Road

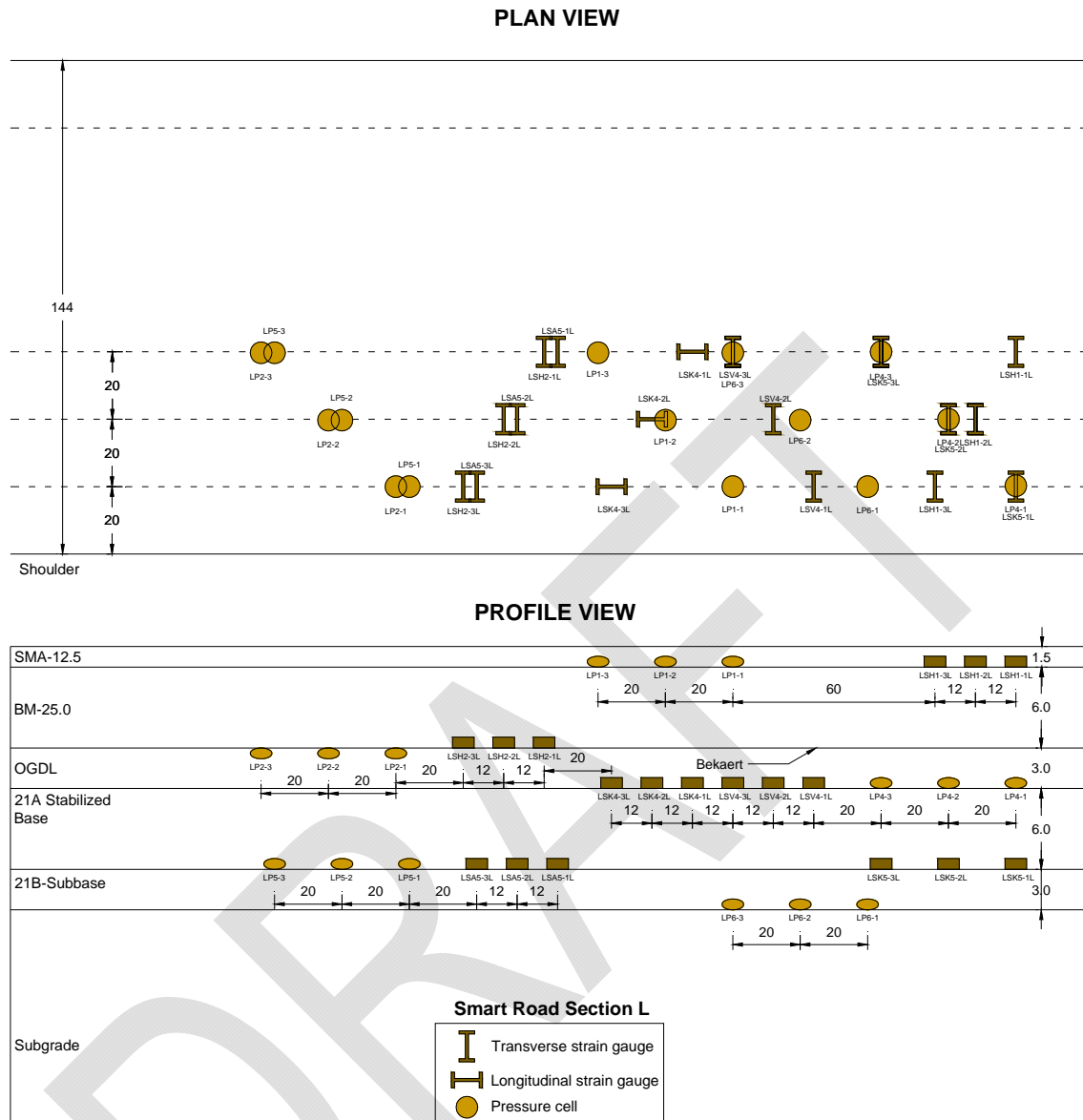


Figure B- 12. Plan and profile view of pavement structure and instrumentation of Section L, Virginia Smart Road

11.APPENDIX C: AVAILABLE PAVEMENT STRUCTURES AND INSTRUMENTATION – ATREL-UIUC THIN SECTIONS

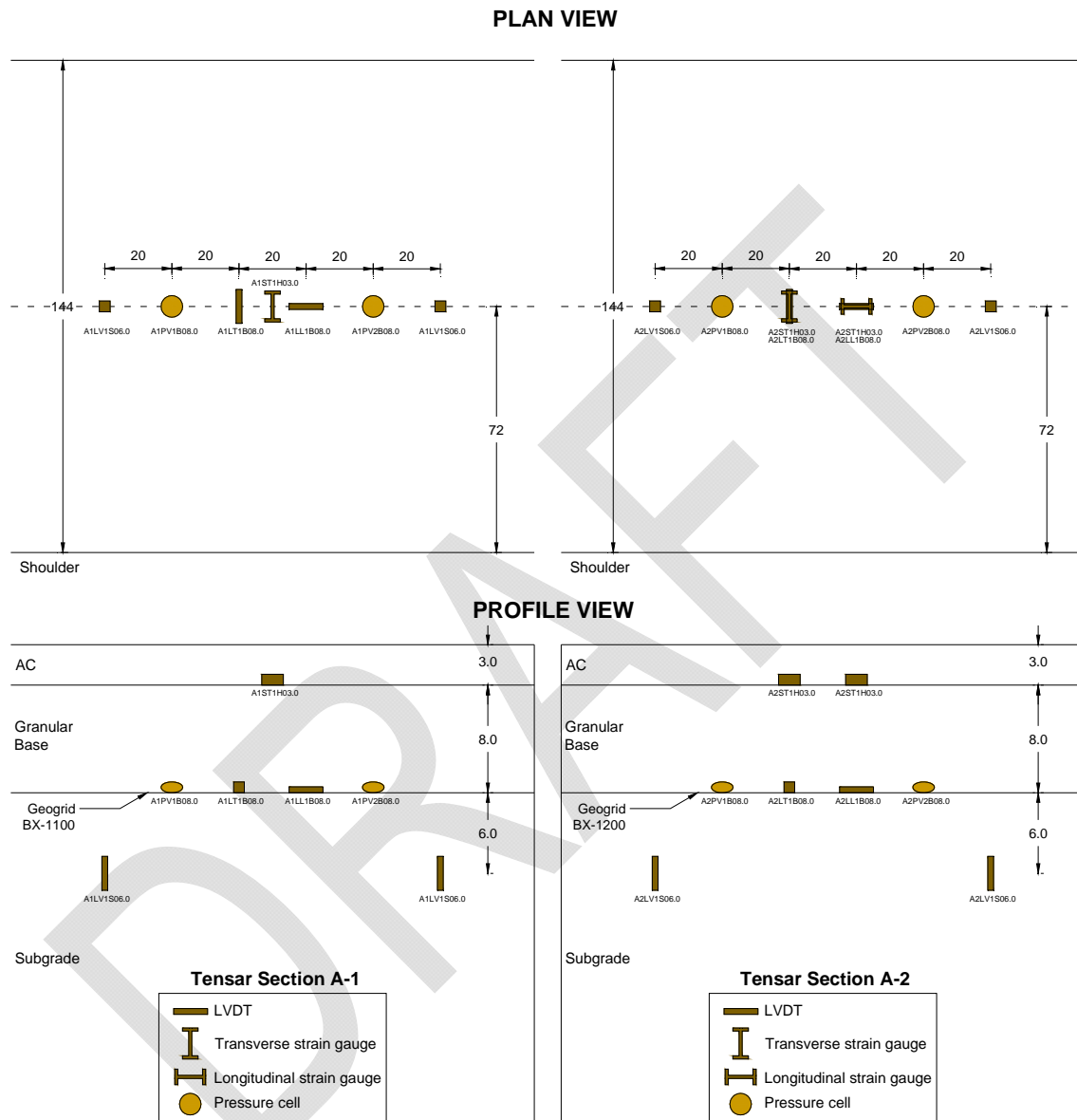


Figure C- 1. Plan and profile view of pavement structure and instrumentation of thin Section A-1 and A-2 at ATREL-UIUC

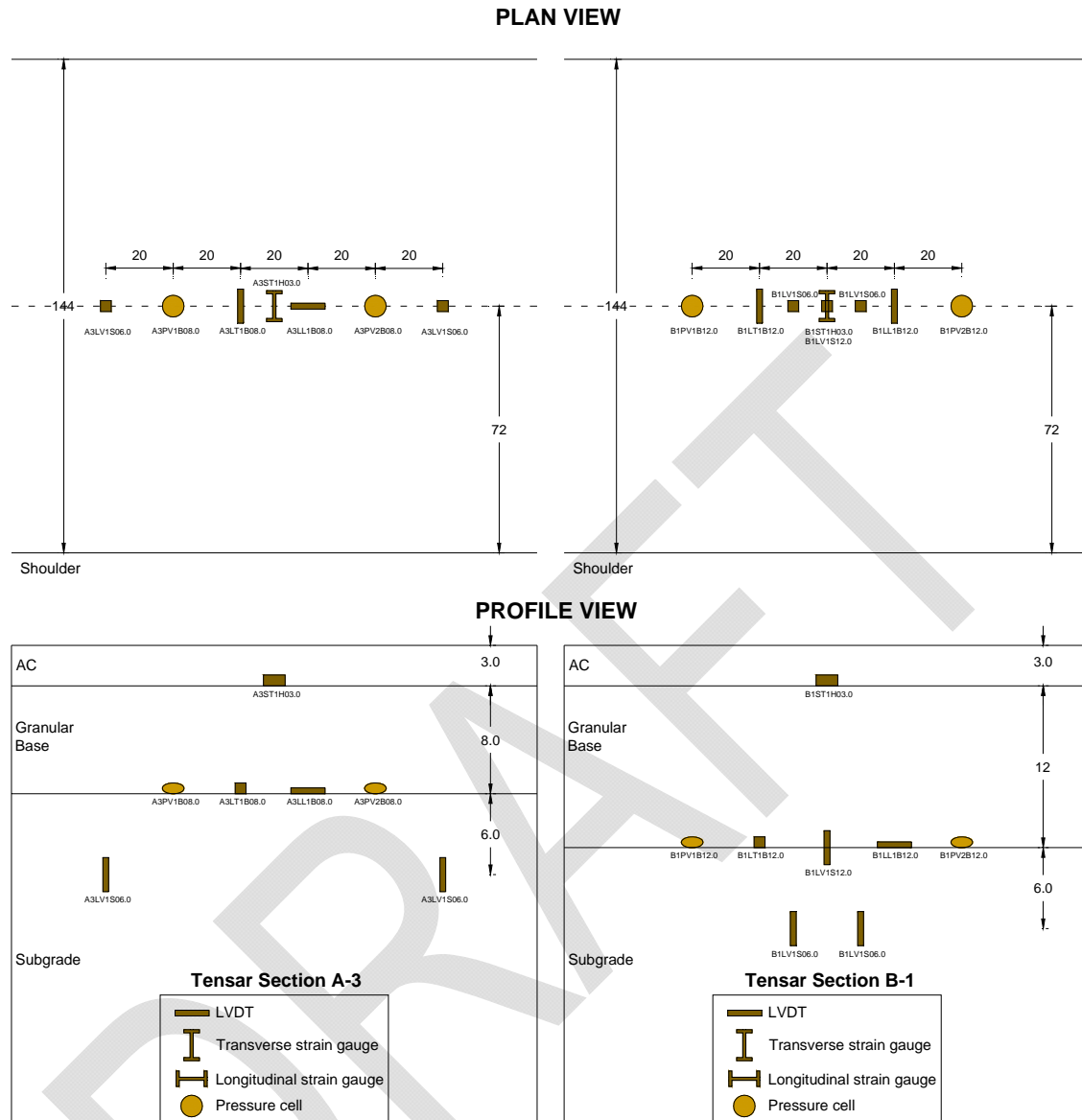


Figure C- 2. Plan and profile view of pavement structure and instrumentation of thin Section A-3 and B-1 at ATREL-UIUC

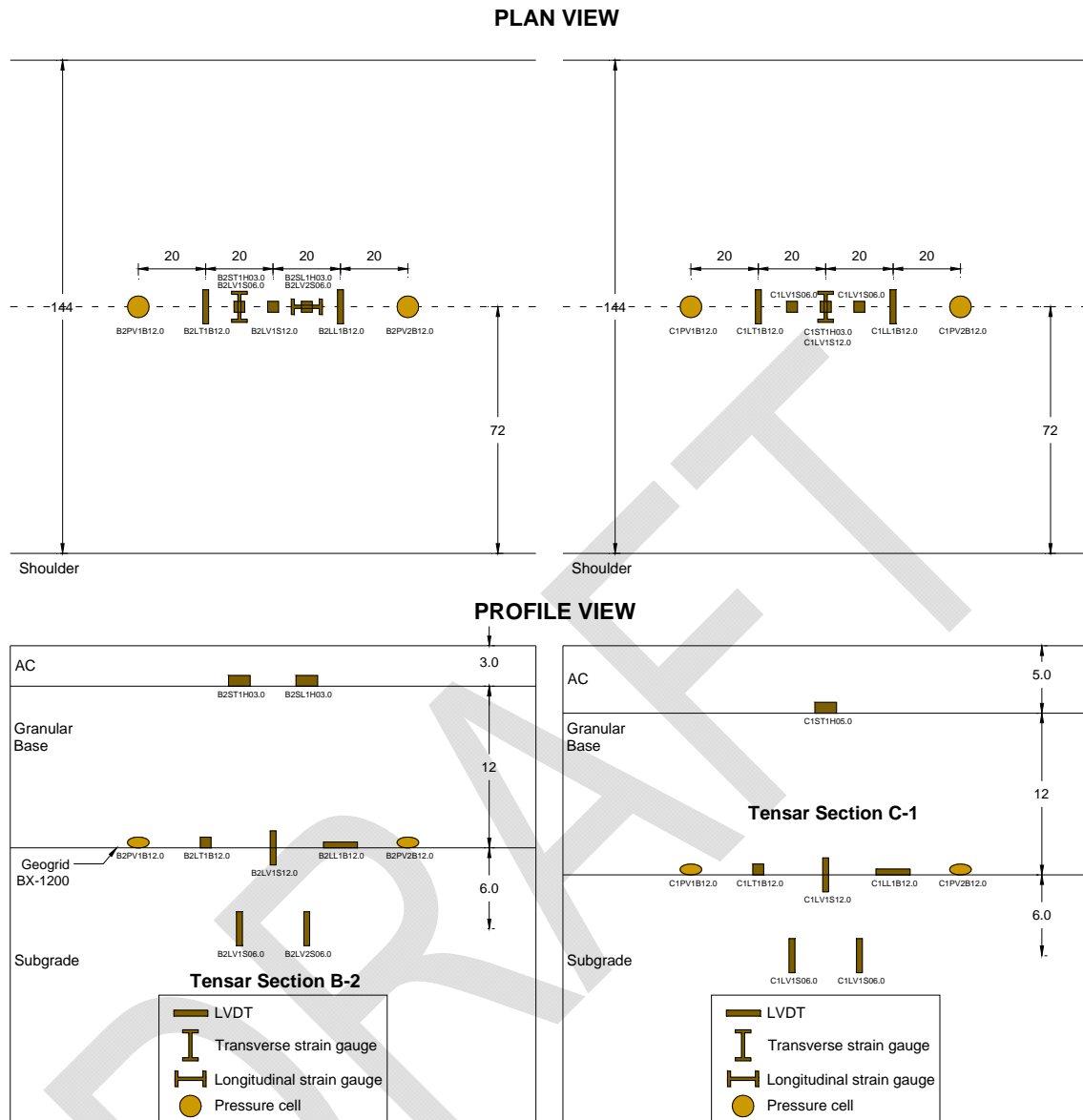


Figure C- 3. Plan and profile view of pavement structure and instrumentation of thin Section B-2 and C-1 at ATREL-UIUC

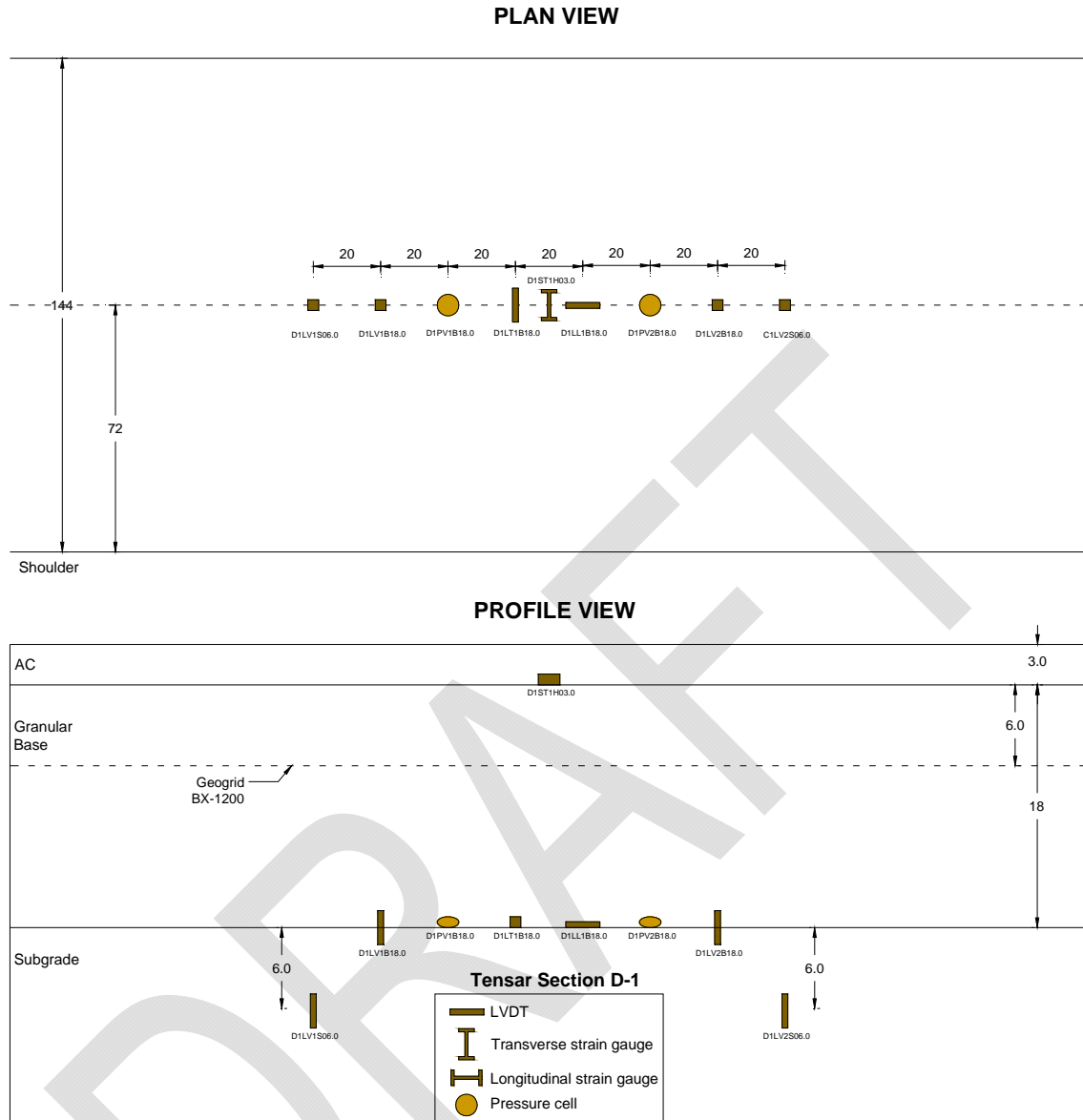


Figure C- 4. Plan and profile view of pavement structure and instrumentation of thin Section D-1 at ATREL-UIUC

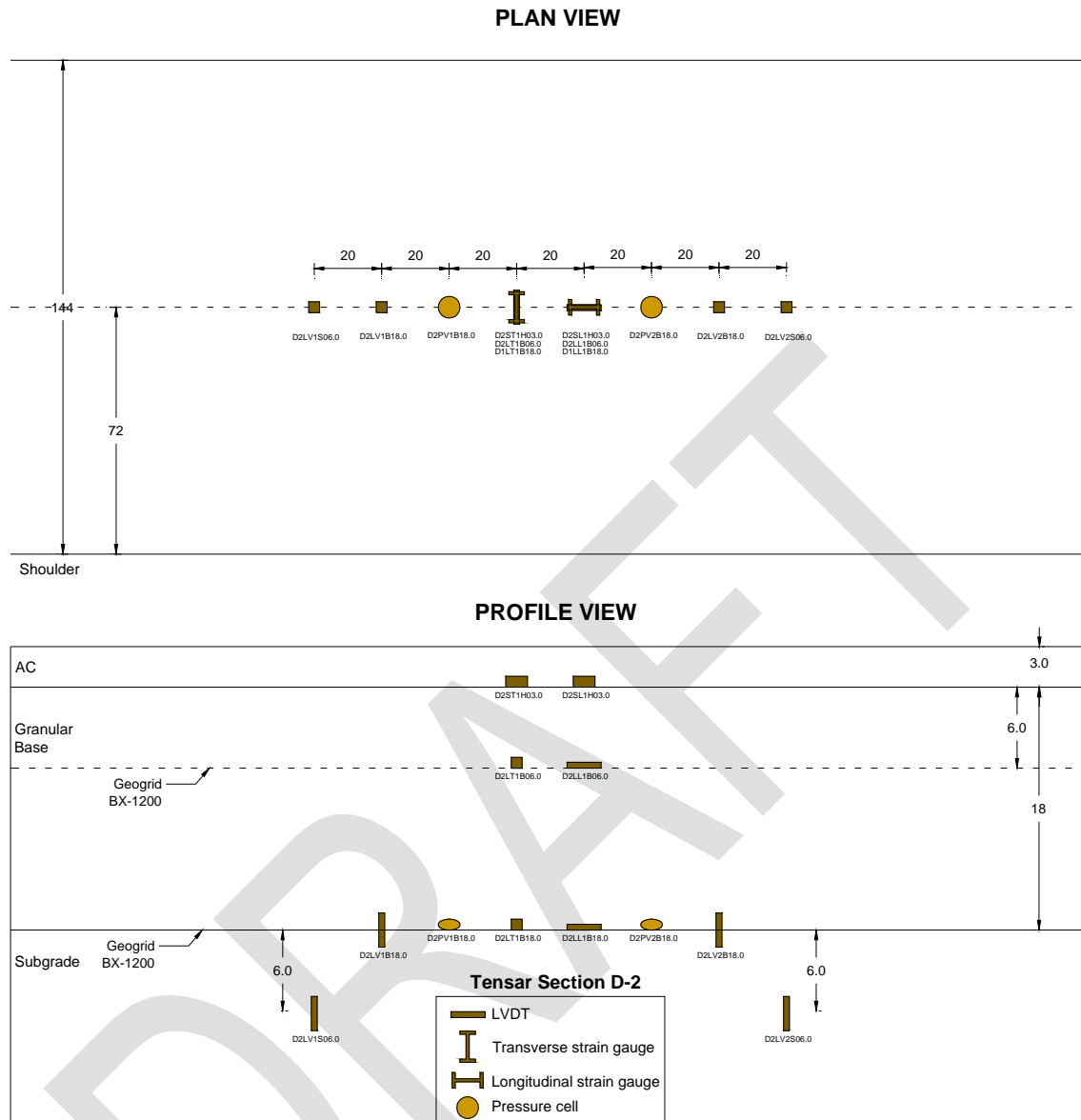


Figure C- 5. Plan and profile view of pavement structure and instrumentation of thin Section D-2 at ATREL-UIUC

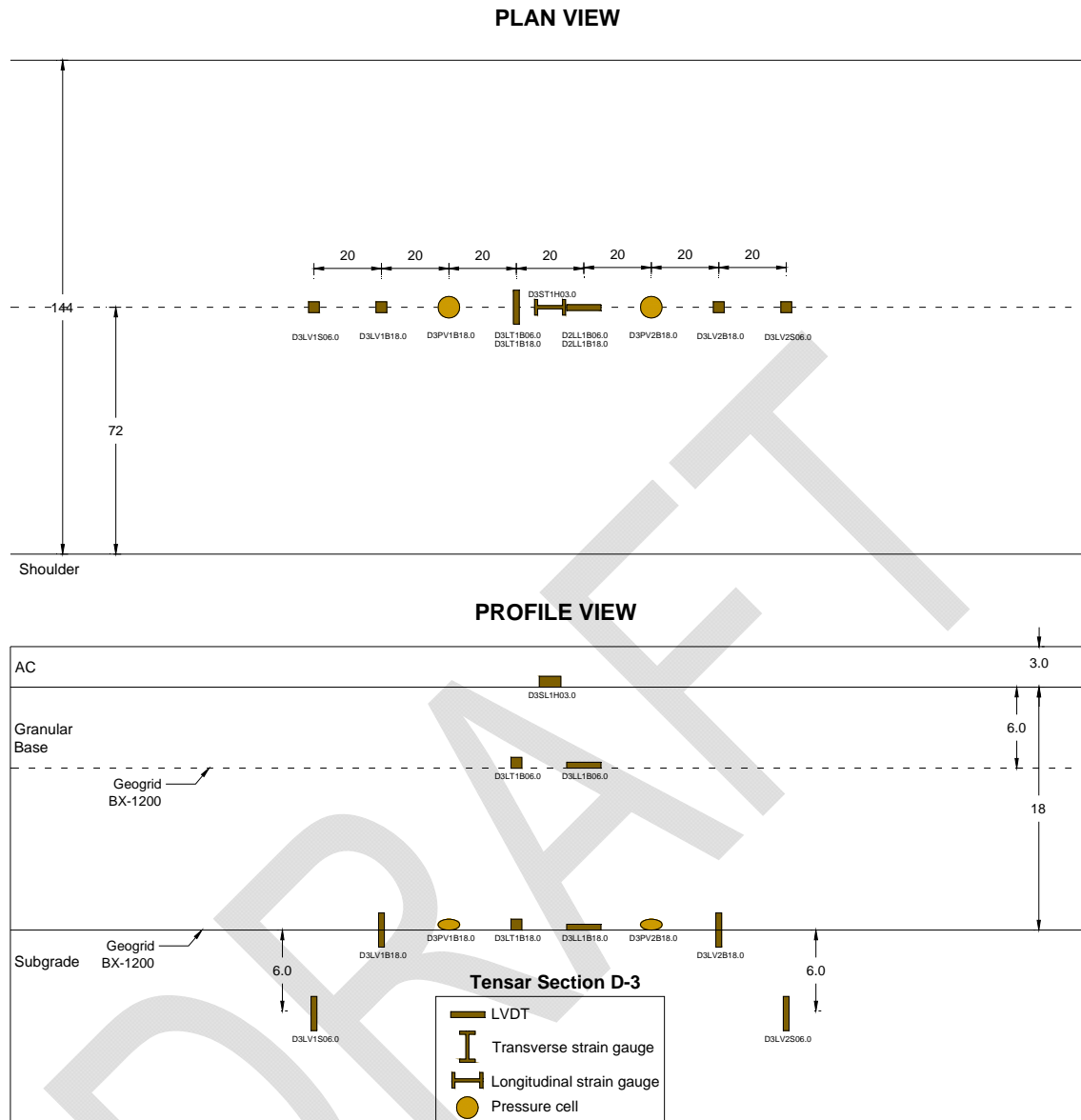


Figure C- 6. Plan and profile view of pavement structure and instrumentation of thin Section D-3 at ATREL-UIUC

12.APPENDIX D: AVAILABLE PAVEMENT STRUCTURES AND INSTRUMENTATION – ATREL-UIUC FULL DEPTH SECTIONS

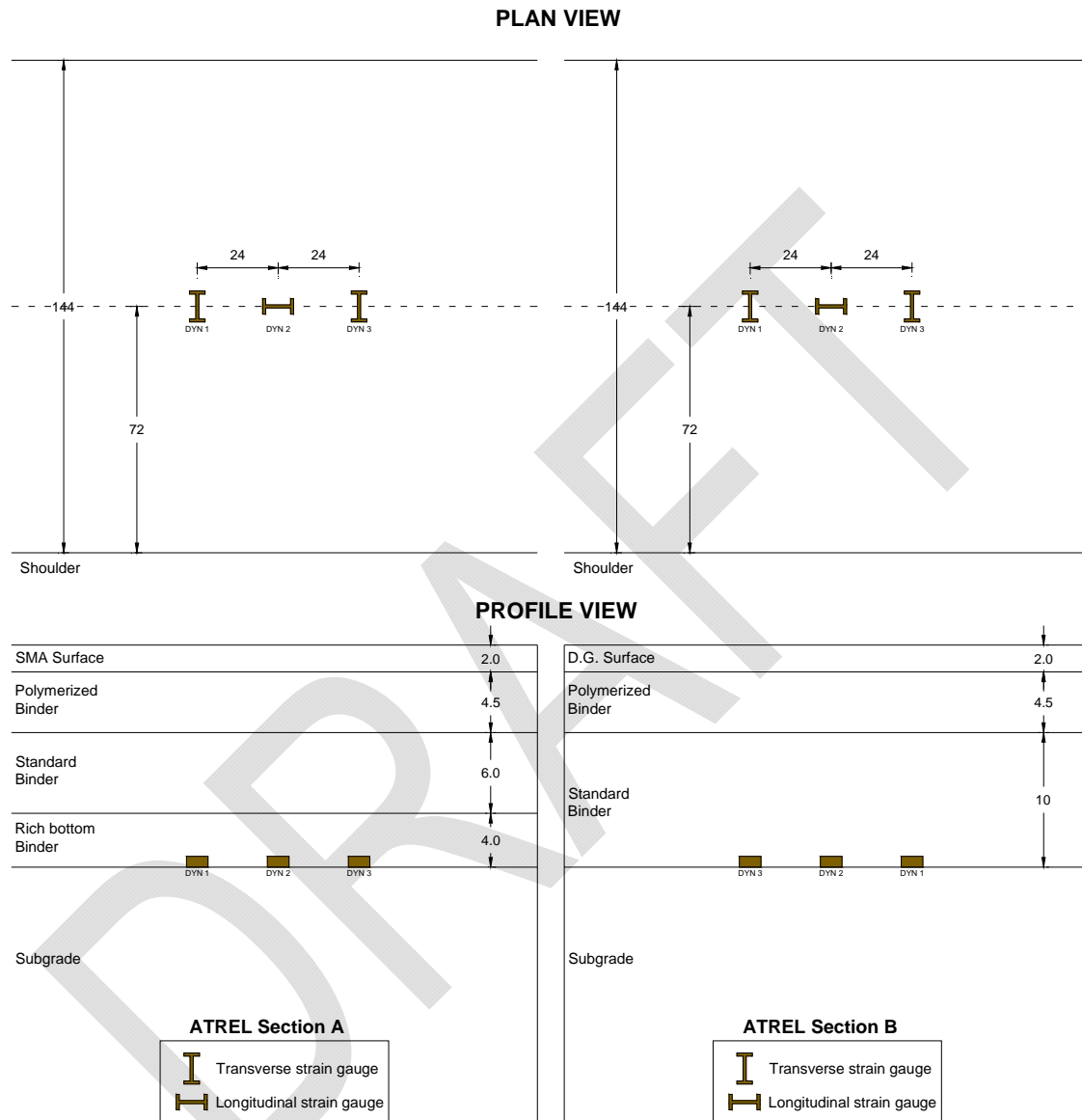


Figure D- 1. Plan and profile view of pavement structure and instrumentation Sections A and B, ATREL-UIUC full depth pavements.

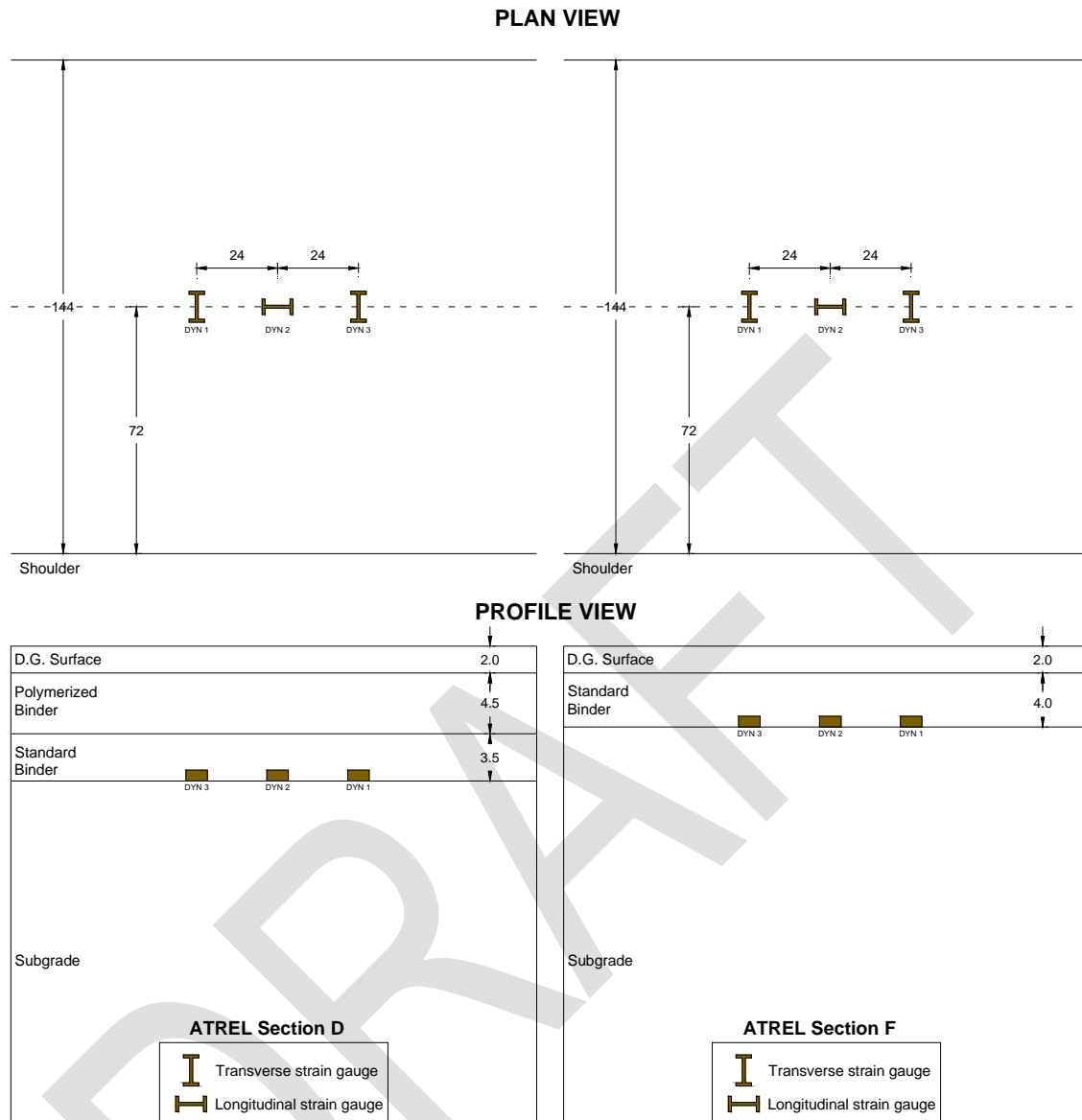


Figure D- 2. Plan and profile view of pavement structure and instrumentation Sections A and B, ATREL-UIUC full depth pavements.

13.APPENDIX E: AVAILABLE PAVEMENT STRUCTURES AND INSTRUMENTATION – OHIO SPS-8

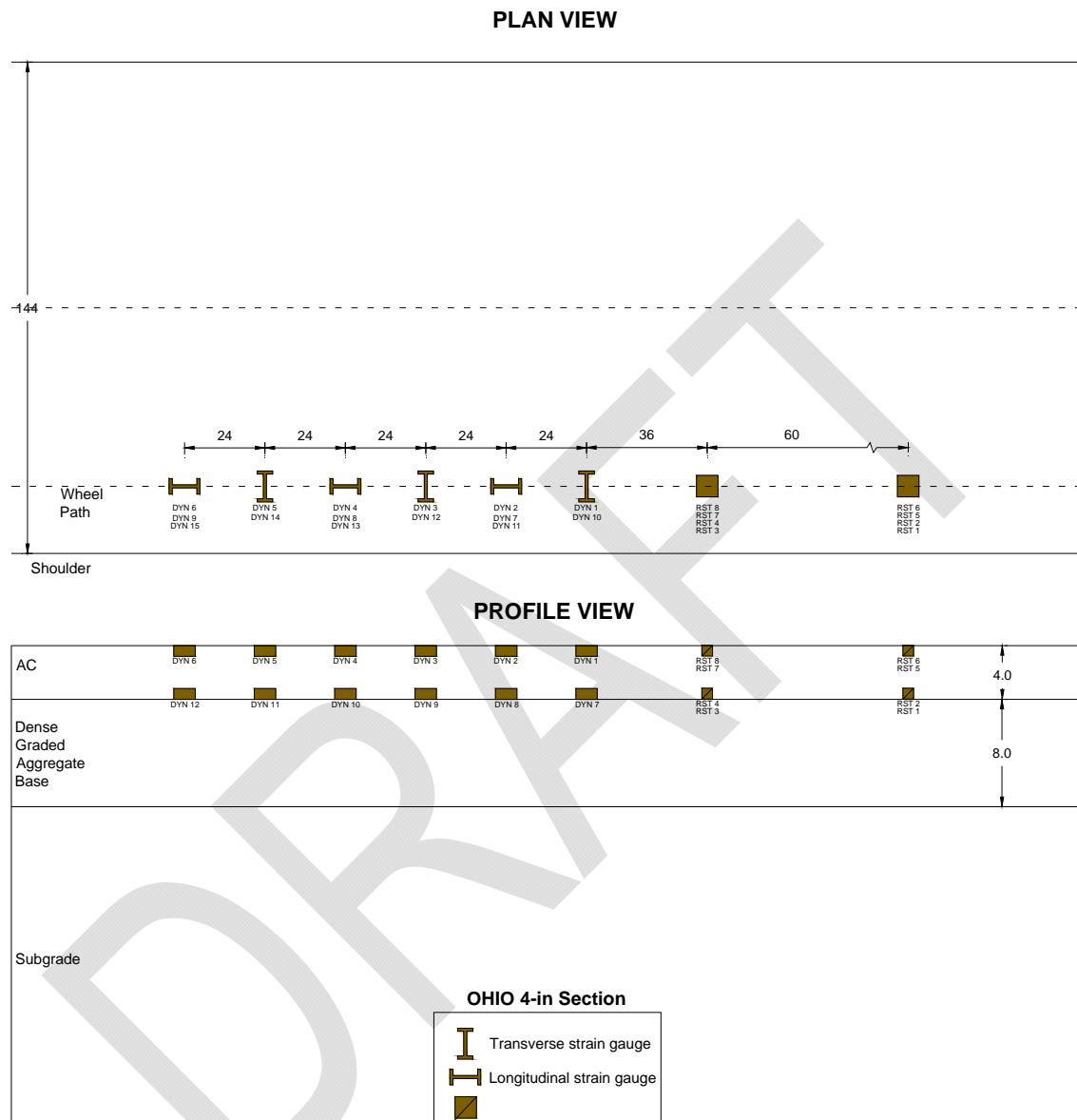


Figure E- 1. Plan and profile view of pavement structure and instrumentation of 4 in section, Ohio SPS-8.

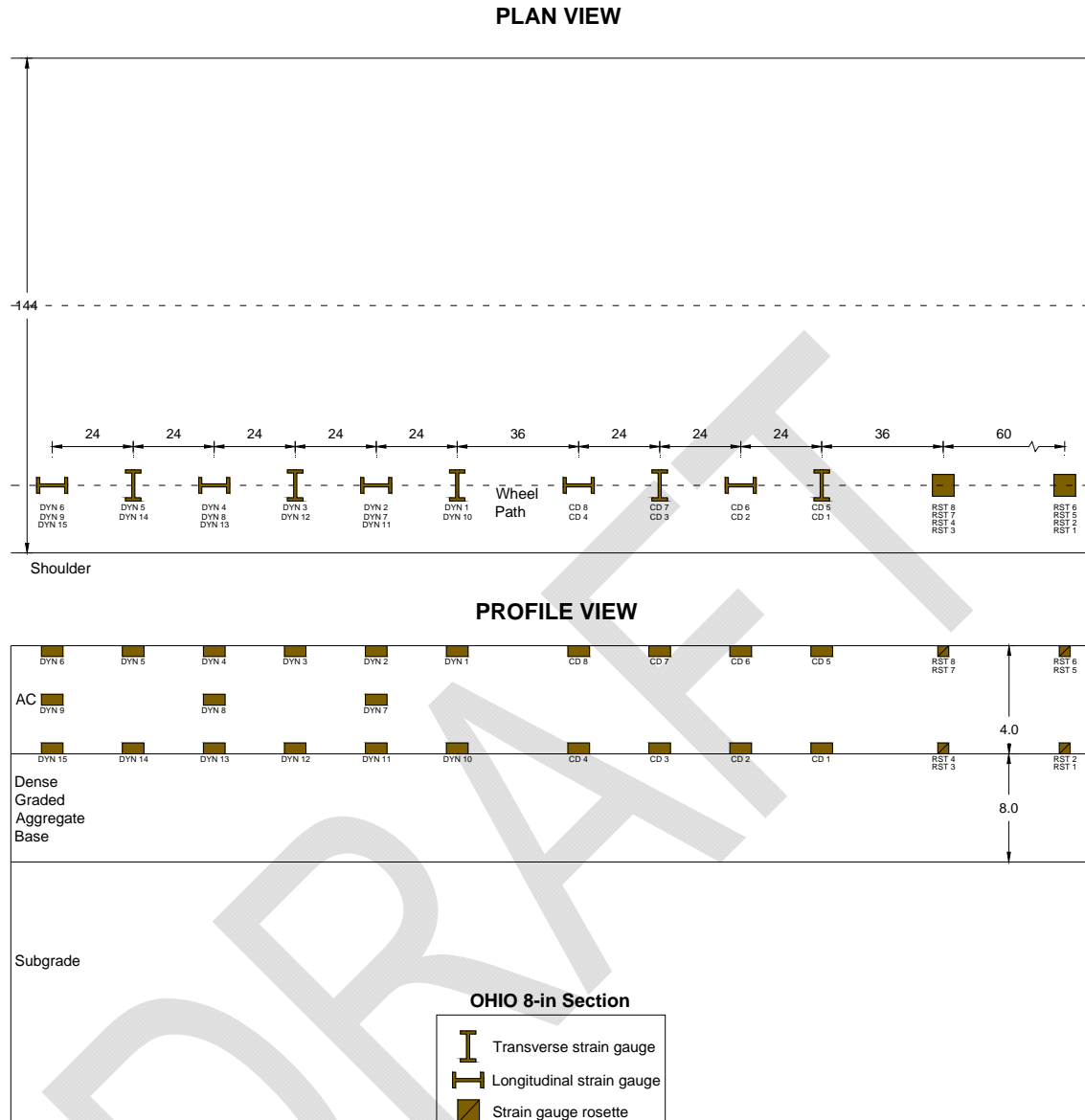


Figure E- 2. Plan and profile view of pavement structure and instrumentation of 8-in section, Ohio SPS-8.

14.APPENDIX F: AVAILABLE PAVEMENT STRUCTURES AND INSTRUMENTATION – UC-DAVIS

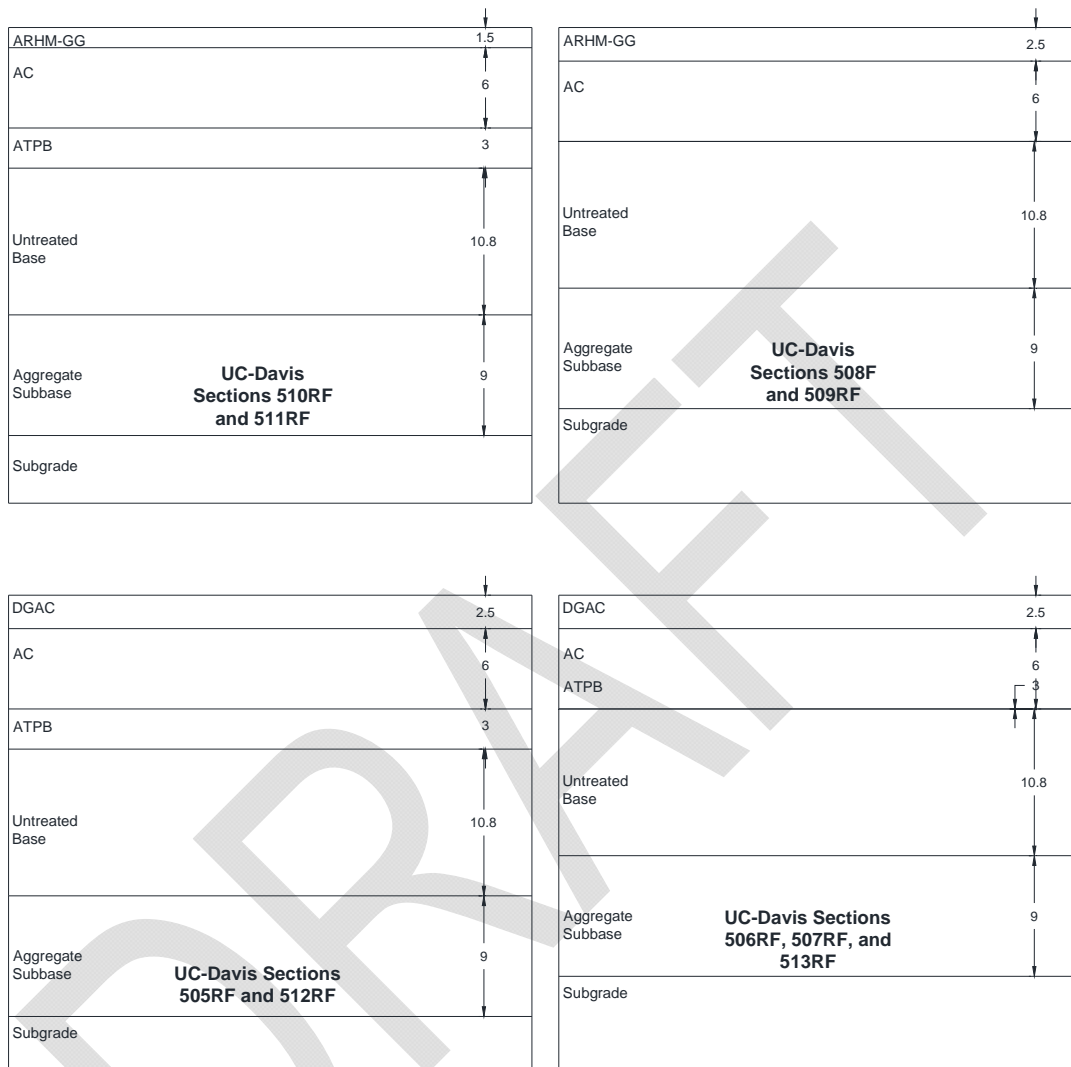


Figure F- 1. Profile view of pavement structure UC-Davis Sections.